NASA Technical Memorandum 81833

SIMULATOR RESULTS OF AN F-14A AIRPLANE UTILIZING AN AILERON-RUDDER INTERCONNECT DURING CARRIER APPROACHES AND LANDINGS

Wendell W. Kelley and Philip W. Brown

May 1980

National Aeronautics and Space Administration

Langley Research Center
Hampton, Virginia 23665

SUMMARY

A piloted simulator study was conducted to evaluate an aileron-rudder interconnect (ARI) control system for the F-14A airplane in the landing configuration. Effects on pilot performance and handling characteristics were investigated. Two ARI configurations were tested and compared to the standard F-14 fleet control system. A nonlinear aerodynamic model of the F-14 was used in conjunction with a six degree-of-freedom motion base simulator. The evaluation task, which utilized three subject pilots, consisted of a night carrier approach and landing.

Results of the study showed that both ARI configurations produced improved pilot performance and pilot ratings when compared to the standard control system. Sideslip due to adverse yaw was considerably reduced by the ARI systems and heading control was more stable and precise. Lateral deviation from centerline was reduced during the approach and lateral touchdown dispersion on the carrier deck was reduced with the ARI control systems.

INTRODUCTION

In cooperation with the Department of the Navy, the NASA Langley Research Center has recently been involved in a simulation and flight study to investigate and improve the handling characteristics of the F-14A airplane, in both the maneuvering and landing configurations. Initially the study was concentrated entirely upon the maneuvering configuration, and efforts were directed toward the development of a control system that would provide improved tracking performance at high angles of attack. It was also desirable to provide a high level of departure/spin resistance for the airplane. The control system which

evolved from that study was characterized by extensive modifications to the roll and yaw control systems of the fleet airplane, the primary modification being an aileron-rudder interconnect (ARI) feature. Initial piloted simulator results are described in reference 1.

Subsequent to the above study, NASA Langley undertook a simulator investigation to determine if the ARI system developed for high-α maneuvering might also be configured to improve the handling characteristics of the F-14 in the landing configuration. This was undertaken in response to fleet pilot comments and recorded flight data which indicated that the F-14 exhibits rather poor lateral/directional handling qualities in the landing configuration. The specific problems noted were a significant amount of adverse yaw following lateral stick inputs and a lightly damped Dutch roll mode which made precise heading prediction and control difficult, especially in a high-workload task such as a carrier landing.

The landing configuration study was conducted in a six degree-of-freedom motion base simulator with an out-the-window visual display depicting a night carrier landing scene. The flight control system was modeled in both the fleet configurations and in two separate experimental ARI configurations, each representing different levels of modification to the high angle-of-attack ARI system. The F-14 aerodynamic data were based upon low-speed wind-tunnel data.

The objectives of the study were to determine whether or not the ARI system, implemented with the airplane in the landing configuration, might provide improved handling qualities and performance, and to determine what level of modification to the ARI system was necessary to achieve the desired improvements. Both F-14 qualified Navy pilots and NASA research pilots were

used in the study. A night carrier landing task was used to determine handling qualities and performance capabilities with each control system.

SYMBOLS

All aerodynamic data and flight motions are referenced to the body system of axes shown in figure 1. The units for physical quantities used herein are presented in the International System of Units (SI) and U.S. Customary Units. The measurements and calculations were made in U.S. Customary Units.

a_n normal acceleration, positive along negative Z body axis, g units ($1g = 9.8\ m/sec^2$)

a_y lateral acceleration, positive along positive Y body axis, g units

b wing span, m (ft)

C_L lift coefficient, $\frac{\text{Aerodynamic lift force}}{\bar{q}S}$

C_ℓ rolling-moment coefficient about X body axis, $\frac{\text{Aerodynamic rolling moment}}{\bar{q}Sb}$

$C_{\ell,t}$ total rolling-moment coefficient

C_m pitching-moment coefficient about Y body axis, $\frac{\text{Aerodynamic pitching moment}}{\bar{q}S\bar{c}}$

$C_{m,t}$ total pitching-moment coefficient

C_n yawing-moment coefficient about Z body axis, $\frac{\text{Aerodynamic yawing moment}}{\bar{q}Sb}$

$C_{n,t}$ total yawing-moment coefficient

C_X X-axis force coefficient along positive X body axis, $\frac{\text{Aerodynamic X-axis force}}{\bar{q}S}$

$C_{X,t}$ total X-axis force coefficient

C_Y Y-axis force coefficient along positive Y body axis, $\frac{\text{Aerodynamic Y-axis force}}{\bar{q}S}$

$C_{Y,t}$ total Y-axis force coefficient

C_Z Z-axis force coefficient along positive Z body axis, $\frac{\text{Aerodynamic Z-axis force}}{\bar{q}S}$

$C_{Z,t}$ total Z-axis force coefficient

$\bar{c}$ wing mean aerodynamic chord, m (ft)

g acceleration due to gravity, m/sec^2 (ft/sec^2)

I_X, I_Y, I_Z moments of inertia about X, Y, and Z body axes, $kg\text{-}m^2$ ($slug\text{-}ft^2$)

I_{XZ} product of inertia with respect to X and Z body axes, $kg\text{-}m^2$ ($slug\text{-}ft^2$)

M_i indicated Mach number

m airplane mass, kg (slugs)

p airplane roll rate about X body axis, deg/sec or rad/sec

$\dot{p}$ airplane roll acceleration about X body axis, deg/sec^2 or rad/sec^2

q airplane pitch rate about Y body axis, deg/sec or rad/sec

$\dot{q}$ airplane pitch acceleration about Y body axis, deg/sec^2 or rad/sec^2

$\bar{q}$ free-stream dynamic pressure, N/m^2 (lb/ft^2)

r yaw rate about Z body axis, deg/sec or rad/sec

$\dot{r}$ yaw acceleration about Z body axis, deg/sec^2 or rad/sec^2

S wing area, m^2 (ft^2)

s Laplace variable, 1/sec

T total instantaneous engine thrust, N (lb)

T_c commanded thrust, N (lb)

t time, sec

u,v,w	components of airplane velocity along X, Y, and Z body axes, m/sec (ft/sec)
$\dot{u}$	airplane acceleration along X body axis, m/sec^2 (ft/sec^2)
$\dot{v}$	airplane acceleration along Y body axis, m/sec^2 (ft/sec^2)
V	airplane resultant velocity, m/sec (ft/sec)
$\dot{w}$	airplane acceleration along Z body axis, m/sec^2 (ft/sec^2)
X,Y,Z	airplane body axes (see fig. 1)
α	angle of attack, deg
α_{bias}	signal used to bias α_i in ARI control systems, deg
α_e	effective angle of attack, $\alpha_i + \alpha_{bias}$, deg
α_i	indicated angle of attack, deg
α_u	angle of attack sensed by autothrottle, units
β	angle of sideslip, deg
δ_a	differential horizontal tail deflection, positive for left roll, deg
δ_h	symmetric horizontal tail deflection, positive for airplane nose-down control, deg
$\delta_{h_{DLC}}$	incremental horizontal tail deflection due to DLC thumbwheel control, positive for airplane nose-down control, deg
δ_{ped}	rudder pedal deflection, positive for right yaw, cm (in)
δ_r	rudder deflection, positive for left yaw, deg
δ_{stkp}	pilot longitudinal stick deflection, positive for pitch up, cm (in)
δ_{stkr}	pilot lateral stick deflection, positive for right roll, cm (in)
$\delta_{SP_{DLC}}$	symmetric spoiler deflection (both wings) due to DLC thumbwheel control, positive for upward deflection, deg
δ_{SPL}	left-wing spoiler deflection, positive for upward deflection, deg
δ_{SPR}	right-wing spoiler deflection, positive for upward deflection, deg

δ_{TW} DLC thumbwheel deflection, positive for aft deflection, deg

$\Delta C_{n_{SPR}}$ increment in yawing-moment coefficient due to right-wing spoiler deflection

Δx distance from approach end of carrier landing deck, measured along deck centerline, positive in direction of landing, m (ft)

Δy lateral distance from extended centerline of carrier landing deck, positive right of centerline from approaching pilot's perspective, m (ft)

ζ_e damping ratio in second-order engine thrust-response model

Θ, ϕ, ψ Euler angles, deg

ω_e natural frequency in second-order engine thrust-response model, rad/sec

$$C_{\ell_p} = \frac{\partial C_\ell}{\partial \frac{pb}{2V}} \qquad C_{\ell_r} = \frac{\partial C_\ell}{\partial \frac{rb}{2V}}$$

$$C_{n_p} = \frac{\partial C_n}{\partial \frac{pb}{2V}} \qquad C_{n_r} = \frac{\partial C_n}{\partial \frac{rb}{2V}}$$

$$C_{n_{\delta_a}} = \frac{\partial C_n}{\partial \delta_a}$$

$$C_{Y_p} = \frac{\partial C_Y}{\partial \frac{pb}{2V}} \qquad C_{Y_r} = \frac{\partial C_Y}{\partial \frac{rb}{2V}}$$

ABBREVIATIONS:

ARI aileron-rudder interconnect

DLC direct lift control

FLOLS fresnel lens optical landing system

PLA power level angle; throttle position

RMS	root mean square
SAS	stability augmentation system
VMS	Visual Motion Simulator

DESCRIPTION OF THE AIRPLANE

General

The F-14 is a two-place, twin-engine jet fighter having a variable-sweep wing and twin vertical tails. A three-view sketch showing the general layout of the airplane is presented in figure 1. In the landing configuration wing sweep is fixed at 20^{o}, while in the maneuvering configuration sweep varies from 22^{o} for low subsonic speeds to 68^{o} for higher speed flight. Each wing is configured with leading-edge slats, trailing-edge flaps and four upper-surface spoiler panels. Figure 2 shows details of the wing flaps, slat and spoiler arrangements. In the landing configuration, leading-edge slats are deflected 17^{o} and trailing edge flaps deflected full down to the 35^{o} position, while the spoilers are normally raised to the 3^{o} position. A speed brake on the upper and lower surfaces of the aft fuselage provides increased drag and allows the use of higher engine thrust settings for the landing approach.

Empty weight of the airplane modeled for the present study was 198,074 N (44,531 lb) and a fuel weight of 17,792 N (4,000 lb) was used for all simulation tests. Table I lists the mass and dimensional characteristics used in the simulation.

Flight Control Systems

This section describes the current F-14 production airplane flight control systems as they were modeled for the simulation study. They are designated Control System A in this report. Modifications to the control systems are discussed in a later section.

The primary flight controls are powered by a system of conventional mechanical linkages and hydraulic actuators, in conjunction with a stability

augmentation system (SAS) which augments the airplane's natural damping characteristics about all three axes (pitch, roll and yaw). All SAS channels are normally engaged for approach and landing. Control surface commands for the SAS functions are generated by roll, pitch and yaw computers which respond to inputs from the pilot's controls and stabilization sensors. The computer outputs are then fed through SAS actuators which drive the control system mechanical linkages to produce surface motions. Commanded surface deflections from the SAS are in series with pilot inputs and do not produce control stick motion.

Each control surface actuator was modeled as a first-order lag with 0.05-second time constant, while the SAS actuators were modeled as unity gain devices with no lag. Rate and deflection limits of each actuator are discussed in the appropriate section.

Pitch control.- Figure 3 shows a schematic diagram of the longitudinal (pitch) channel of the airplane which was modeled for the study. The pitch controls consist of an all-moveable horizontal tail (stabilizer) which is controlled by pilots inputs at the control stick and a washed-out pitch-rate feedback signal from the SAS. The two signals combine to drive the stabilizer actuator which was modeled as a first order lag with a rate limit of 36 deg/sec. Symmetric stabilizer deflection limits were 10^{o} and -33^{o}, and the pitch SAS had an authority limit of $\pm 3^{o}$ deflection. SAS deflection rates were limited to 20 deg/sec.

Direct lift control.- The wing spoilers may be set to one of two positions for the approach and landing, depending upon whether or not the pilot selects direct lift control (DLC). If DLC is not selected, all the spoilers are deflected 4.5^{o} downward from their zero-deflection position (fig. 2). In

this mode of operation, flight path angle is controlled primarily by pitch attitude and thrust adjustments.

When DLC is selected, the spoilers are extended 7.5^{o}, making their neutral setting 3.0^{o} above the zero-deflection position. Subsequently, when the spoilers are actuated symmetrically on each wing, lift is rapidly modulated to give quicker flight-path angle response than could be generated with pitch control alone.

The pilot commands DLC spoiler actuation by a thumbwheel on the control stick. Figure 4 shows the relationship between thumbwheel actuation and spoiler deflection. Symmetric deflection of the horizontal tail also occurs during thumbwheel activation in order to counteract pitching moments generated by the spoilers. Figure 5 illustrates the horizontal tail deflection schedule as a function of thumbwheel position. Spoiler actuator models were rate limited at 150 deg/sec and deflection limits were -4.5^{o} to 55^{o}.

Lateral control.- The lateral system uses a combination of differential stabilizer deflection (δ_a) and spoiler deflection (δ_{sp}) for roll control. There are no wing aileron surfaces. Figure 6 shows a schematic diagram of the roll channel. Without roll SAS engaged, differential tail deflection is controlled solely by a mechanical linkage from the control stick and has a maximum deflection of $\pm 7^{o}$. When roll SAS is engaged another $\pm 5^{o}$ deflection is provided through a series actuator, which receives electrical inputs from a lateral control stick deflection sensor and stabilization signals from the roll gyro. The differential tail actuator model was rate limited at 36 deg/sec. The SAS actuator model was limited to 33.4 deg/sec deflection rate.

Whether roll SAS is engaged or disengaged, spoilers are used for roll control and are actuated via electrical signals from lateral stick deflection.

Figure 7 shows the spoiler control system schematic, including DLC inputs. Lateral spoiler gearing schedules, which are a function of whether DLC is engaged or disengaged, are shown in figure 8.

Directional control.- Conventional rudders on each vertical tail are used for directional control. Figure 9 shows a schematic diagram of the yaw channel of the airplane. Full rudder authority ($\pm 30^{o}$) is available through a mechanical linkage to the rudder pedals. With yaw SAS engaged, stabilization signals are derived from yaw rate gyro and lateral accelerometer feedbacks. The rudder actuator model was rate limited at 106 deg/sec while the SAS actuator model was limited to 63.4 deg/sec.

DESCRIPTION OF SIMULATOR

Cockpit

The NASA Langley Visual Motion Simulator (VMS) is a general purpose simulator consisting of a two-man cockpit mounted on a six degree-of-freedom motion base. Although the cockpit was designed to represent a transport type airplane, several modifications were accomplished which provided the hardware and instrumentation necessary for a simulator study of the F-14 airplane. An F-14 stick grip was mounted on a MacFadden hydraulic control loader and programmed to represent actual F-14 stick forces. Floor-mounted rudder pedals were also programmed to represent F-14 force-feel characteristics. A single-lever throttle grip provided simultaneous thrust control for both engines and a switch was provided for automatic throttle operation when desired.

The cockpit instrumentation consisted of a conventional flight director system and associated instruments. An angle-of-attack indexer provided on-speed indications during the approach and landing.

Visual Display

The visual display system was designed to provide a basic representation of the visual cues associated with a night carrier approach. The display, shown in figure 10, was generated by a computer-controlled monochromatic raster-scan television system, and provided a landing scene out the forward viewing screen of the simulator cab.

Dimensions of the simulated carrier landing deck, modeled after the U.S.S. Enterprise, were approximately 21.3m × 228m. Only the runway edge lighting, centerline stripe, dropline and fresnel optical lens landing system (FLOLS) were displayed. No horizon line was shown. The vertical dropline, which was suspended from the aft end of the ship and aligned with the deck centerline, provided lateral offset cues and bank angle information to the pilot during the approach.

In actual carrier operations, the FLOLS assembly is the primary source of vertical guidance during an approach in visual conditions. It consists of a fresnel optical lens units ("ball") mounted between a pair of horizontal reference (datum) lights to provide the pilot with information regarding airplane height above or below the desired glidepath. The datum lights and FLOLS ball are in a fixed position relative to one another. Thus, the geometric relationship of the ball, the datumn lights and the pilot's eye position during the approach provides the pilot with a direct indication of his position above or below the glidepath. In the simulator, the position of the ball was determined by calculations of the displacement of the airplane center-of-gravity from the ideal glidepath. The desired glidepath angle was 3.5^{o} relative to the carrier deck.

Computer Program and Equipment

The VMS was controlled by a real-time digital computer system which integrated the airplane equations of motion at a fixed rate of 32 times per second. The equations used nonlinear aerodynamic data which was stored in tabular form as functions of angle-of-attack. Appendix A describes the equations of motion used in the simulation. The engine model and automatic throttle are described in Appendix B.

AIRPLANE FLIGHT CHARACTERISTICS

Pilot Comments

The following summary of F-14 lateral/directional handling characteristics was obtained from interviews with several F-14 qualified Navy pilots, some with test pilot experience. The pilots were asked to comment on airplane handling qualities during all phases of the approach and landing, particularly during day and night carrier approaches.

The main handling qualities problem in the landing configuration is adverse yaw following lateral stick inputs. Unless a generous amount of rudder is used, there is substantial adverse yaw both rolling into and out of turns. The adverse yaw and resultant yaw excursions result in some difficulty making precise line-up corrections during an approach and contributes to a fairly high pilot workload. Although the problem exists in all phases of the approach, the primary area of concern is from an altitude of 61 m (200 ft) down to touchdown, since that is where small line-up errors become important and pilot gain goes up considerably. Turbulence may complicate the problem considerably.

The airplane's heading tends to wander when the pilot is attempting to hold a specific heading, such as might occur on an instrument flight task. The Dutch roll mode also appears to be lightly damped.

The carriage of missile stores does not appear to affect lateral/directional characteristics in the landing configuration.

Flight Data

Analysis of flight data in the landing configuration reinforces pilot comments. Figure 11 shows the response of an F-14 to a lateral stick input, reversing bank angle from $+30^{o}$ to -50^{o}. Rudders were not used. The data were taken from a series of flight maneuvers which was flown in a test airplane to document the aerodynamic characteristics of the F-14 for the simulator study. Note that a step lateral stick input of approximately 1.9 cm (0.75 in.) results in a 12^{o} sideslip angle (β) which reaches peak amplitude 3.0 seconds after the lateral control input. Note also that a 1.5 second delay exists in yaw rate (r) response before the aircraft begins to turn in the proper direction, and that there is a momentary tendency to turn in the opposite direction. Both of these characteristics contribute greatly to difficulties in precise heading control and tend to substantiate the pilot comments. To eliminate SAS effects on the lateral/directional data, both the roll and yaw SAS were disengaged. Thus, the Dutch roll characteristics which are shown are more lightly damped than the airplane would exhibit if the SAS system were engaged. However, the adverse yaw characteristics are essentially identical to the SAS-engaged case.

Superimposed on the flight data in figure 11 are simulator time histories of the same flight maneuver. Note that good agreement exists in most flight

parameters up until the time the simulator and flight control inputs no longer match.

Spoiler Effects

Wing spoiler contribution to adverse yaw is evident from analysis of the aerodynamic data. Figure 12 represents yawing moment due to right wing spoiler deflection. (Left wing spoiler effects are identical except for a sign reversal.) Although the normal approach angle-of-attack is 10.5^{o}, the $\alpha = 12^{o}$ curve, which is representative of approach conditions, is used here to demonstrate an example of spoiler effects. Reference to figure 8(b) shows that a lateral stick deflection of 3.81 cm (1.5 in) to the right causes the right wing spoilers to deflect 5.5^{o}. Using the $\alpha = 12^{o}$ data in figure 12, it can be seen that this spoiler deflection results in a net change of -0.0025 in the airplane yawing moment. The negative yawing moment following a right lateral stick input is adverse; that is, it tends to turn the airplane opposite the direction which was intended by the control input. Furthermore, differential tail contribution to yawing moment, which is shown in figure 13, is favorable at this angle-of-attack. Therefore, although some of the sideslip in rolling maneuvers is kinematically induced, much of the adverse yaw noted in flight data is generated by spoiler deflections.

The case illustrated above demonstrates spoiler effects when DLC was not engaged. However, a similar effect exists for the DLC engaged case.

CONTROL SYSTEM MODIFICATIONS

ARI High-α Configuration

The control systems which were used to investigate F-14 handling qualities in the landing configuration were based upon modifications to an existing

experimental aileron-rudder interconnect (ARI) system for the airplane which was designed to improve stability and control characteristics during high-α maneuvering. Developed by the NASA Langley Research Center, the high-α ARI featured modifications to the roll and yaw channels of the standard fleet control system.

Figure 14 shows a schematic of the high-α ARI roll channel. Major differences from control system A are an extra stick-to-differential-tail gain path and increased roll-rate damping. It should be noted that the high-α ARI was designed to be effective at higher angles-of-attack while not affecting handling characteristics at low-to-medium α. As a result, α-scheduling components are a major feature of the design. Note for instance that for $M \leq 0.55$ the SAS stick-to-differential-tail gain is -4.28 for $\alpha_i \leq 14^0$, which provides the same gain as control system A. As α_i increases from 14^0 up to 40^0 the gain linearly decreases, providing less differential tail movement per unit lateral stick deflection. Note also that the α-scheduling breakpoints vary with Mach number.

Roll rate damping is generally increased with the ARI for $\alpha \geq 15^0$, and a rudder pedal fadeout feature is added.

The ARI yaw channel is shown in figure 15. Two features were added to control system A. A lateral-stick-to-rudder interconnect counteracts adverse yaw and provides turn coordination at higher α. Although the lateral-stick-to-rudder interconnect is not, technically speaking, an aileron-rudder interconnect, it was designated ARI to comply with established nomenclature. The other added feature was a feedback of roll rate to rudder which helps to increase lateral/directional damping.

ARI Landing Configurations

The objectives of the present study were to analyze the previous ARI design and determine what further modifications might be necessary in order to improve handling characteristics in the landing configurations. The approach taken was not only to maximize improvements in the handling qualities but also to minimize any impact on the design of the ARI as it already existed. Therefore, numerous combinations of gain changes and SAS circuit modifications were investigated on the piloted simulator. From these investigations were selected the two best configurations, one which provided the minimum ARI design impact and the other which utilized further modifications in order to achieve more optimum handling qualities. The simulator sessions which were used in this effort involved NASA engineering test pilots flying numerous flight maneuvers in the moving-base facility described earlier. The maneuvers included carrier approaches and landings, instrument turns, and other tasks designed to highlight adverse flying qualities.

The two candidate ARI system designs which were selected for further evaluation were designated control system B and control system C, and are described below. Since the ARI modifications did not affect the pitch control channel, that system remains unchanged for control system A, B, and C.

Control System B

Figure 16 illustrates the roll channel of control system B. Minimum impact to the ARI design was achieved by simply biasing the angle-of-attack signal coming into the ARI. The relationship between true angle-of-attack (α) and angle-of-attack sensed by the ARI test noseboom (α_i) is shown in figure 17. Note that at the proper approach angle-of-attack ($\alpha = 10.5^{o}$) the ARI noseboom

senses $\alpha_i = 12^0$, which is the quantity available for ARI input. By summing α_i with a bias angle-of-attack (α_{bias}) the ARI senses a higher effective angle-of-attack (α_e) than is actually being flown. This in turn causes the ARI functions, which would normally be ineffective at approach α due to α-scheduling, to be effective.

An α_{bias} setting of 8.96^0 was determined to give the best combination of roll and yaw response to lateral stick inputs using the existing high-α ARI gains. Note that during an approach α_e is 20.96^0 which reduces the δ_a/δ_{stkr}, gain from that of control system A. Figure 18 shows the relationship of δ_a/δ_{stkr} as a function of α_e. Operation in the landing configuration should always occur at $M \leq 0.55$, so the higher Mach scheduling curves will not affect control gains.

The only other change to the ARI roll channel involved the α switch in the roll rate damping loop. This was changed so that the higher roll rate damping remained in effect for all positive α, and eliminated the problem of discrete gain switching during low-α maneuvering.

The yaw channel of control system B, shown in figure 19, is identical to the high-α configuration except the addition of α_{bias}. For the approach condition ($\alpha_e = 20.96^0$) the effective ARI gain is (2.60)(.896) = 2.33 and the effective δ_r/p gain is (0.2)(.896) = 0.179.

Control System C

The design approach for this ARI configuration was to adjust any SAS gain or α-schedule which might result in better handling qualities than control system B provided. Major design changes in the ARI system were not considered.

Figure 20 shows the yaw channel of control system C. The only gain change which was beneficial was an increase in the LSRI gain from 2.60 to 3.19. This provided slightly more rudder for turn coordination and resulted in quicker yaw response for initiation of turns. The actual ARI gain at approach α was (3.19)(.896) = 2.86.

Several combinations of gain changes involving p, r, and a_y feedback were also investigated. No gain configurations which were tested provided improved handling qualities over the gains taken from the high-α configuration.

The roll channel of control system C is shown in figure 21. Two changes were made from control system B. First, the stick-to-differential-tail gain was slightly increased to match the increased ARI gain. This was accomplished by moving the α breakpoints in the δ_a/δ_{stkr} loop from 14^o and 40^o to 17^o and 43^o, respectively. The δ_a/δ_{stkr} gain which resulted from this schedule is shown in figure 18.

The other gain change was an increase in the roll rate damping multiplier from 4.0 to 5.0, which provided better damping to accompany the increased ARI and δ_a/δ_{stkr} gains.

EVALUATION PROCEDURES

Evaluation of airplane handling qualities and pilot performance was accomplished during a series of simulator sessions involving three pilots. Pilot 1 was a NASA engineering test pilot with over 2000 hours in fighter type airplanes and previous Navy carrier landing experience, but with no actual F-14 flight time. Pilot 1 had considerable experience flying F-14 simulations at NASA Langley Research Center.

Pilots 2 and 3 were operational Navy pilots were current F-14 experience and recent F-14 carrier landings. Pilot 2 had 1700 hours flying time in fighter airplanes, 1200 hours of which was in the F-14. Pilot 3 had 900 hours in fighter airplanes, 700 hours of which was in the F-14.

Carrier Landing Task

Simulated carrier landings were used as an evaluation task to compare pilot performance with each of the control system configurations. Each pilot was briefed on the simulator facility and cockpit features but were not briefed in detail on the differences between control system configurations. Pilot 1 was already familiar with each control system due to his previous F-14 simulator work.

Each carrier landing run was begun at a point 1828 m (6000 ft) from the desired touchdown point on the carrier, and displaced laterally 45.7 m (150 ft) to the right of course. Altitude at that point was 138 m (454 ft) above sea level, which was 119 m (391 ft) above carrier deck level. The airplane was in a trimmed condition on the desired -3.5^{0} glidepath to touchdown. The autothrottle was engaged for all approaches.

Although no carrier motion was included, a 30-knot headwind was used which resulted in an approximate 100-knot closure speed on the carrier. This was considered a reasonable simulation of the combined headwind and carrier speed (wind over deck) which might be encountered in an operational environment. The ship burble was not modeled. Turbulence was not present for the runs included in this report.

Pilots were instructed to make a prompt lateral correction to get the airplane on the approach centerline and to maintain the airplane on the centerline

as closely as possible throughout the approach and touchdown. The primary cue for lateral corrections was the visual display of the carrier deck and vertical dropline at the approach end of the deck.

Pilots also were instructed to maintain the proper glidepath throughout the approach. The FLOLS provided a vertical guidance visual cue for this task.

Although cockpit instrumentation also provided deviation-type indicators for both lateral and vertical guidance to touchdown, the pilots rarely used those indicators. The approach and landing was almost entirely an out-the-window visual task.

Cockpit motion was used for all approaches. At the instant of touchdown, a vertical acceleration was introduced at the cockpit to provide a touchdown motion cue to the pilot. At this instant the simulation was halted and the visual display was frozen in the attitude existing at touchdown.

After approximately 10 practice runs each evaluation pilot performed approximately 12 approaches and landings with control system A. At the end of the run sequence, pilot comments were recorded and a Cooper-Harper pilot rating (ref. 2) was assigned to the control system for that task. The same procedure was used for control systems B and C except only five to six practice approaches were necessary for the pilots to adapt to the handling characteristics of the new control configurations.

RESULTS AND DISCUSSION

Both time history and statistical data were recorded for each control system and evaluation pilot. Time histories are discussed below, followed in a later section by statistical data on both the approaches and touchdowns. The

time history traces are representative of the performance by each pilot/control system combination and do not necessarily represent the best or worst performance noted during the run session.

Approach Time Histories - Control System A

Figures 22 through 24 show time history results of a typical approach for the three pilots using control system A. Each pilot had a tendency to overshoot the final approach course and usually crossed back over the course one or more additional times prior to landing the airplane. Adverse yaw, a lightly damped Dutch roll, and difficulty in predicting the results of a control input were cited as the primary contributing factors.

Roll rate (p) and consequently bank angle (ϕ) tended to be oscillatory and of a fairly large magnitude during the final portion of the approach, although Pilot 1 did not have that problem on the particular run selected for inclusion in this report.

The amount of sideslip (β) which occurred during the run varied considerably from pilot to pilot. However, each pilot was consistent in that the maximum sideslip occurred on the latter part of the approach, where the workload increased considerably as he attempted to land precisely on the carrier centerline. Note that the maximum sideslip angles were approximately 2^{o}, 2.5^{o}, and 6^{o} for Pilots 1, 2, and 3 respectively during the final moments of the approach.

Yaw rate (r) and heading (ψ) were both quite oscillatory throughout the approach for all pilots.

Approach Time Histories - Control System B

Figures 25 through 27 show results of typical approaches using the ARI configuration with minimum design changes. The amount of final approach course

overshoot was greatly reduced from control system A. Also, there was not a tendency to overshoot in the opposite direction after the correction back to course was begun.

Yaw rate and ψ were much less oscillatory and responded positively to pilot inputs with practically no delay due to adverse yaw. This was directly attributable to the rudder coordination feature of the ARI yaw channel.

Roll rate and ϕ oscillations, although existent for this configuration, were generally of a slower frequency and smaller amplitude than control system A.

Sideslip excursions were also greatly reduced throughout the approach. Note that the largest magnitude of β for all pilots was approximately 1.0^{o} - 1.5^{o}.

Approach Time Histories - Control System C

Approaches with control system C are shown in figures 28 through 30. Final approach intercept and tracking were generally as good as, and in most cases better than, the results from control system B. Although Pilot 3 overshot final in the example shown, that was not typical for either pilot. Note that the correction back to course was positive and precise.

Heading control was slightly better than with control system B and much improved over control system A. After the pilots made their initial correction to get on the approach centerline, only very small heading changes were necessary to complete the approach and landing.

Sideslip angle during the approach was greatly reduced from control system A and slightly reduced from control system B.

Pilot Ratings

At the end of each run session with a particular control system configuration, each pilot rated the control system for the approach task. Figure 31(a) shows the Cooper-Harper rating scale which was supplied to the pilots for their use, and figure 31(b) shows the results for each pilot. There was consistently a 2-point improvement in pilot ratings when going from the fleet control system to ARI configuration B. Pilot 1 also rated the more advanced ARI configuration C to be 1-point better than configuration B. Pilots 2 and 3,although showing some performance improvement in going from control system B to C, rated them equally on the Cooper-Harper scale.

Appendix C contains an amplification of the rating process by Pilot 1.

Statistical Data

Lateral deviation from centerline, Δy, is shown in statistical form in figure 32. These data show the root-mean-square (RMS) value of lateral deviation during two segments of the approach; Segment 2 covering the last 518 m (1700 ft) of the approach, measured along the approach centerline, and Segment 1 from 518 m (1700 ft) out to 1036 m (3400 ft) on the approach. Segment 2 corresponds roughly to the last 10 seconds of the approach, while Segment 1 represents the 10 seconds of flight prior to Segment 2.

Although there was considerable variation among pilots, a reduction in lateral deviation was noted for all pilots in each segment when the ARI control systems were used. Segment 2 shows remarkable similarity in performance between pilots. In each case a reduction in lateral deviation was noted when going from control system A to B and a subsequent reduction, although generally smaller, occurred in going from control system B to C.

Figure 33 shows RMS sideslip angle for the same approach segments. A large reduction in β occured for all pilots in each segment when control system B was used. Note also that a slight further reduction was consistently obtained when going from control system B to C.

Carrier Landing Data

Figures 34-36 show landing dispersion data for each pilot/control system combination. The width of the Δy scale approximates the width of the landing deck.

Each pilot showed a reduced lateral touchdown dispersion when either ARI control configuration was compared to control system A. This was particularly true for Pilots 1 and 2, where most touchdowns occurred within ± 2.0 m of the deck centerline using either control system B or C. This was considerably better than the dispersion noted with control system A. A similar, though not as large, reduction was noted for Pilot 3.

Longitudinal dispersion was also reduced for Pilots 1 and 2. This was attributed to the fact that the ARI systems made the lateral tracking task so much easier that they had more time to devote to tracking the glideslope.

INTERPRETATION OF RESULTS

The fidelity of the simulation in representing the actual F-14 airplane was evaluated by comparing simulation results with actual airplane flight test data and by having pilots with F-14 experience fly the simulator. The agreement between flight and simulator data was generally very good and pilot comments were positive. Therefore, a similar trend of results and pilot opinions is expected when the ARI system is flight tested in the landing configuration.

Although turbulence effects were not included in the results of this report, simulated approaches were also flown with moderate turbulence and similar beneficial effects of the ARI systems were noted. However, ship burble effects were not included in the simulator model.

Approaches were also flown in crosswind conditions and during single-engine operation. No degradation in control characteristics was noted for the ARI systems.

Limited flight tests will be conducted later this year at the NASA Dryden Flight Research Center to investigate the ARI concept for the landing configuration. However, final results and recommendations regarding ARI suitability for the landing configuration will most likely have to come from more extensive flight tests and should include approaches to a carrier or field carrier landing facility.

CONCLUSIONS

A piloted simulator study was conducted to evaluate pilot performance and handling characteristics of an F-14 airplane in a night carrier landing task configured with either of two aileron-rudder interconnect (ARI) control systems. Control system B used an existing ARI design and included a minimum of modifications. Control system C included further modifications for improved performance. Both were compared with the standard F-14 fleet configuration (control system A). Results of the study were as follows:

1. The simulator provided good verification of flight data and pilot comments regarding F-14 handling qualities. A considerable amount of adverse sideslip existed following lateral stick inputs. Some difficulty was encountered when attempting precise lateral line-up corrections during high-workload tasks such as a carrier landing.

2. The airplane adverse yaw characteristics were primarily a result of spoiler aerodynamics during lateral control inputs.

3. During carrier approaches, lateral deviation from the approach centerline was much less oscillatory, and lateral errors were significantly reduced, with either ARI configuration when compared to the fleet control system.

4. Sideslip angles and heading errors were both considerably reduced with the ARI systems, and heading control was much more stable.

5. A considerable reduction in lateral touchdown dispersion on the carrier deck resulted when the ARI systems were used.

6. Evaluation pilots rated the ARI systems 2.0 points higher than the unmodified control system using the Cooper-Harper rating scale.

7. Of the two ARI configurations tested, control system C generally resulted in better pilot performance than control system B.

Langley Research Center
National Aeronautics and Space Administration
Hampton, VA 23665
May 15, 1980

APPENDIX A

Equations of Motion

The equations used to describe the motions of the airplane were nonlinear, six-degree-of-freedom, rigid-body equations referenced to a body-fixed axis system and are given as follows:

Forces

$$\dot{u} = rv - qw - g\sin\theta + \frac{\bar{q}S}{m} C_{X,t} + \frac{T}{m}$$

$$\dot{v} = pw - ru + g\cos\theta \sin\phi + \frac{\bar{q}S}{m} C_{Y,t}$$

$$\dot{w} = qu - pv + g\cos\theta \cos\phi + \frac{\bar{q}S}{m} C_{Z,t}$$

Moments:

$$\dot{p} = \frac{I_Y - I_Z}{I_X} qr + \frac{I_{XZ}}{I_X} (r + pq) + \frac{\bar{q}Sb}{I_X} C_{\ell,t}$$

$$\dot{q} = \frac{I_Z - I_X}{I_Y} pr + \frac{I_{XZ}}{I_Y} (r^2 - p^2) + \frac{\bar{q}S\bar{c}}{I_Y} C_{m,t}$$

$$\dot{r} = \frac{I_X - I_Y}{I_Z} pq + \frac{I_{XZ}}{I_Z} (\dot{p} - qr) + \frac{\bar{q}Sb}{I_Z} C_{n,t}$$

Euler angles were computed by using quarternions to allow continuity of attitude motions. Auxiliary equations included:

$$\alpha = \tan^{-1} \left(\frac{w}{u}\right)$$

$$\beta = \sin^{-1} \left(\frac{v}{V}\right)$$

$$V = \sqrt{u^2 + v^2 + w^2}$$

$$a_n = \frac{qu - pv + g\cos\theta\cos\phi - \dot{w}}{g}$$

$$a_y = \frac{-pw + ru - g\cos\theta\sin\phi + \dot{v}}{g}$$

Aerodynamics

The aerodynamic data used in the simulation were derived from static and dynamic (forced oscillation) wind tunnel tests of subscale models of the F-14 in the landing configuration. The data extended over an angle-of-attack range of -5^{o} to 30^{o} and was input to the computer program in tabulated form as a function of angle-of-attack. Aerodynamic derivatives which were a function of roll rate and yaw rate were derived from tests performed at NASA Langley Research Center facilities. All other aerodynamic data were taken from references 3 and 4 which describe earlier F-14 simulation studies in the landing configuration.

APPENDIX B

Engine Model and Automatic Throttle

The engine thrust response was simulated by the following second-order model, taken from reference 3:

$$\frac{T}{T_c} = \frac{\omega_e^2}{s^2 + 2\zeta_e\omega_e s + \omega_e^2}$$

Where:

	ω_e, rad/sec	ζ_e
Increasing thrust	3.464	1.617
Decreasing thrust	3.000	1.817

The relationship of T_c to PLA was determined by the following equation:

T_c (both engines) =-32439 + 1908 x PLA (deg)

Where: Maximum PLA limit = 60^0

Minimum PLA limit = 20^0

The F-14 automatic throttle system is designed to maintain angle-of-attack at the desired final approach value automatically. The autothrottle control law was modeled in the simulator and is shown in figure 38.

APPENDIX C

PILOT RATINGS AND DETAILED SUPPLEMENTAL COMMENTARY

Background

Description of the pilot's function is shown below in a sketch which illustrates a simplified control system block diagram and expanded pilot transfer function block. These provide a context for pilot comments which supplement the numerical pilot ratings given on the Cooper-Harper handling qualities rating scale, Fig. 31(a).

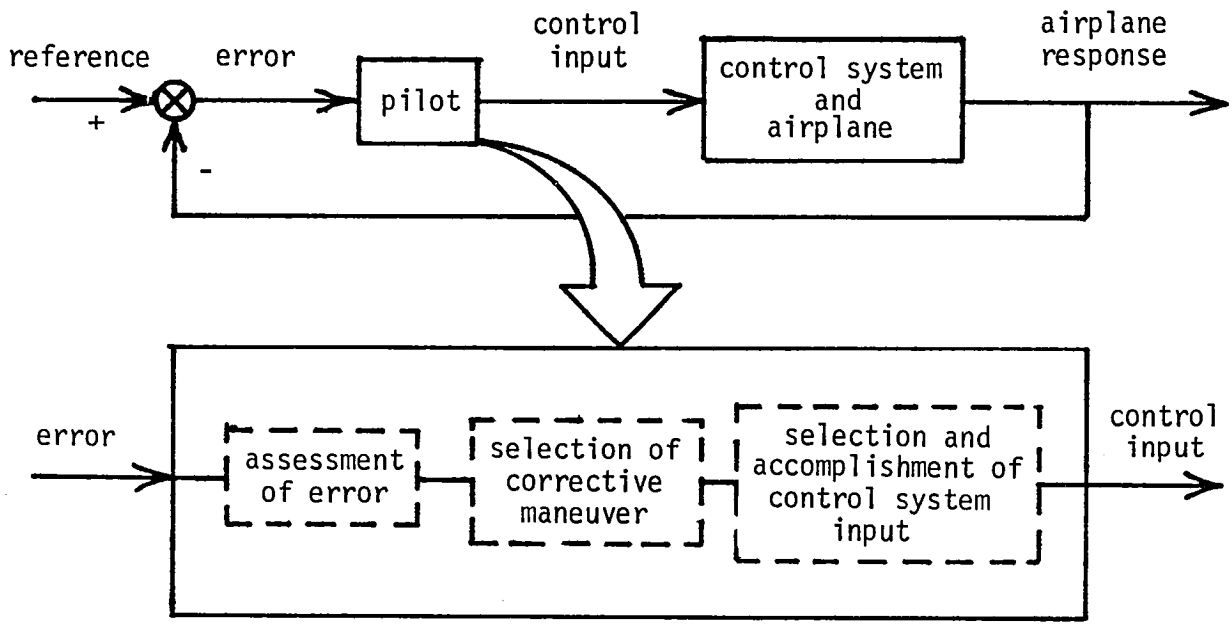

Pilot ratings are formed as a consequence of performing the three subtasks within the expanded pilot transfer function block. A description of each task is necessary for an understanding of their role in supplementing the numerical pilot ratings.

Description of Pilot Subtasks

In performing the subtasks, the pilot must continually be aware of airplane flightpath which encompasses both track and glideslope information. The characteristics of the flight control systems evaluated, however, affect in a more direct manner the pilot's awareness of track than his awareness of glideslope. The unfavorable effect on glideslope awareness is more the result of the heavy pilot workload required to solve the track problem. Therefore, in the following subtask description, track awareness is emphasized.

Assessment of error. This subtask involves both perception and prediction processes. The pilot must perceive error accelerations, rates and attitudes. Accurate perception leads to an awareness of airplane track which is vital to the task. The airplane's Dutch roll and adverse/proverse yaw characteristics strongly influence the pilot's perception capability. Oscillatory motions reduce the pilot's ability to see error amplitudes and inhibit his sensing of airplane track. Uncoordinated flight typified by adverse or proverse yaw also strongly inhibits his sensing of track and excites the Dutch roll.

The prediction process could be called "motion predictability". This parameter is a measure of the pilot's ability to estimate the initial and long term effects of airplane accelerations and hence, future rates, attitudes and flightpaths. Airplane Dutch roll and adverse/proverse yaw characteristics have a strong effect on this type of predictability.

Selection of corrective maneuvers. Given a set of error conditions, an airplane with good handling qualities, and a certain speed of closure with the carrier, the pilot has a good concept of what maneuver to use for an expeditious return to the centerline and glideslope. The actual maneuver he selects, however, may be somewhat different from this ideal because of his knowledge that airplane handling qualities deficiencies demand an unacceptably high or unattainable level of pilot compensation.

Selection and accomplishment of control system input. The pilot selects and makes control system inputs in order to fly as closely as possible the selected corrective maneuver. In order to do this the pilot desires a high degree of airplane "control input-airplane response predictability"; this parameter is a measure of the pilot's ability to estimate the initial effects of control system force and/or displacement inputs on airplane accelerations and rates. Flight control system stick breakout forces, damping, force/displacement gradients and gearing are the variables which strongly influence this type of predictability.

Predictability

"Predictability" is an overall measure not specifically shown in the pilot transfer function, which incorporates both motion and control input - airplane response predictability; it is approximately inversely proportional to the amount of pilot attention required to fly the selected corrected maneuver; it is sensed by the pilot and can sometimes be measured by the amount of time required to establish a flightpath correction. Both control input-airplane response and motion predictability inform the pilot on initial effects of pilot loop closure. Motion predictability encompasses the longer term or future result.

The pilot desires a high rather than low level of predictability because the pilot is then required to do less monitoring of airplane response to his loop closure; he more easily achieves the corrections he desires and hence his work load is lessened.

For the carrier landing task, the ideal corrective maneuvers are small and frequently made. Low predictability is incompatible with such maneuvering because the pilot cannot make expeditious short term corrections with certainty. He has to lower his gains, allowing enough time to elapse after an input to be sure of the input's corrective effect. This is an example of ideal maneuver modification in the maneuver selection process.

Pilot Ratings and Comments

Table II presents pilot ratings and comments for all three simulated F-14 flight control systems for Pilot 1.

REFERENCES

1. Nguyen, Luat T.; Ogburn, Marilyn E.; Pollock, Kenneth S.; Deal, Perry L.; Brown, Philip W.; and Whipple, Raymond D.: Piloted Simulator Study of High-angle-of-attack Characteristics of F-14 Airplane with Maneuver Slats. NASA TM-80058, 1979.

2. Cooper, George E.; and Harper, Robert P.: The Use of Pilot Rating in the Evaluation of Aircraft Handling Qualities. NASA TN D-5153, 1969.

3. McNeill, Walter E.; Rebel, James M.; Agnew, William H.; and Fortenbaugh, Robert L.: A Simulator Analysis of the F-14A Airplane Automatic Carrier Landing System, 1975.

4. Fortenbaugh, Robert L.: A Simulator Comparison of an Integrated Direct-Lift-Control Automatic Carrier Landing System with a Conventional Automatic Carrier Landing System. Final Report. NADC-72210-VT, Naval Air Development Center, 1973.

TABLE I.- MASS AND DIMENSIONAL CHARACTERISTICS OF SIMULATED AIRPLANE

Weight, N (lb)	215,880	(48,531)
Moments of Inertia, Kg-m^2 (slug-ft^2)		
I_X	89,647	(66,120)
I_Y	360,215	(265,681)
I_Z	444,287	(327,689)
I_{XZ}	-3,440	(-2,537)
Wing Dimensions:		
Span, m (ft)	19.55	(64.13)
Area, m^2 (ft^2)	52.5	(565)
Mean aerodynamic chord, m (ft)	2.99	(9.80)
Center of gravity, percent of mean aerodynamic chord	13.4	

TABLE II.- PILOT 1 RATINGS AND COMMENTS FOR THREE SIMULATED F-14 CONTROL SYSTEMS

Flight Control System	Technique	Cooper Harper Pilot Rating	Pilot Subtasks			Predictability			Remarks
			Assessment of Error	Selection of Corrective Maneuver	Selection and Accomplishment of Control System Input	Motion	Control Input - Airplane Response	Overall	
A	Feet on floor	7	Very Poor	Difficult, due to poor error assessment.	Fair	Very Poor	Fair	Very Poor	Lateral PIO tendency due to airplane dynamics.
	Rudder as necessary	6	Poor	Slightly better than above.	Fair	Poor	Fair	Poor	Same lateral PIO tendency as above. Rudder usage improves lineup control but pilot compensation it requires detracts from attention available for glideslope control. Tendency toward lateral-directional and track oscillations in close. Therefore, must often open rudder loop.
B	Feet on floor, or, rudder as necessary	4	Good	Fair, affected by control input - airplane response predicta-bility.	Fair to Poor	Good	Fair to Poor	Good to Fair	Use of rudder seldom necessary. Lateral PIO tendency due to control input - airplane response predictability. Easy to make excessive amplitude inputs inadvertently. Best technique is making series of increasing force pulses, in order to overcome control breakout force and achieve correct amplitude and duration input.
C	Feet on floor	3	Excellent	Fair to good, affected by control input - airplane response predicta-bility.	Fair to Good	Very Good	Fair	Good	Use of rudder almost never necessary. Less lateral PIO tendency than flight control system B. Less overcontrolling tendency than flight control system B but still a limiting factor in pilot gain selection.

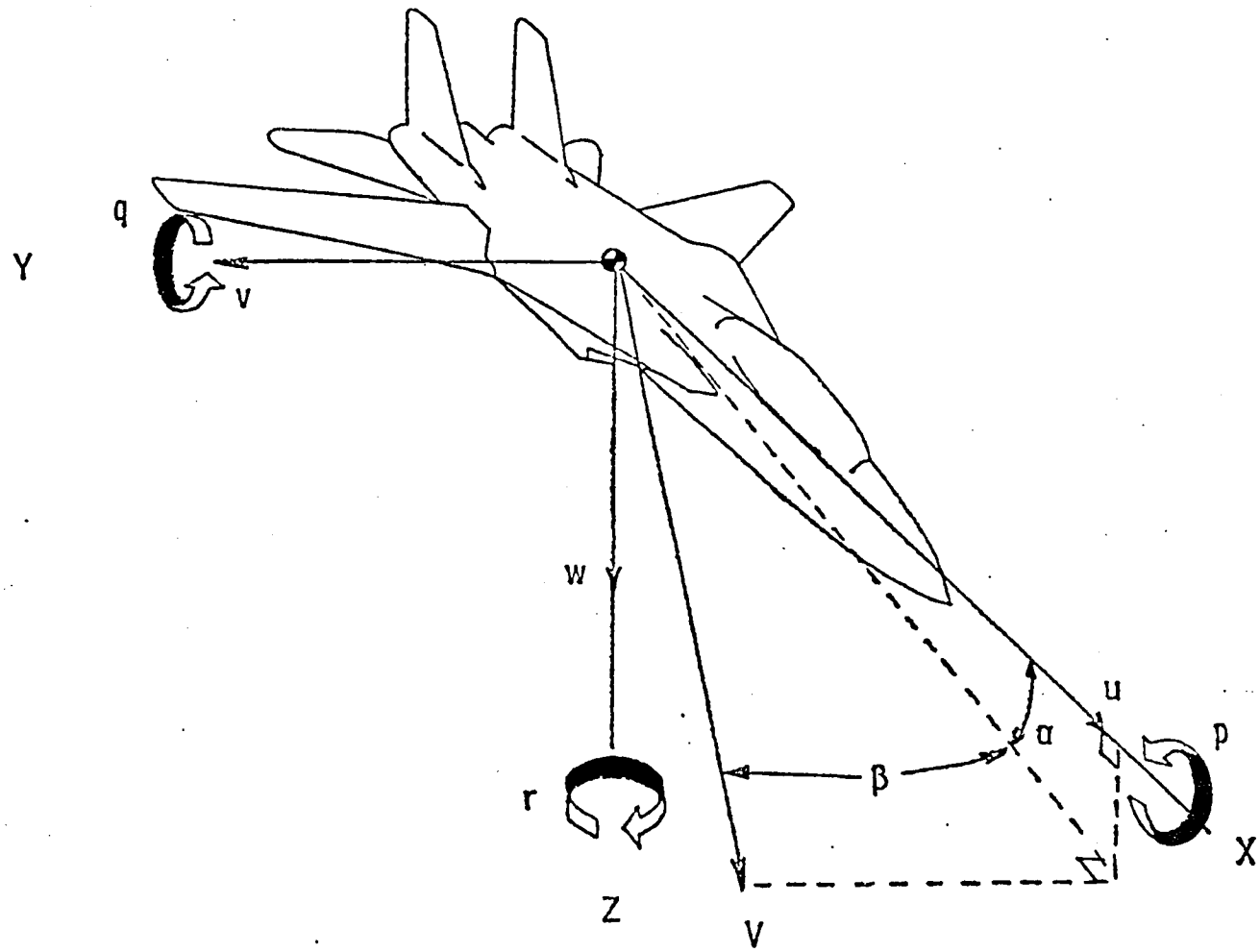

(a) The body system of axes.

Figure 1.- Axis system used in simulation and three-view drawing of airplane.

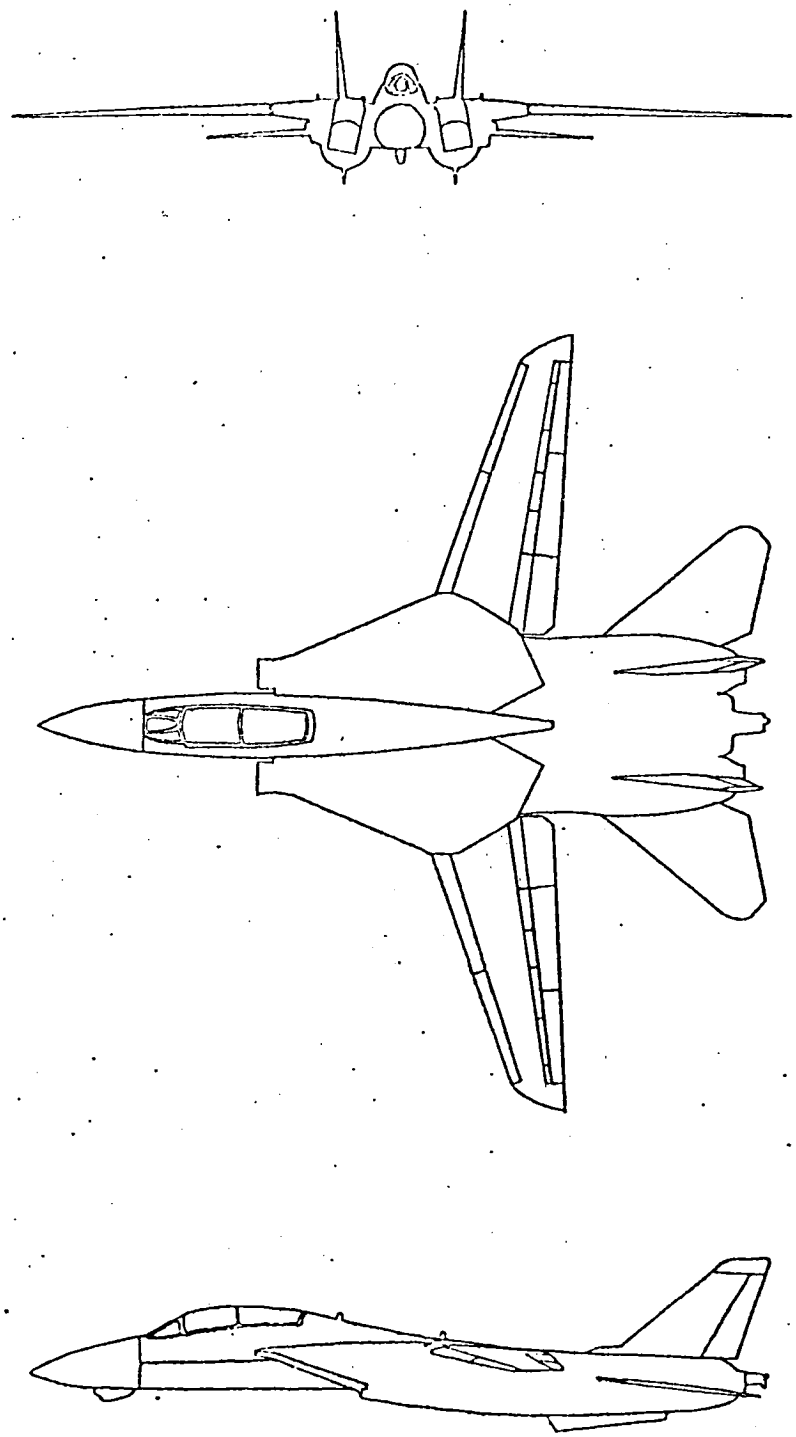

(b) Three-view drawing of F-14.

Figure 1.- Concluded.

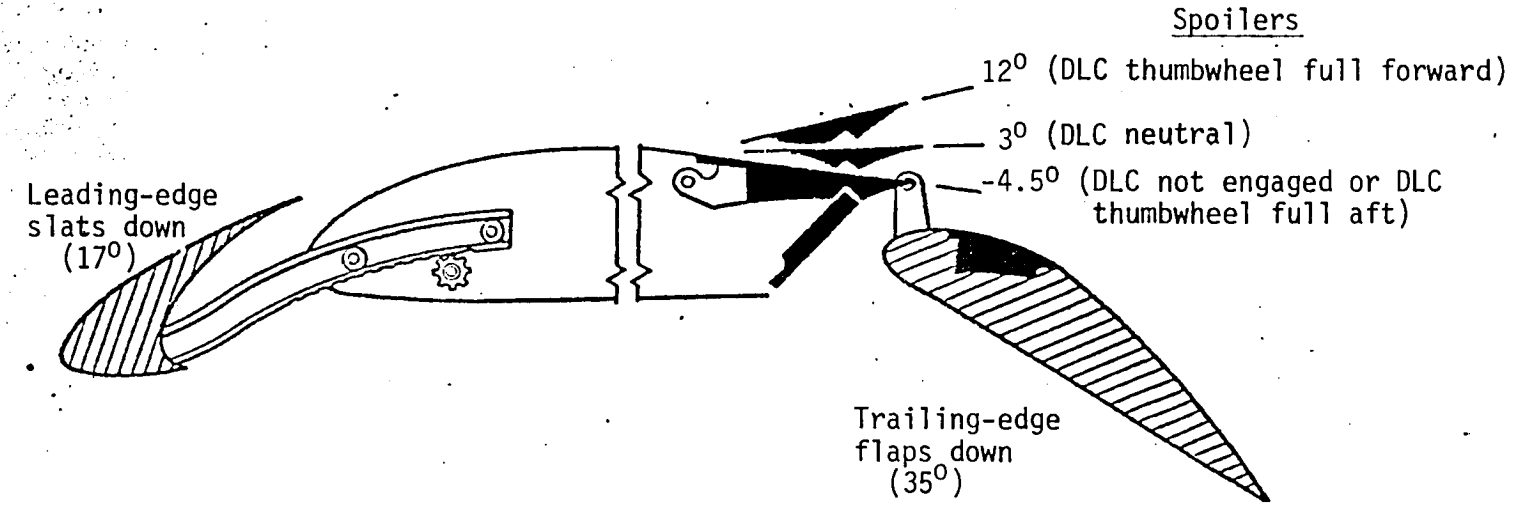

Figure 2.- Wing Control Surfaces.

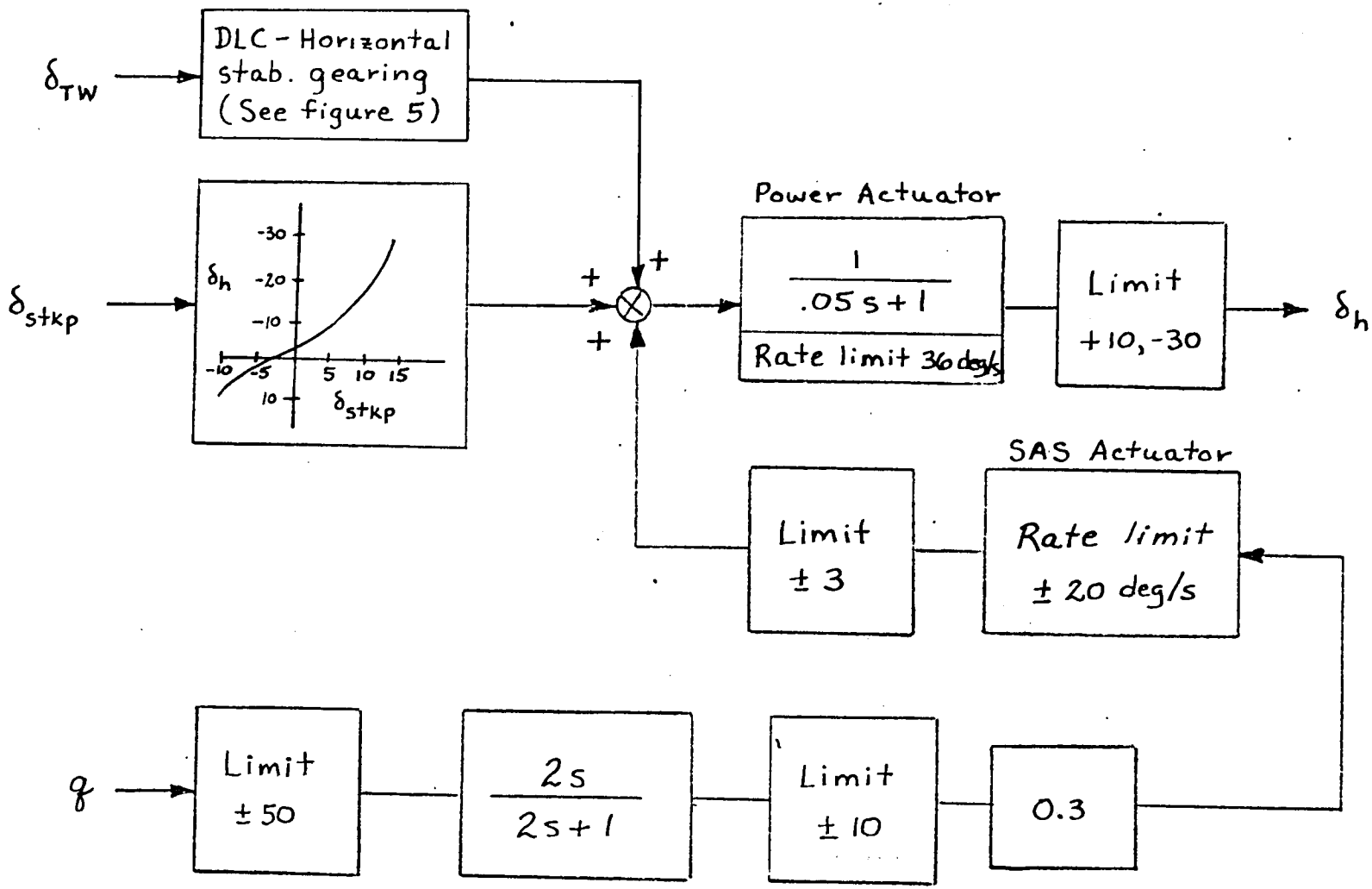

Figure 3.- Schematic of pitch channel - All control configurations.

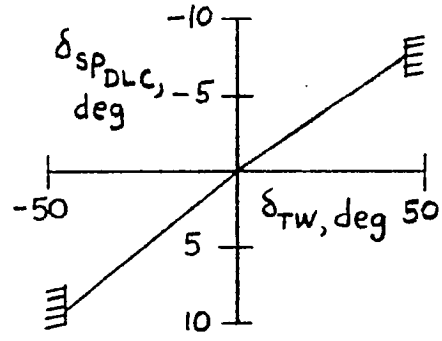

Figure 4.- Incremental spoiler command as function of DLC thumbwheel position.

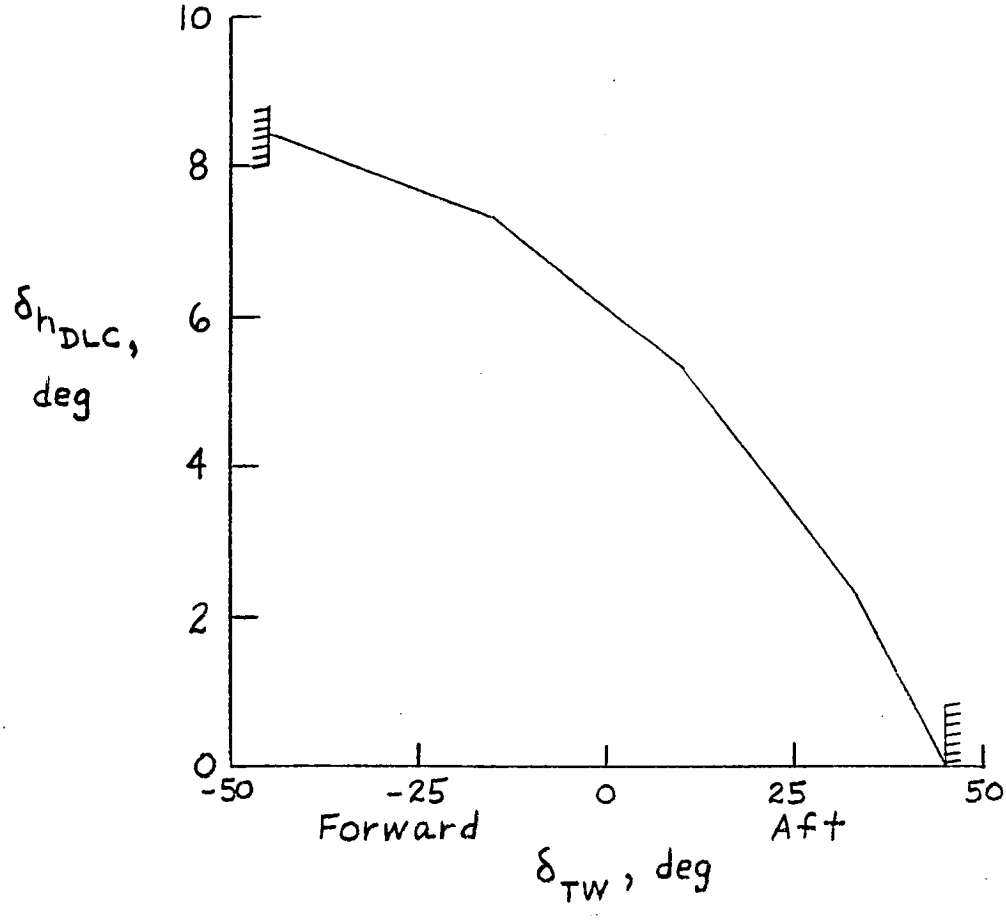

Figure 5.- Incremental horizontal stabilizer command as function of DLC thumbwheel position.

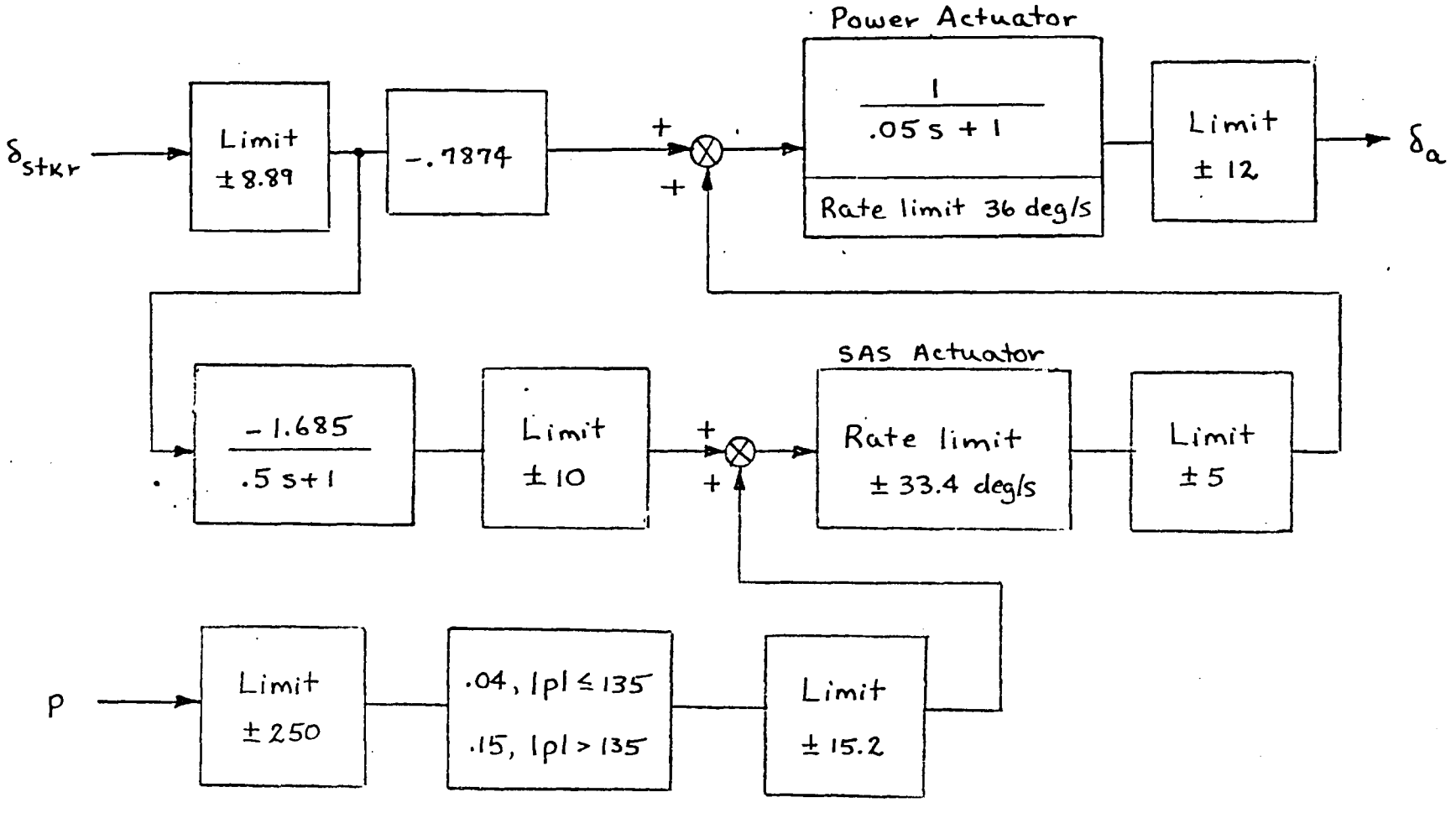

Figure 6.- Schematic of roll channel - Control system A.

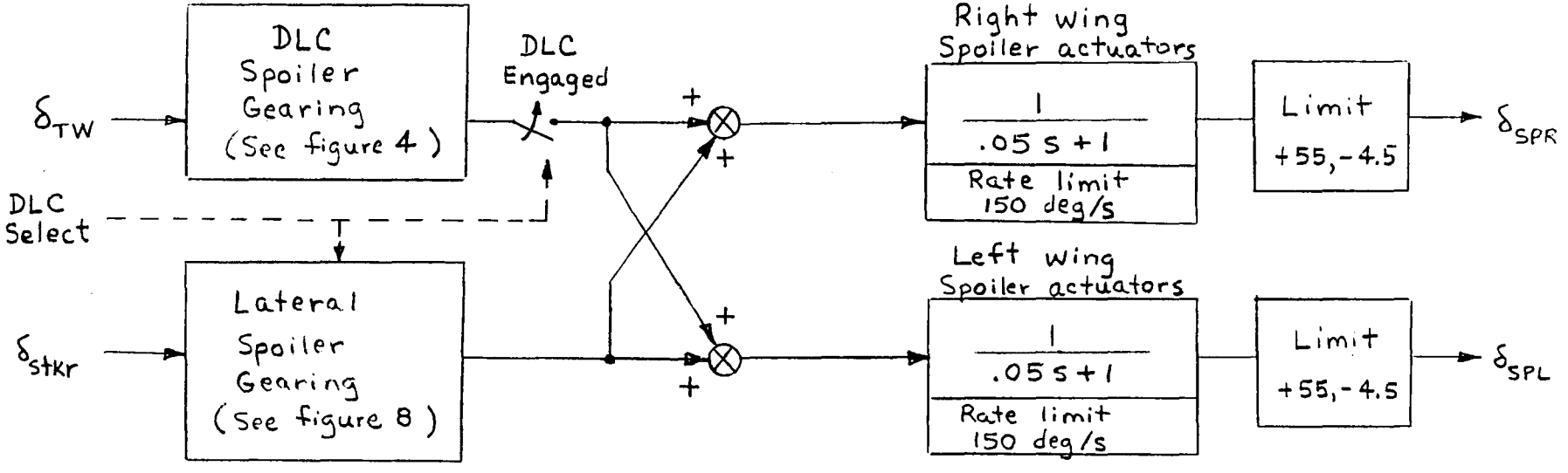

Figure 7.- Schematic of spoiler control system - All control configurations.

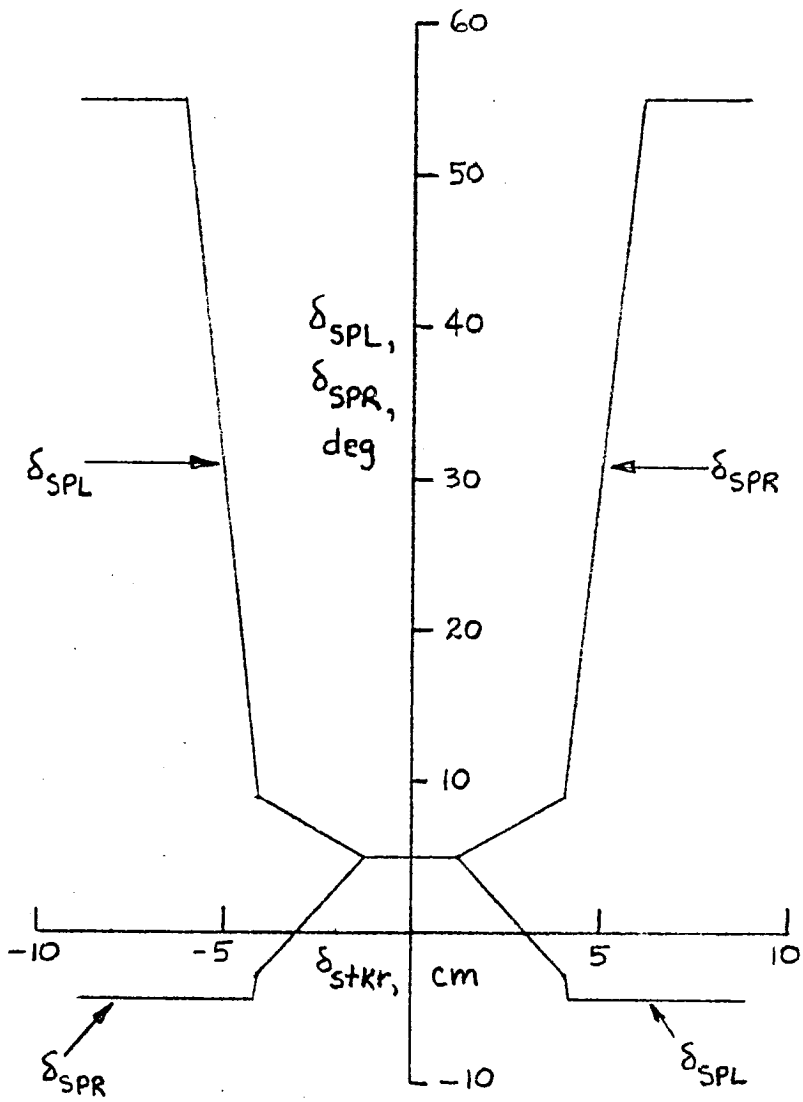

(a) DLC engaged.

Figure 8.- Spoiler deflections as a function of lateral stick input.

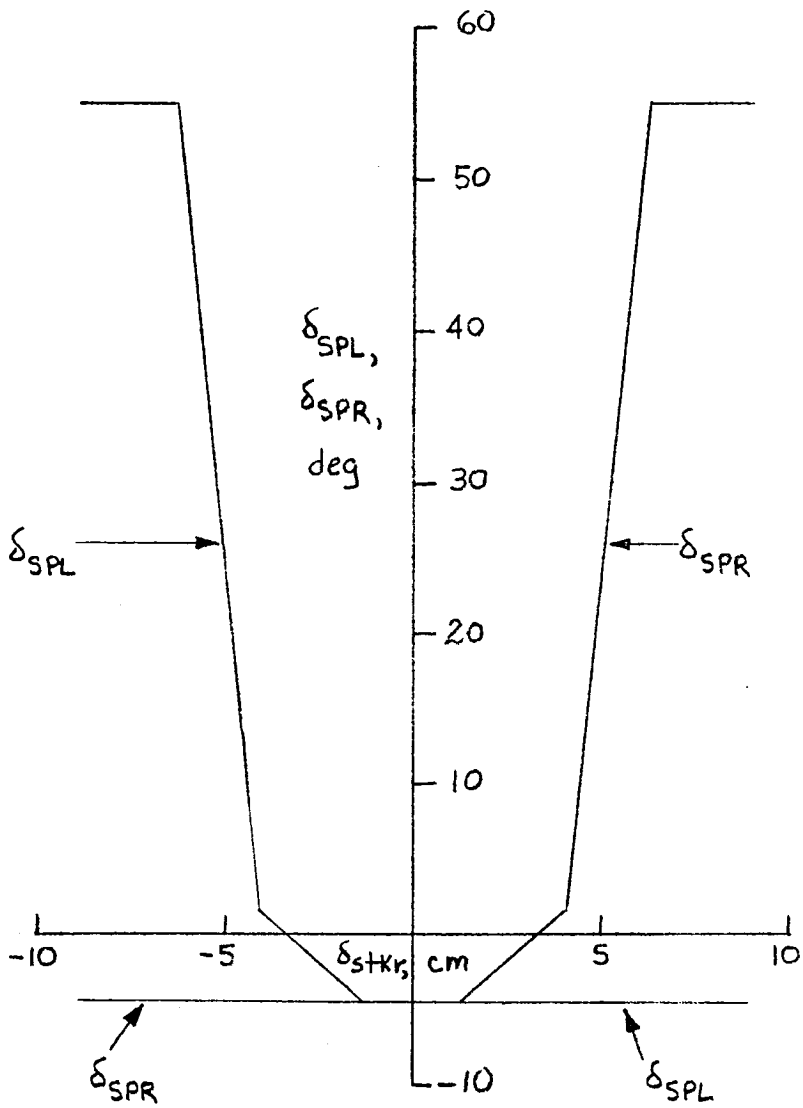

(b) DLC not engaged.

Figure 8.- Concluded.

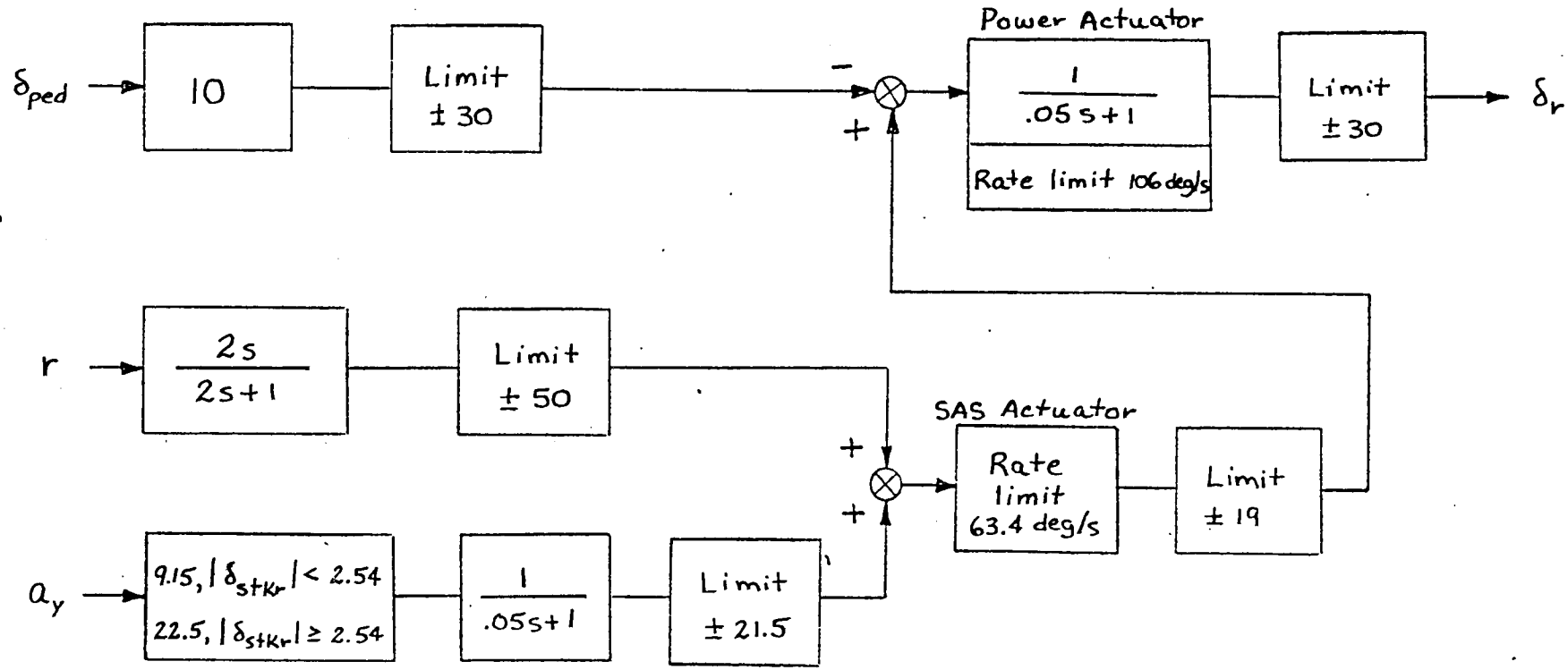

Figure 9.- Schematic of yaw channel - Control system A.

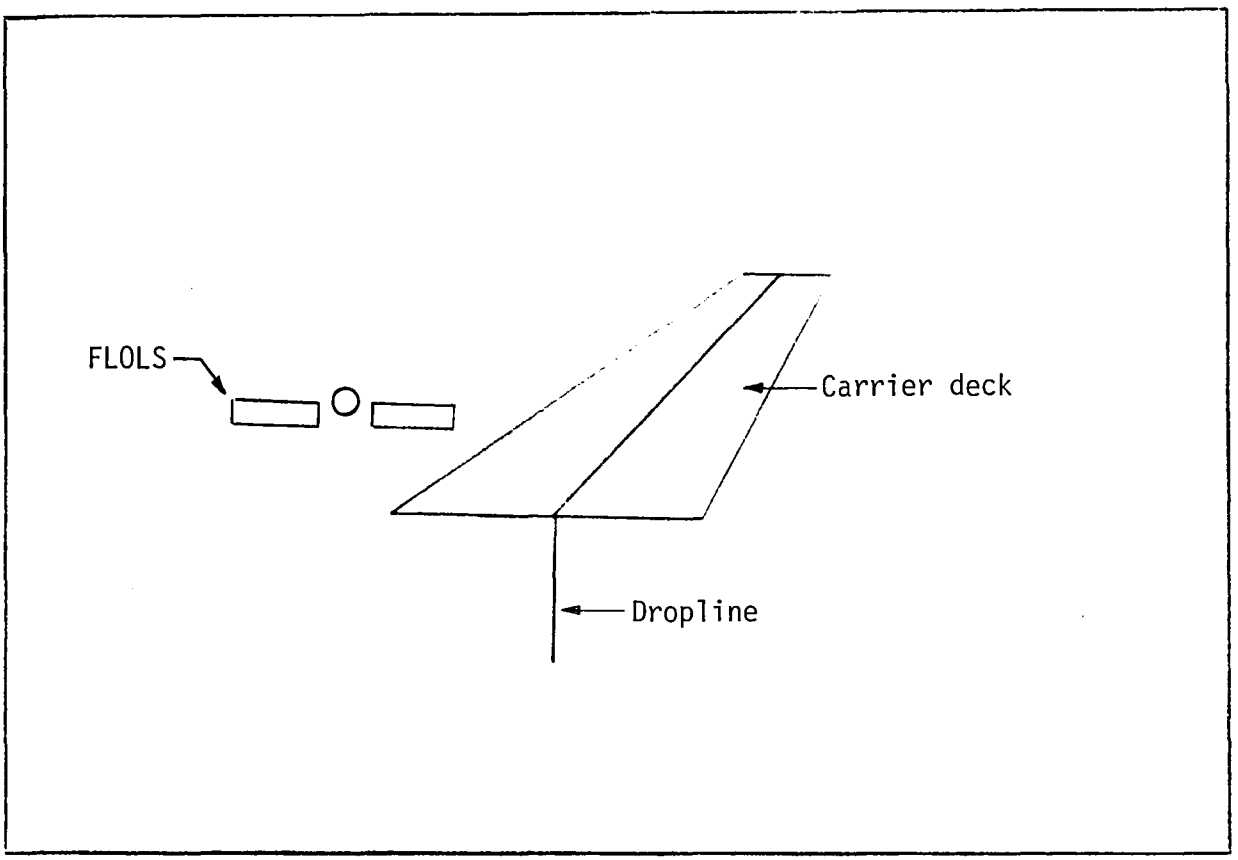

Figure 10.- Sketch of carrier landing visual display (shown for airplane slightly high and right of course).

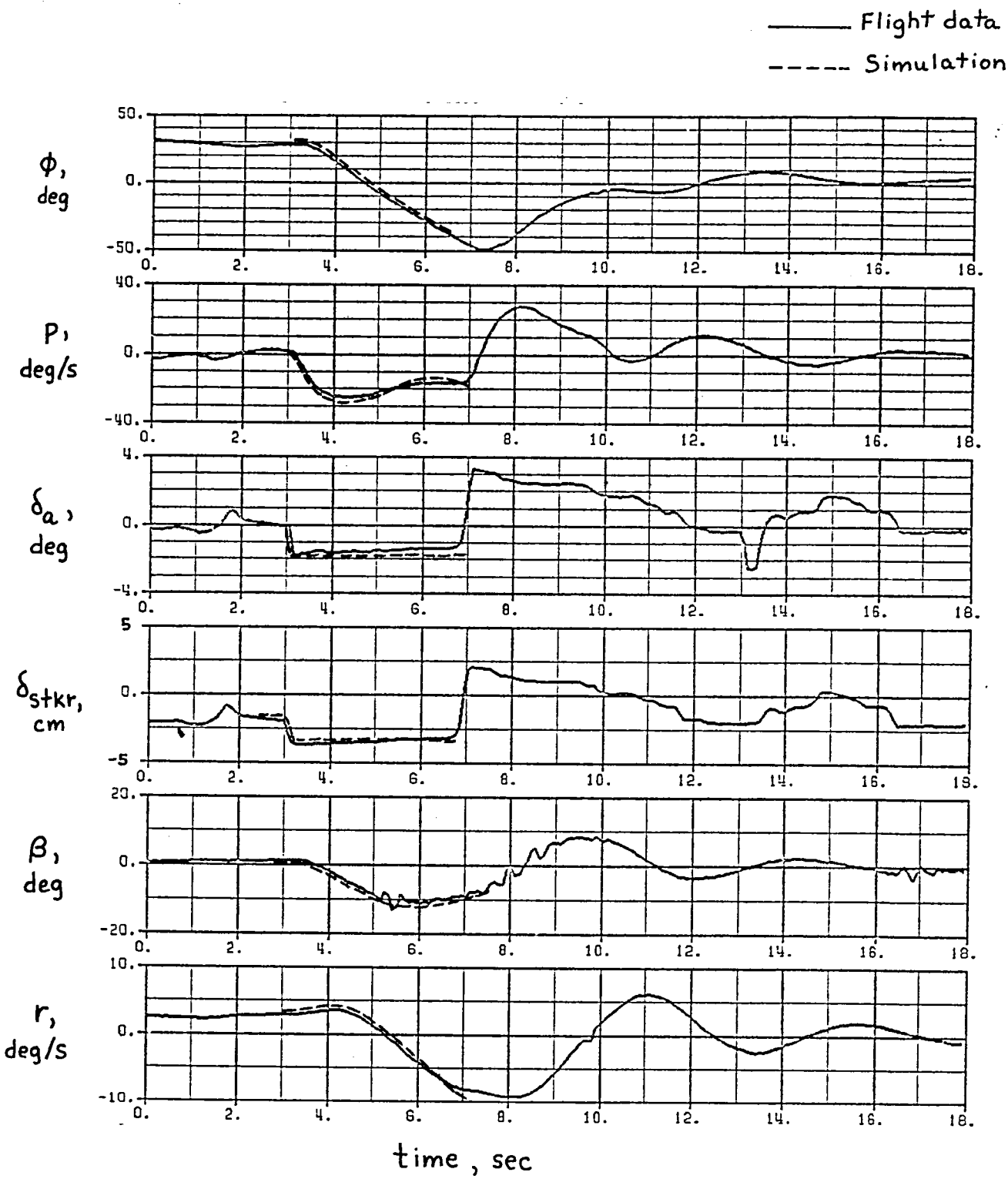

Figure 11.- Response of airplane to lateral stick input.

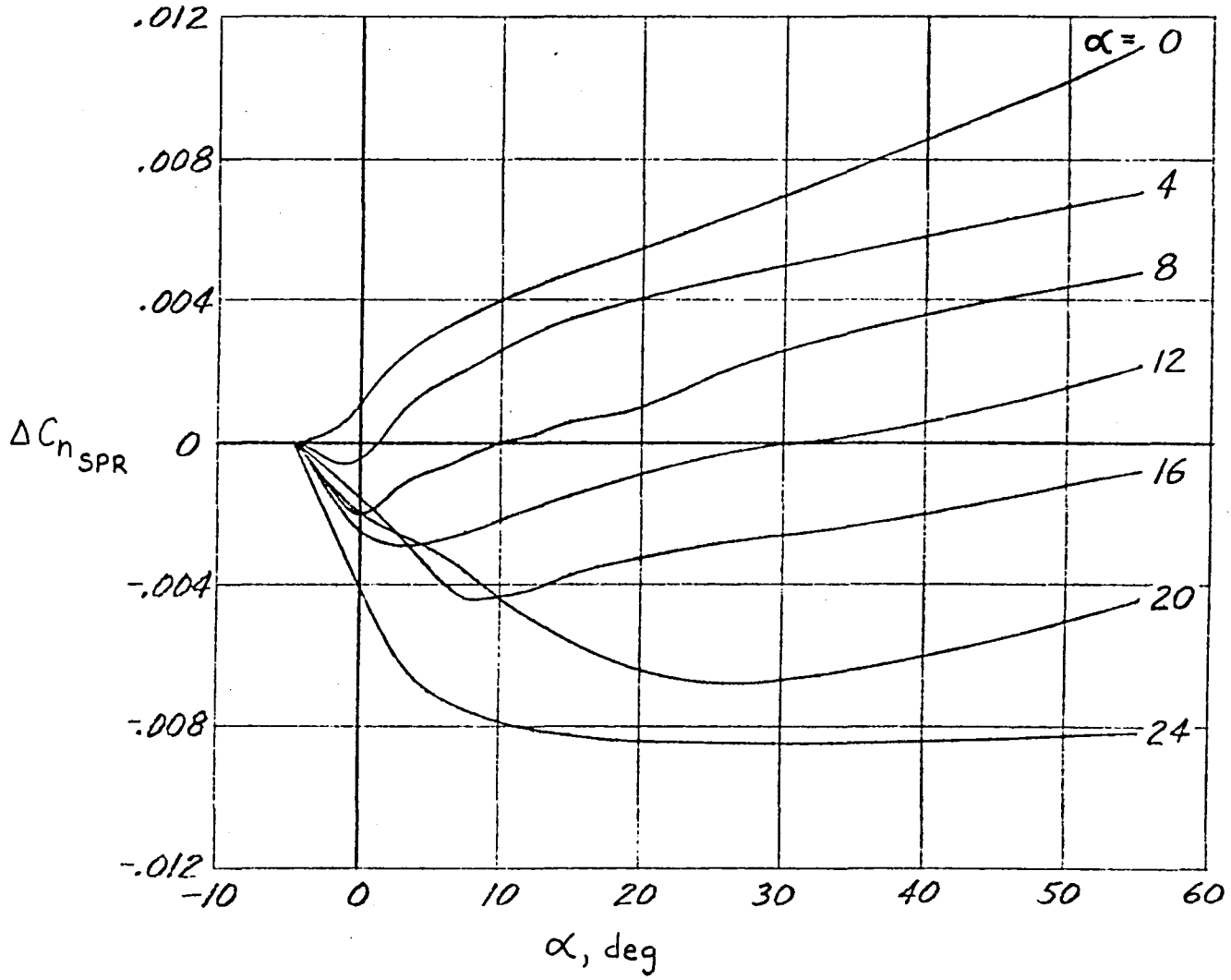

Figure 12.- Yawing moment due to spoiler deflection.

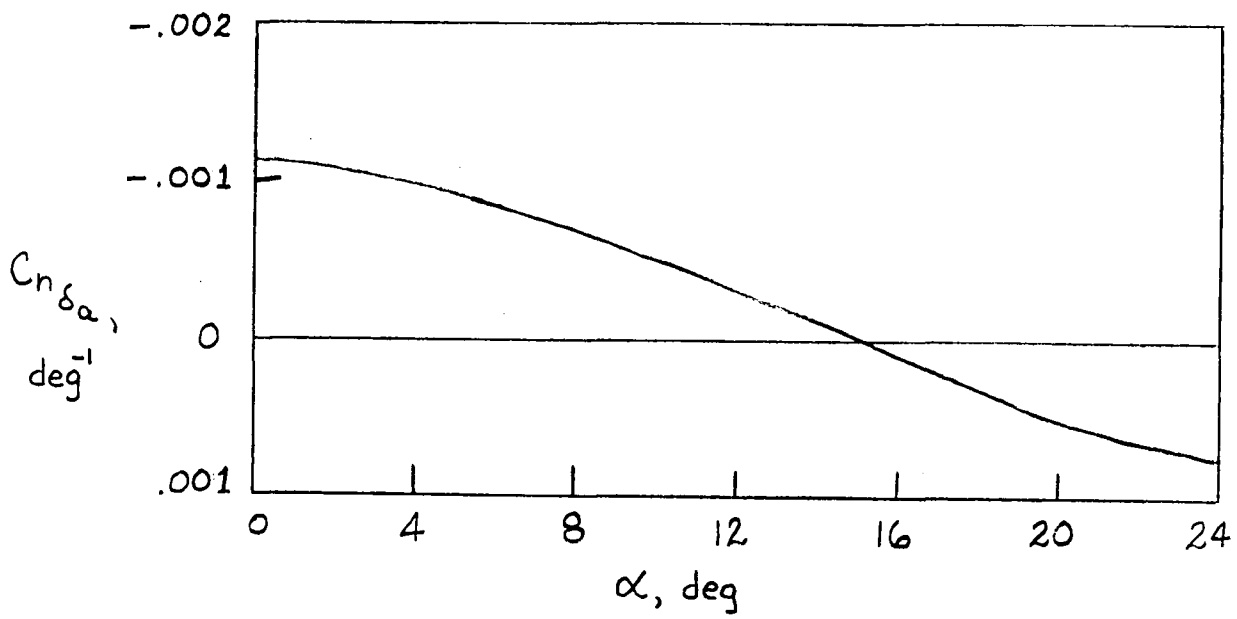

Figure 13.- Yawing moment due to horizontal stabilizer deflection.

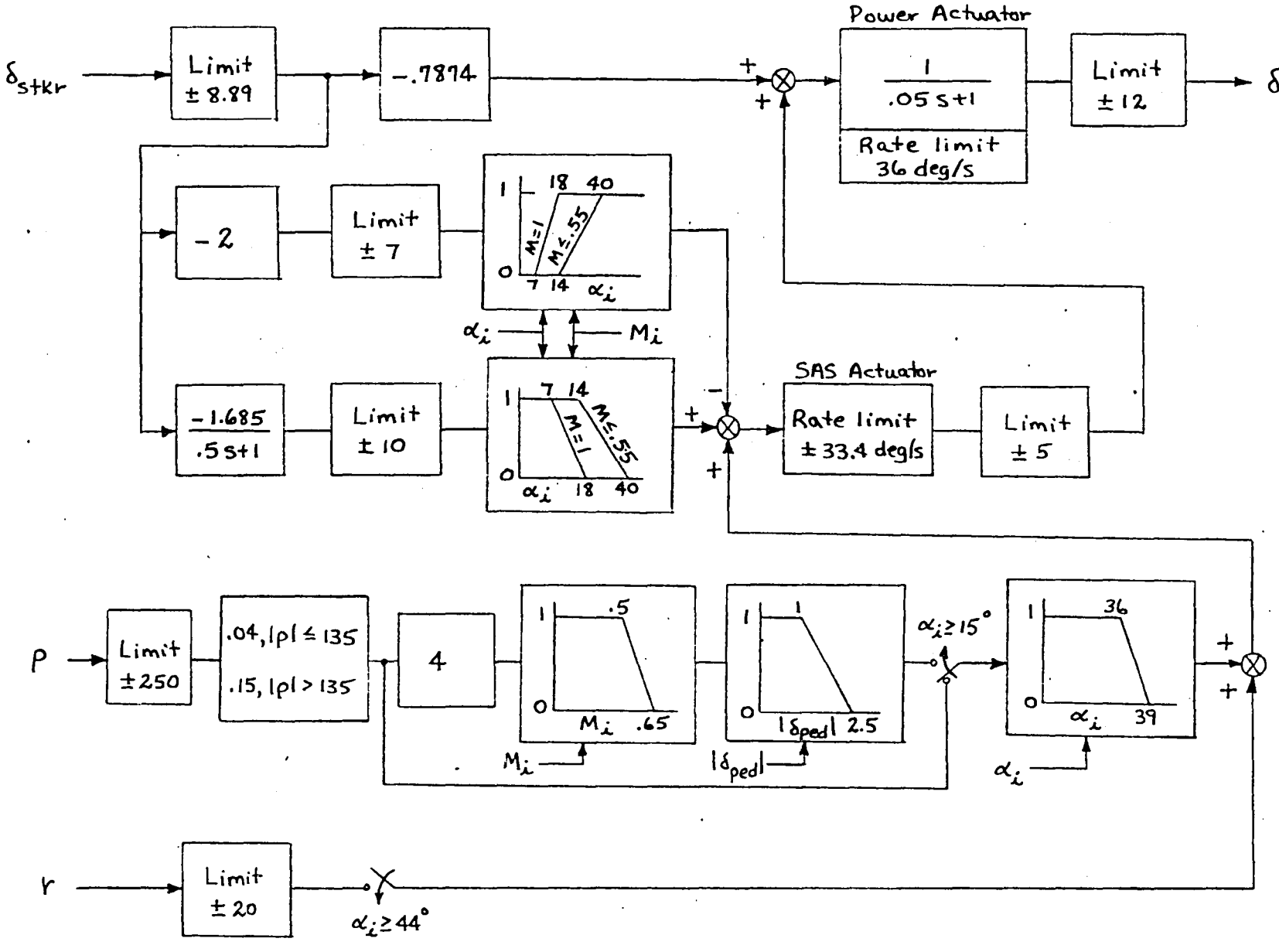

Figure 14.- Schematic of roll channel - High-α ARI system.

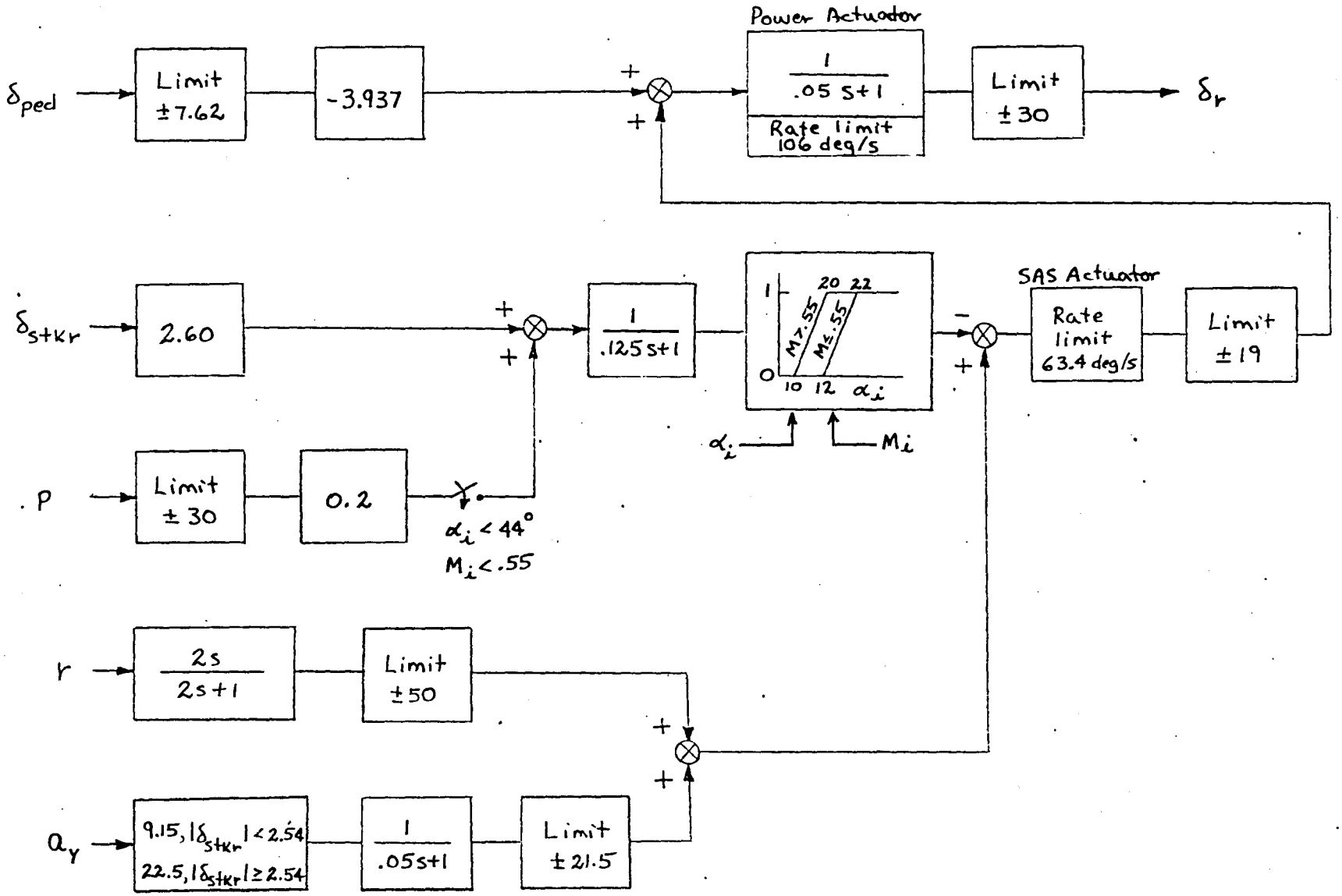

Figure 15.- Schematic of yaw channel - High-α ARI system.

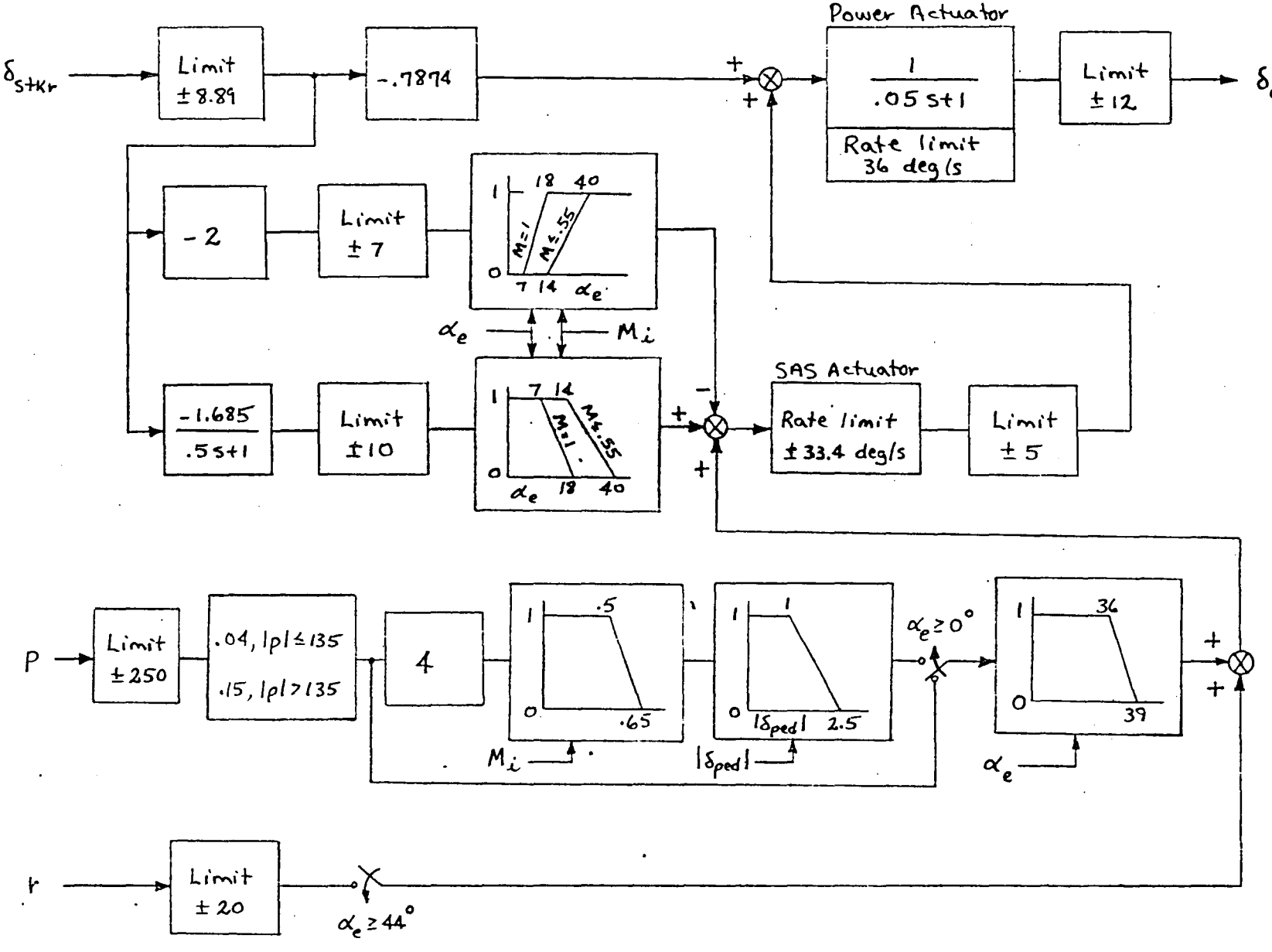

Figure 16.- Schematic of roll channel - Control system B.

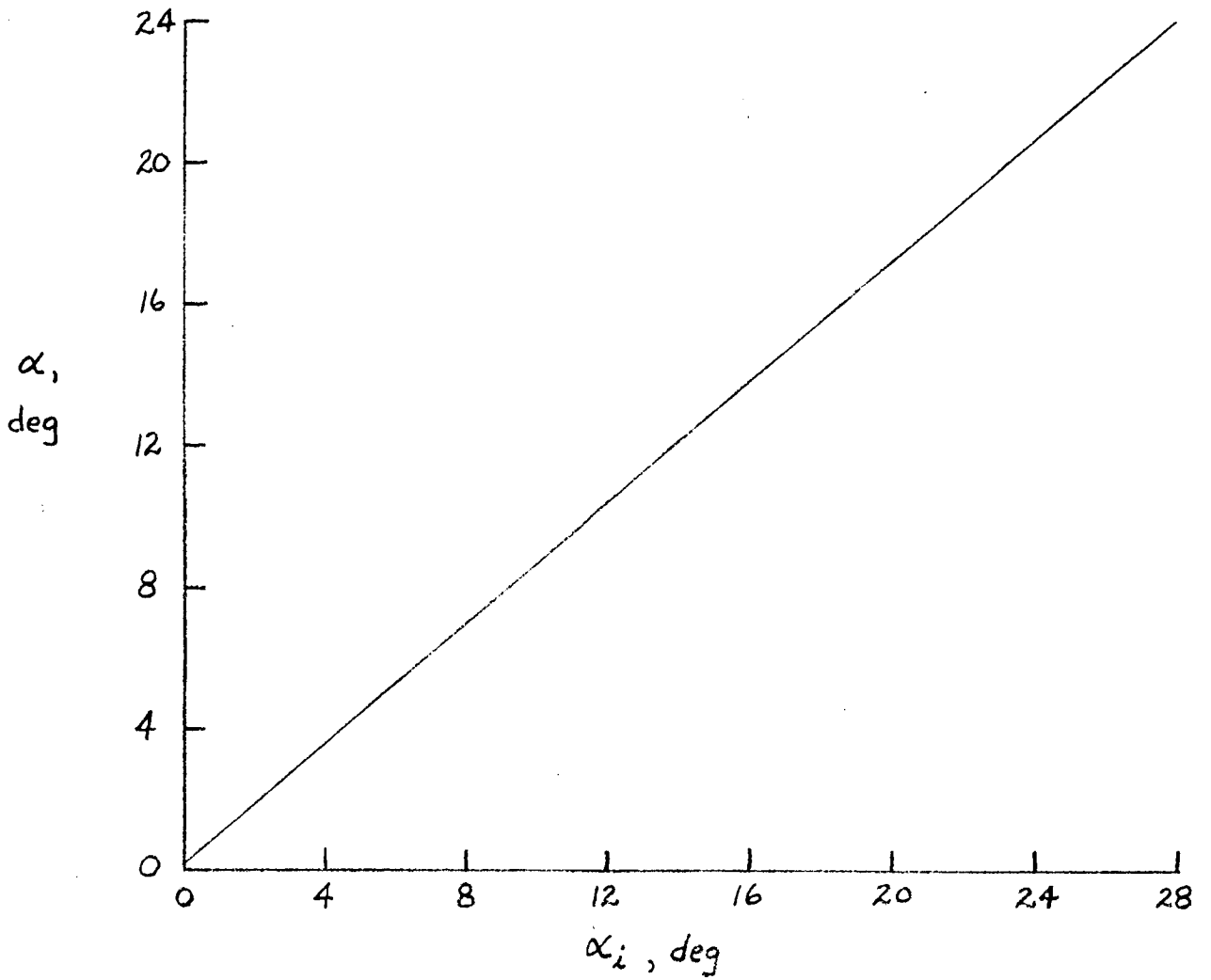

Figure 17.- Relationship of true angle-of-attack to indicated angle-of-attack.

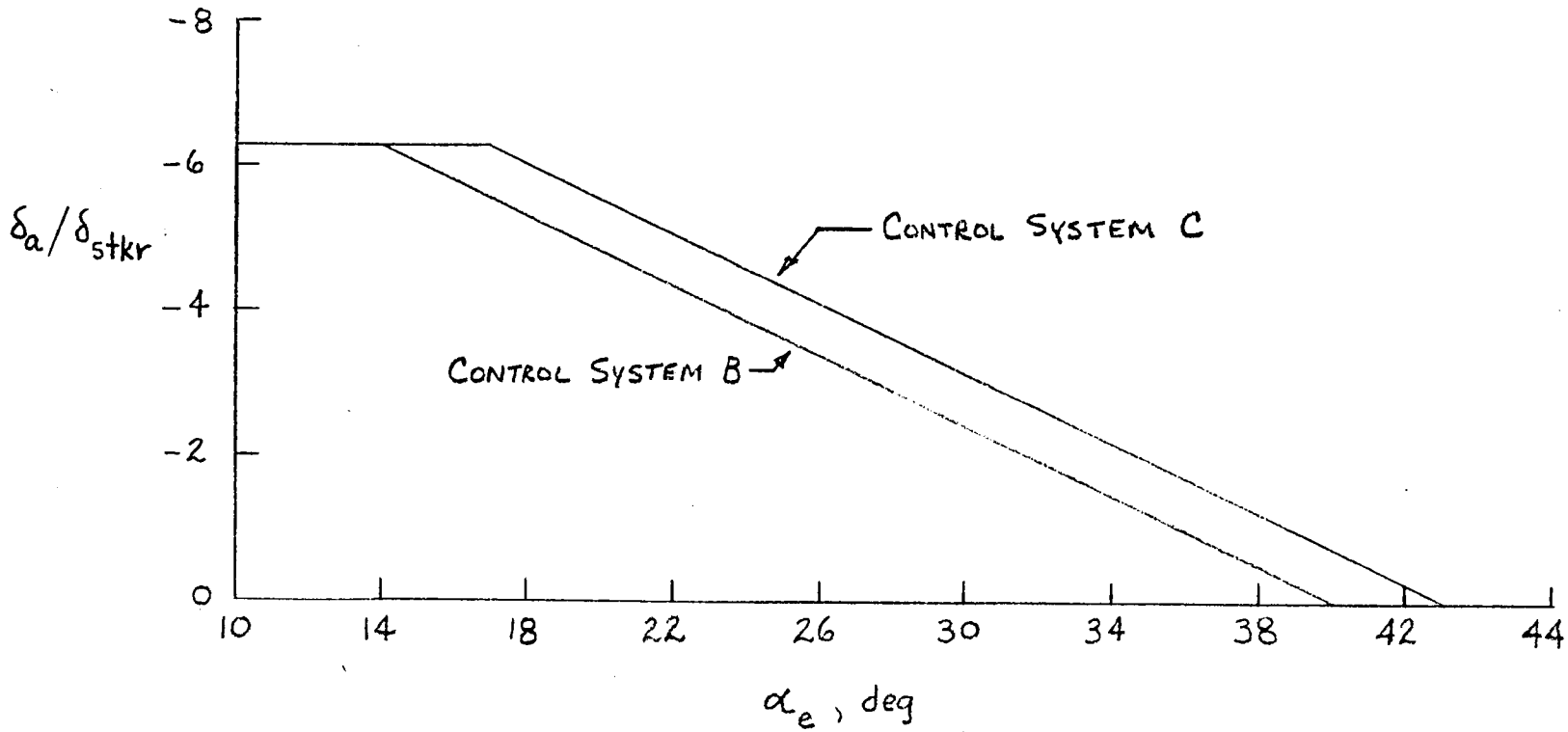

Figure 18.- Stick-to-differential-tail gain for Control systems B and C.

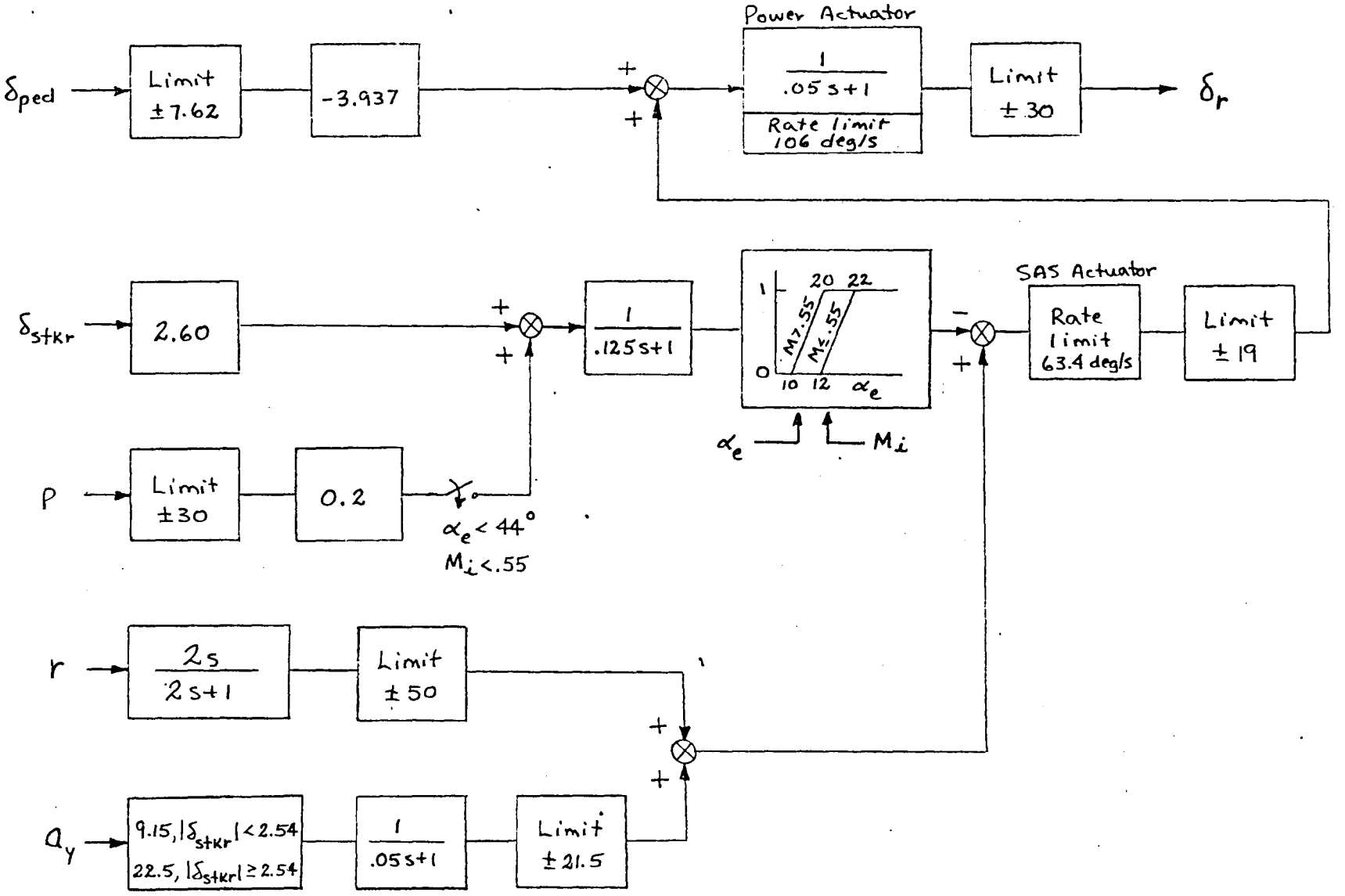

Figure 19.- Schematic of yaw channel - Control system B.

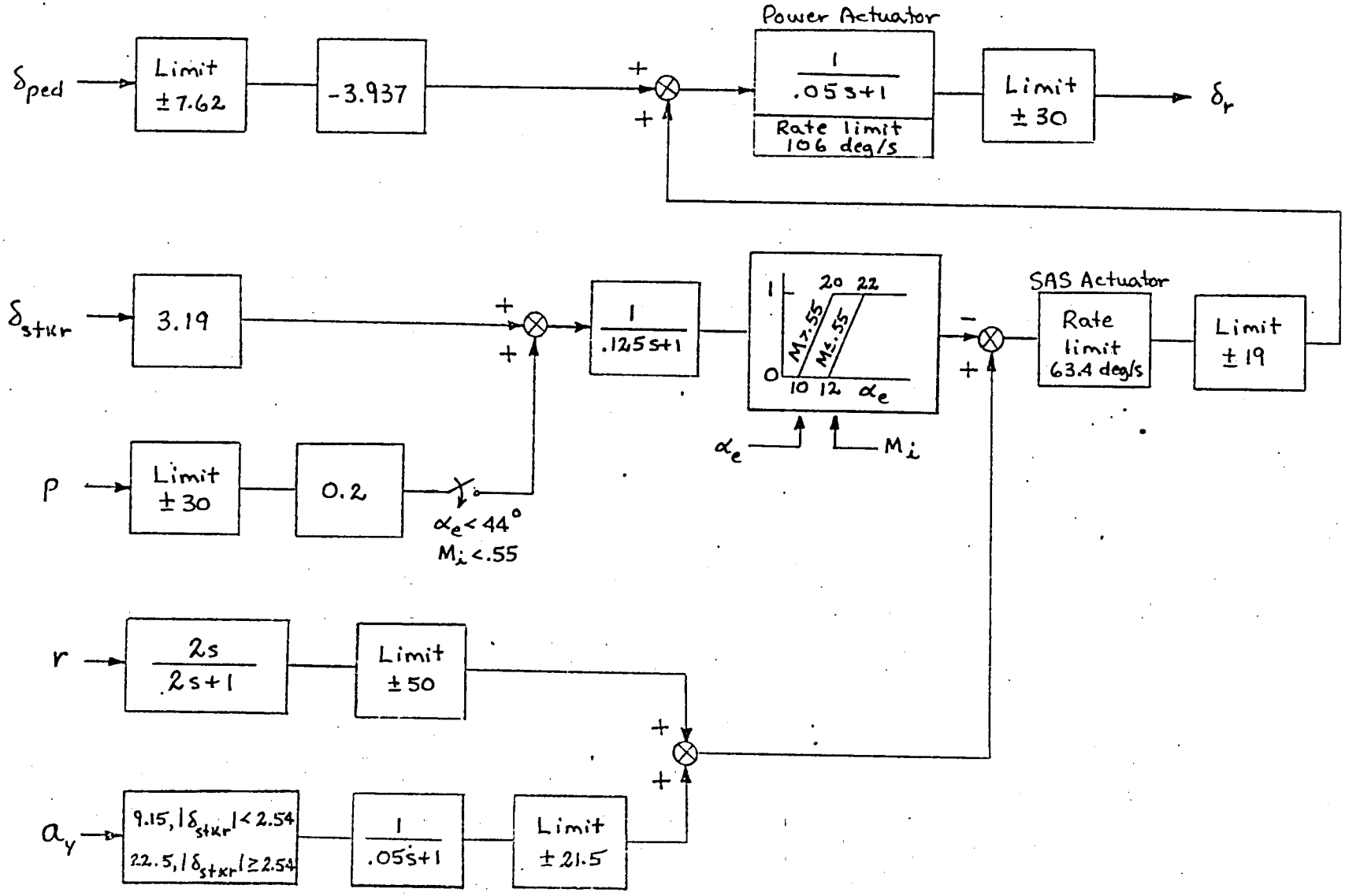

Figure 20.- Schematic of yaw channel - Control system C.

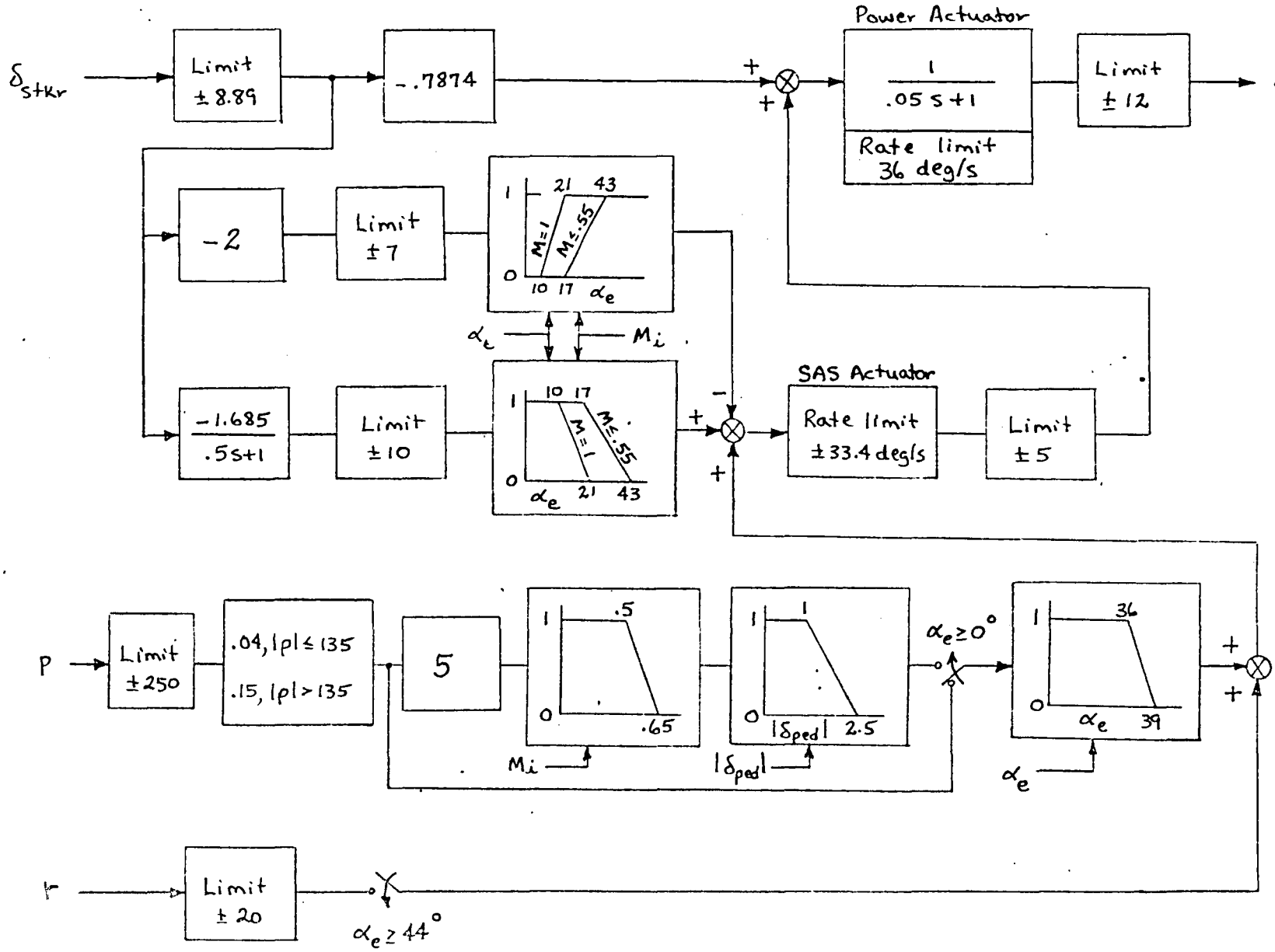

Figure 21.- Schematic of roll channel - Control system C.

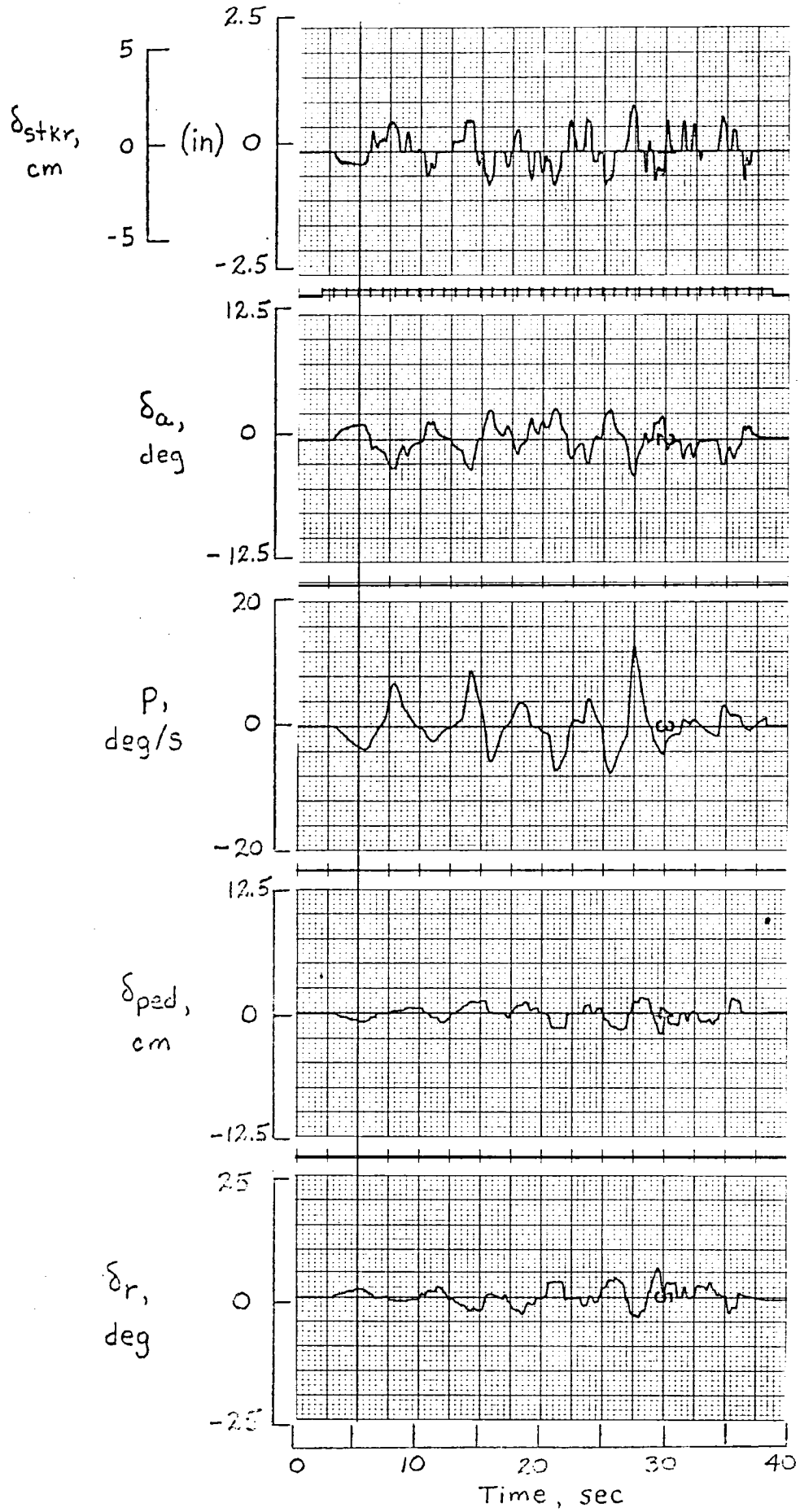

Figure 22.- Carrier approach - Pilot 1, control system A.

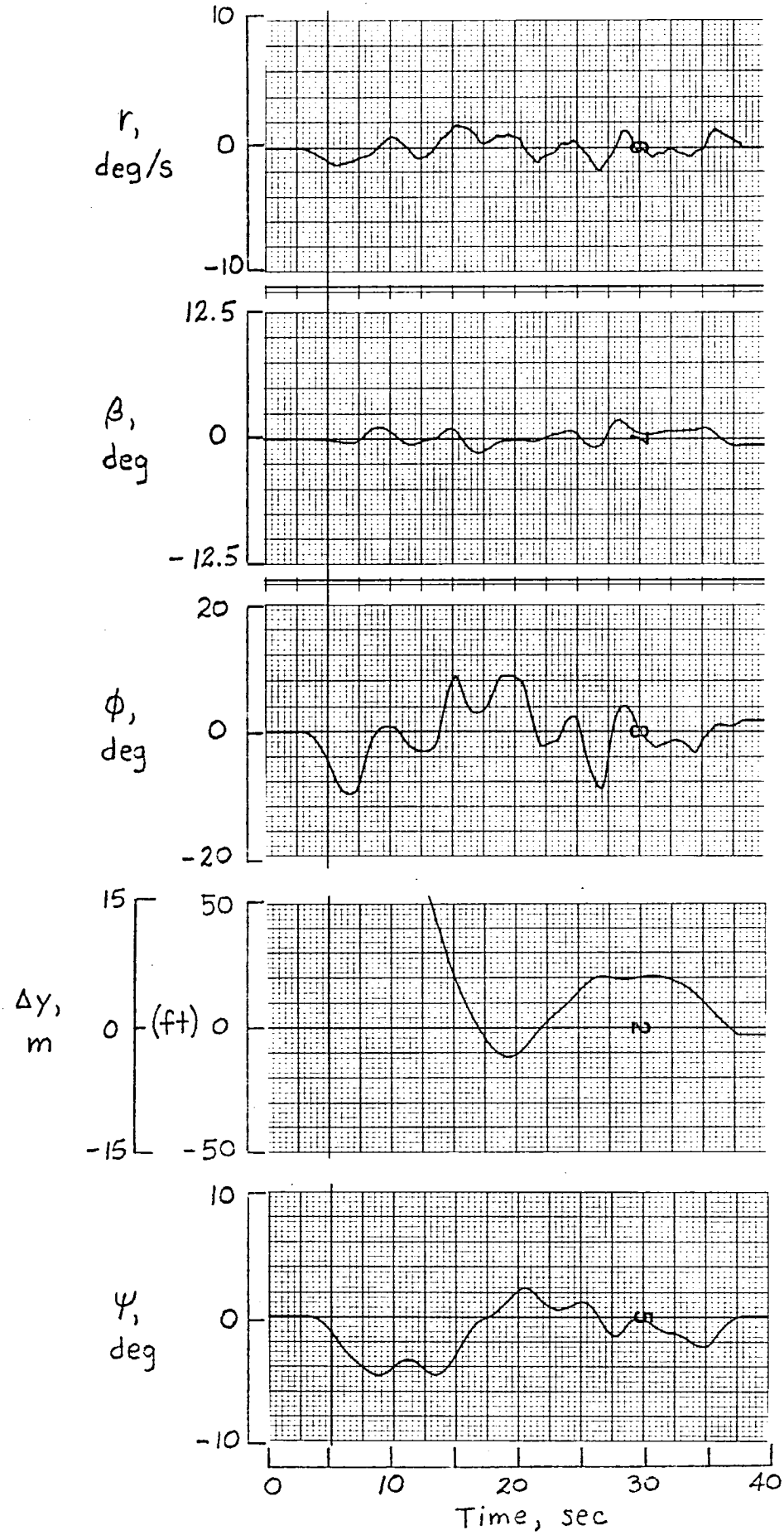

Figure 22.- Concluded.

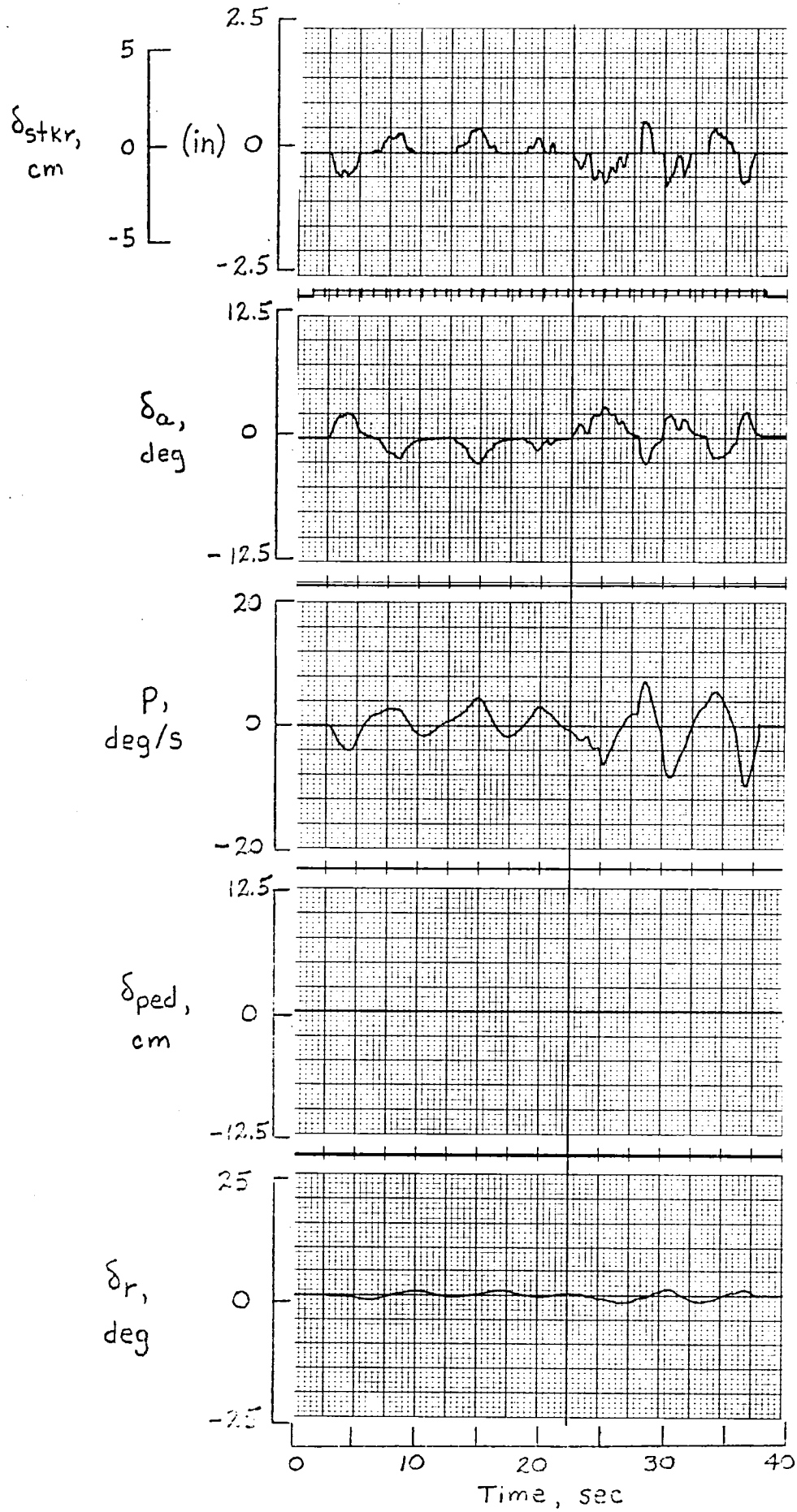

Figure 23.- Carrier approach - Pilot 2, control system A.

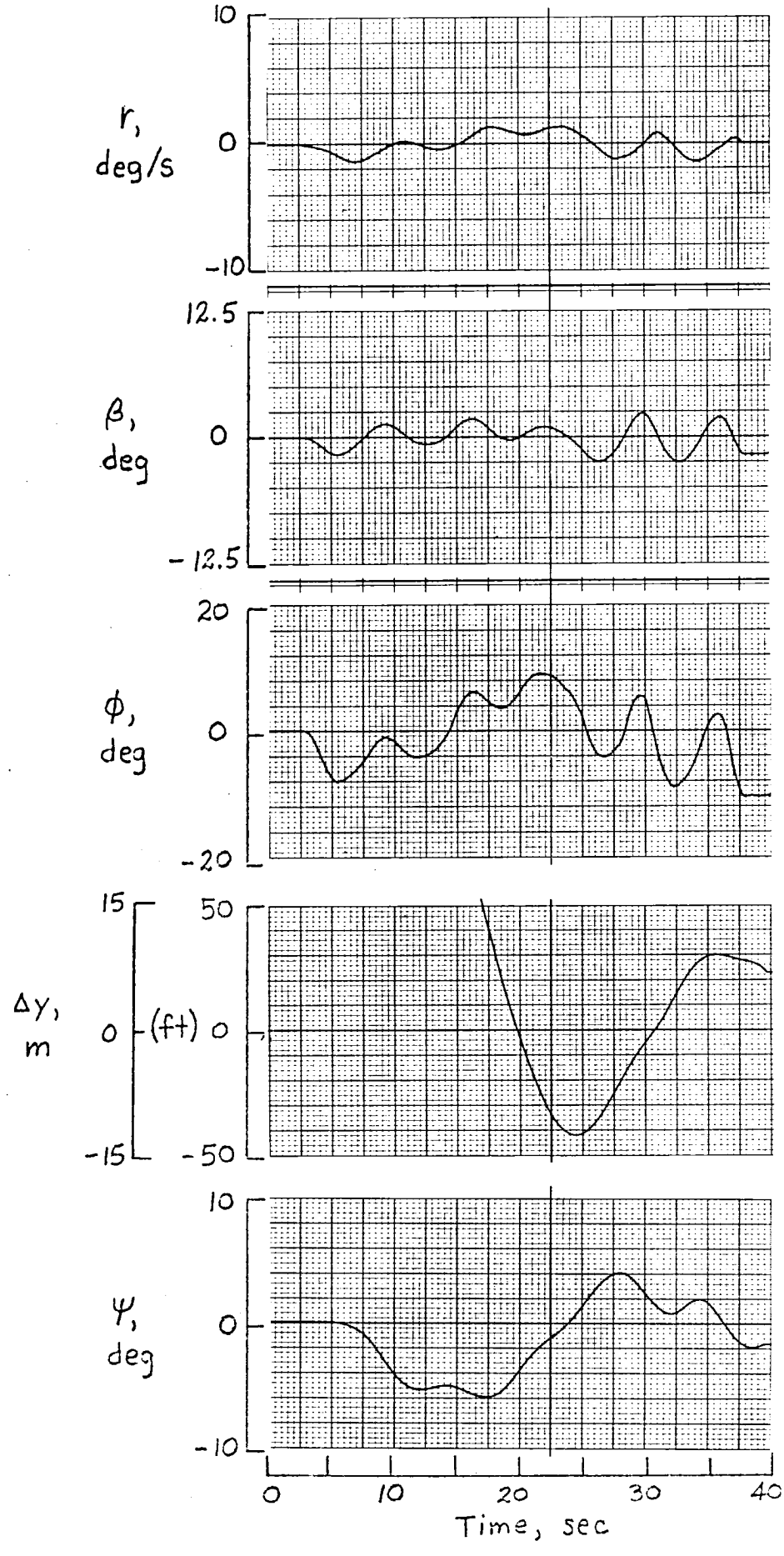

Figure 23.- Concluded.

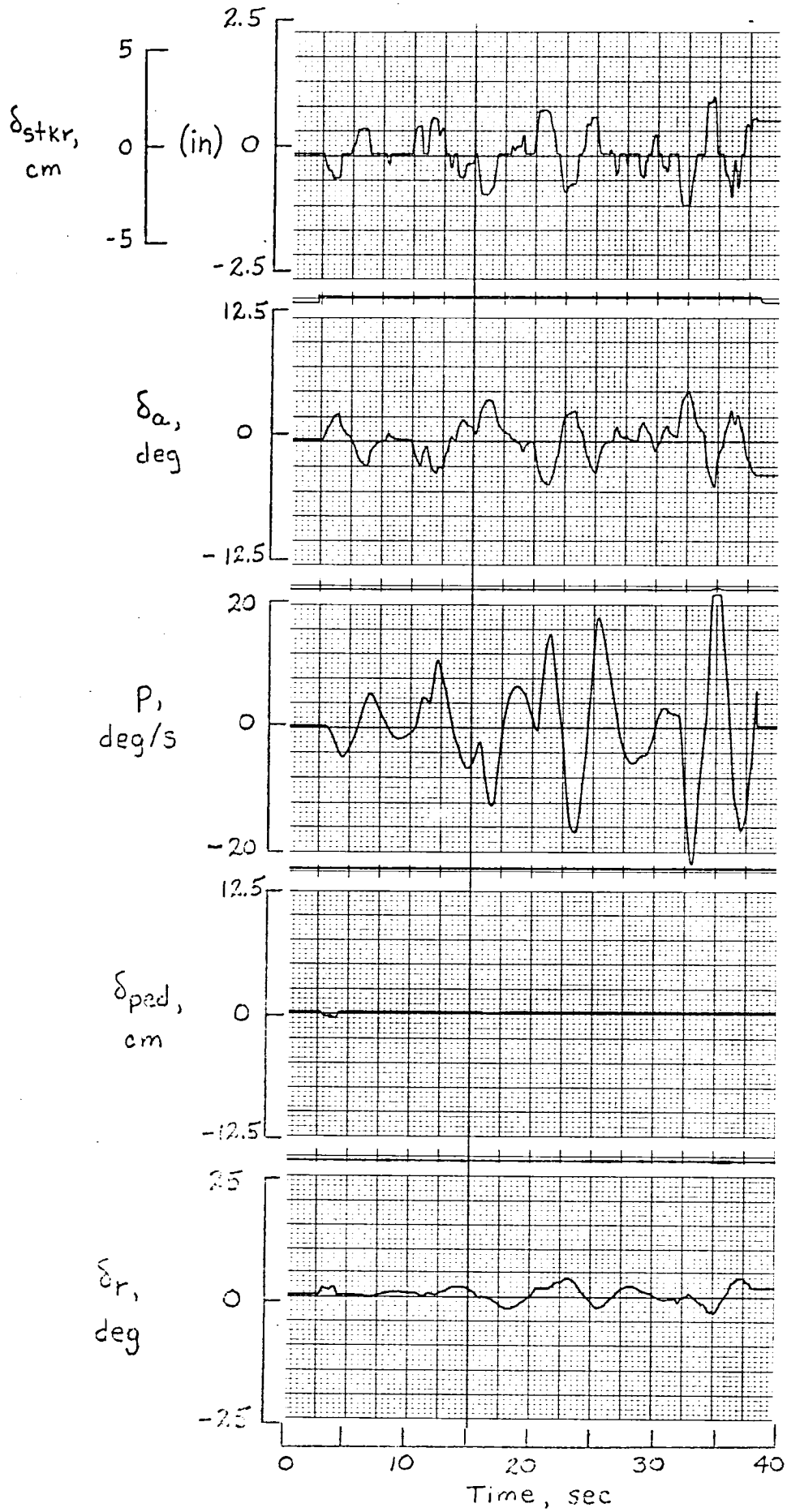

Figure 24.- Carrier approach - Pilot 3, control system A.

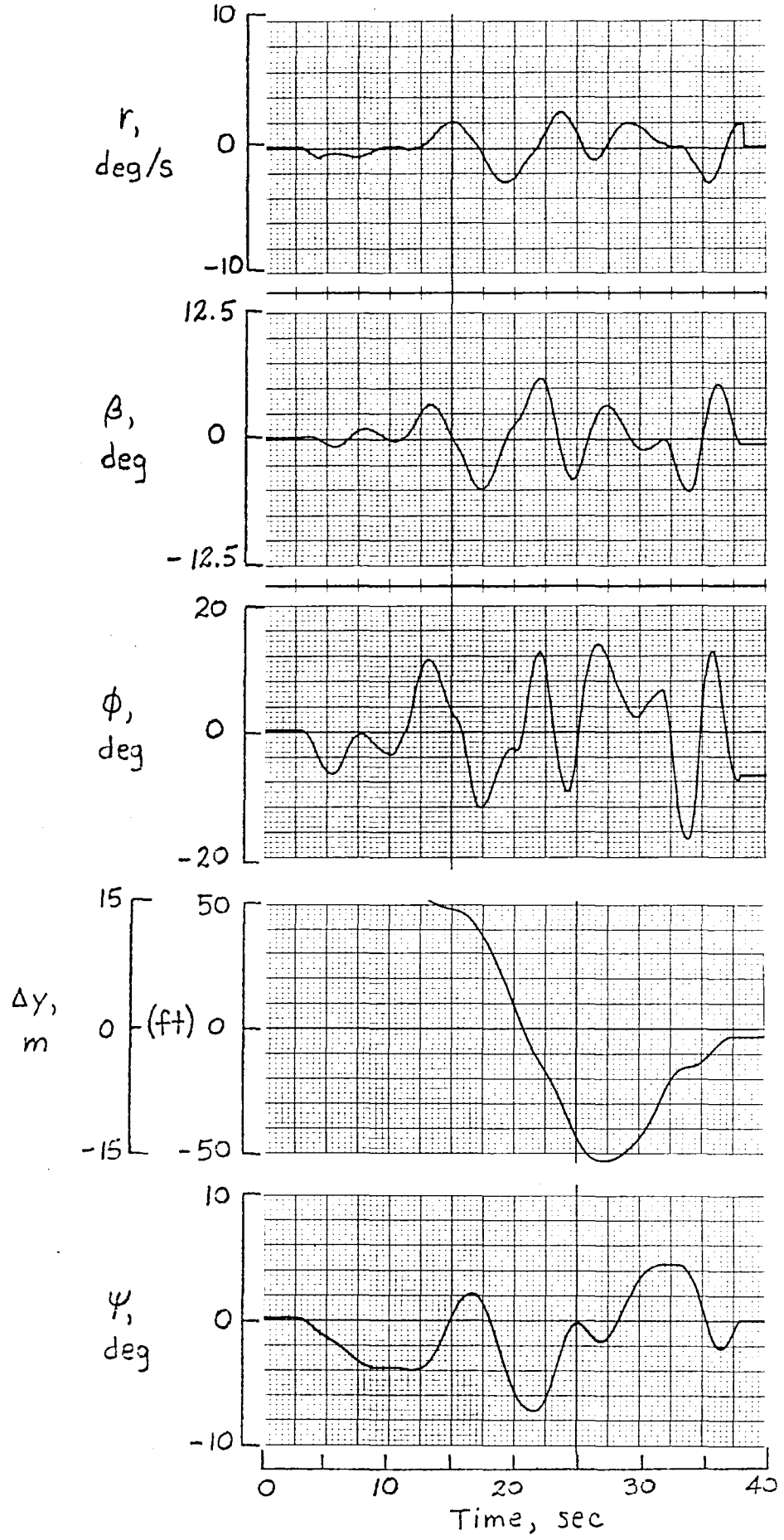

Figure 24.- Concluded.

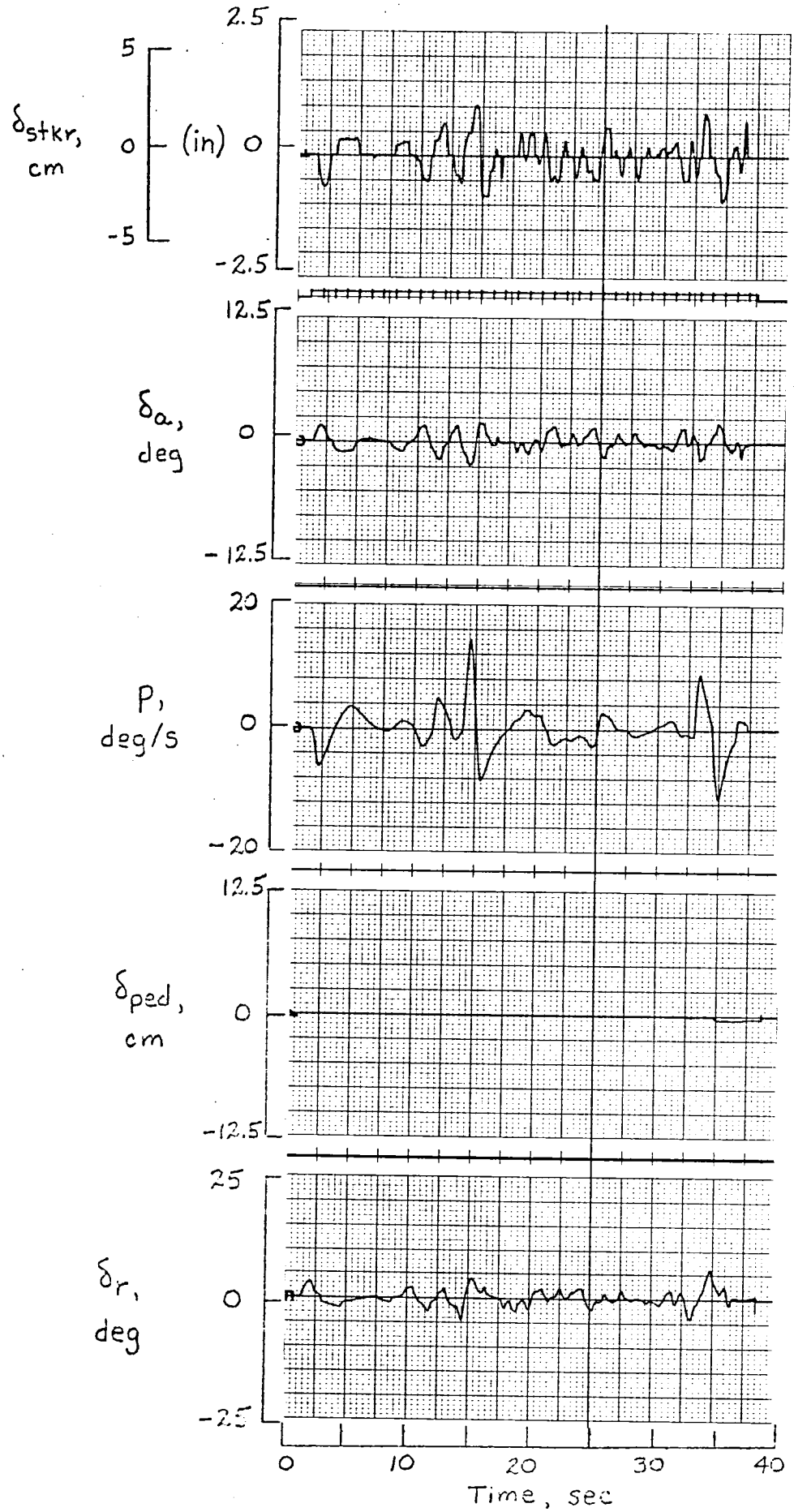

Figure 25.- Carrier approach - Pilot 1, control system B.

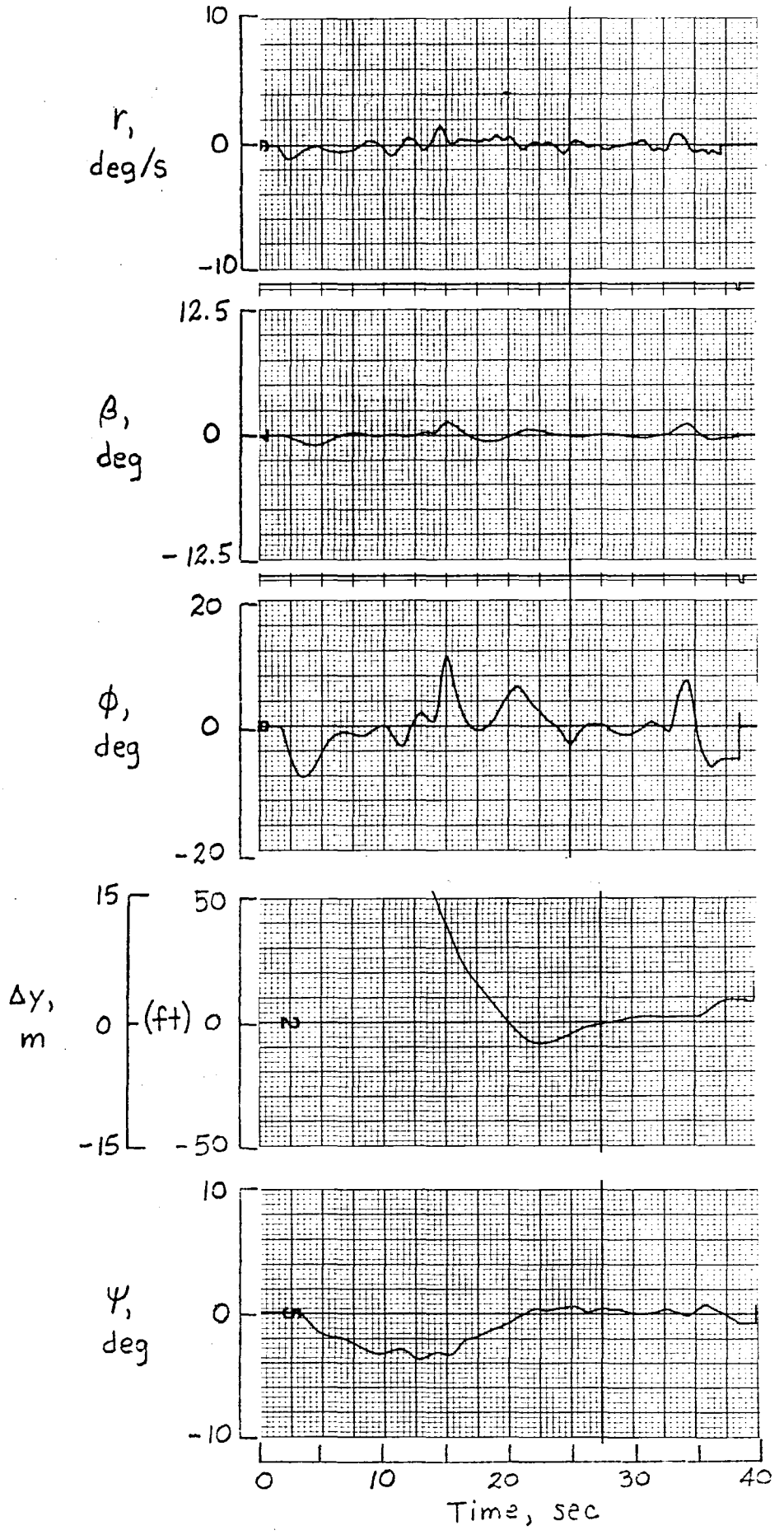

Figure 25- Concluded.

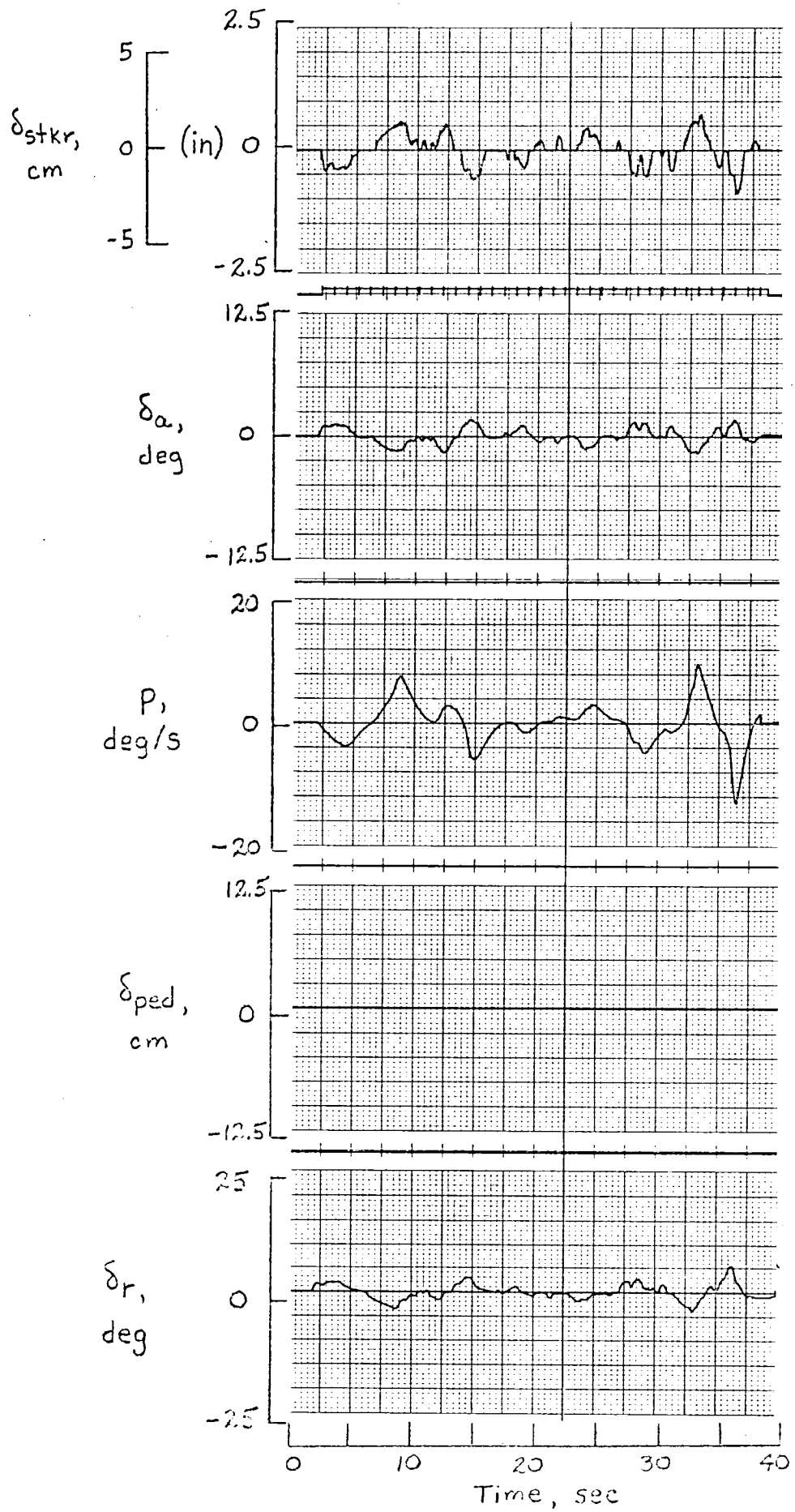

Figure 26.- Carrier approach - Pilot 2, control system B.

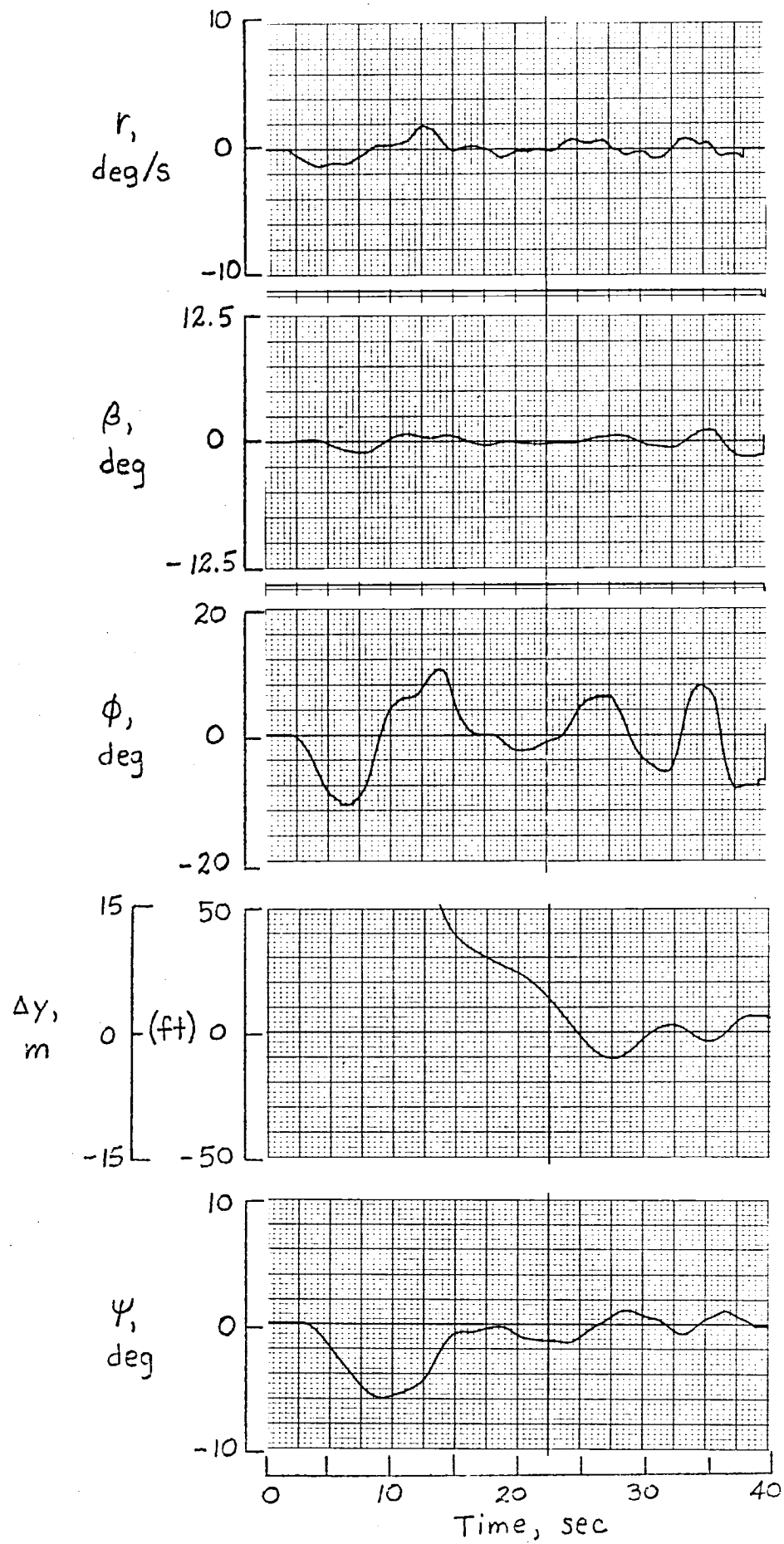

Figure 26.- Concluded.

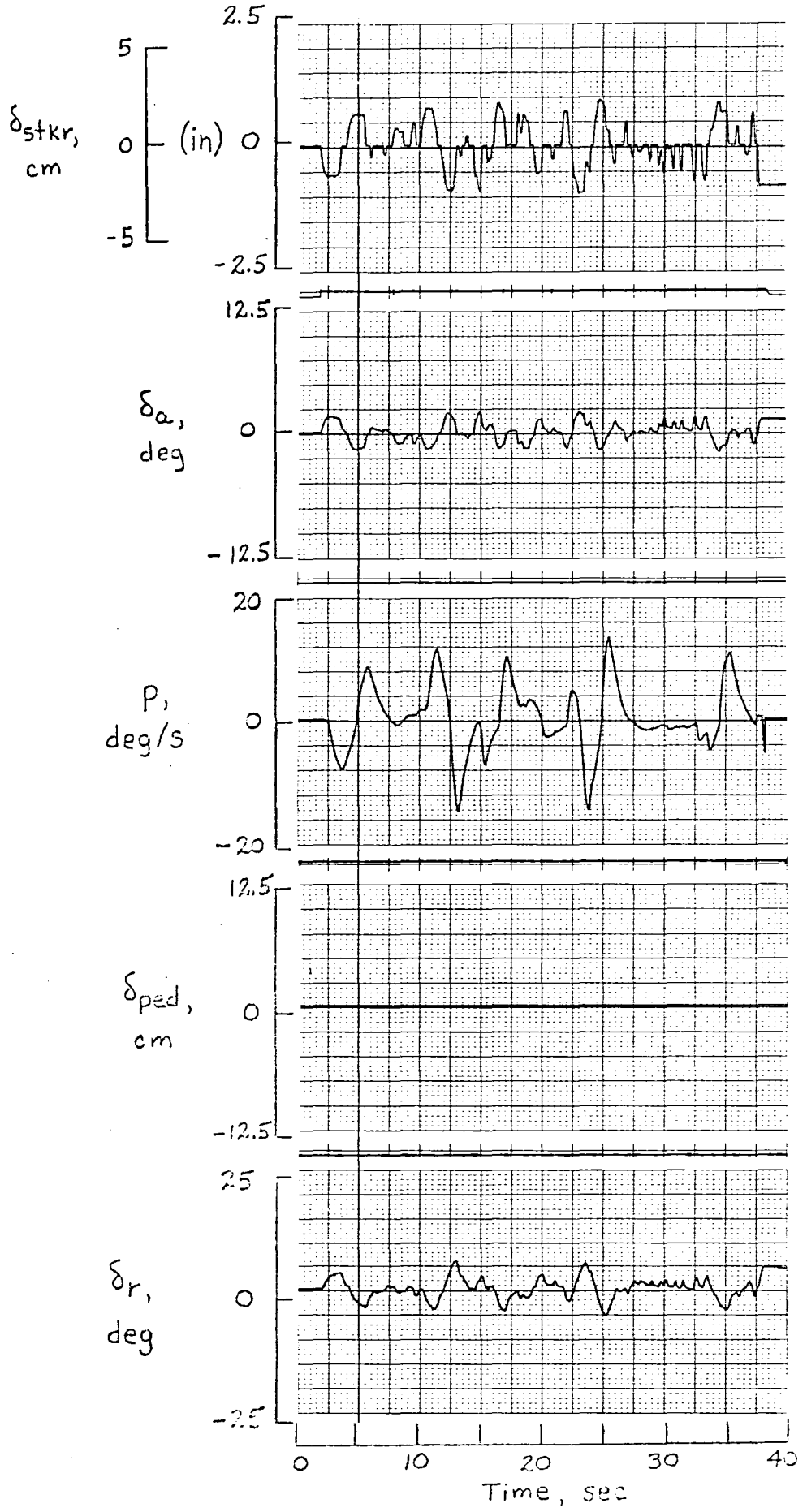

Figure 27.- Carrier approach - Pilot 3, control system B.

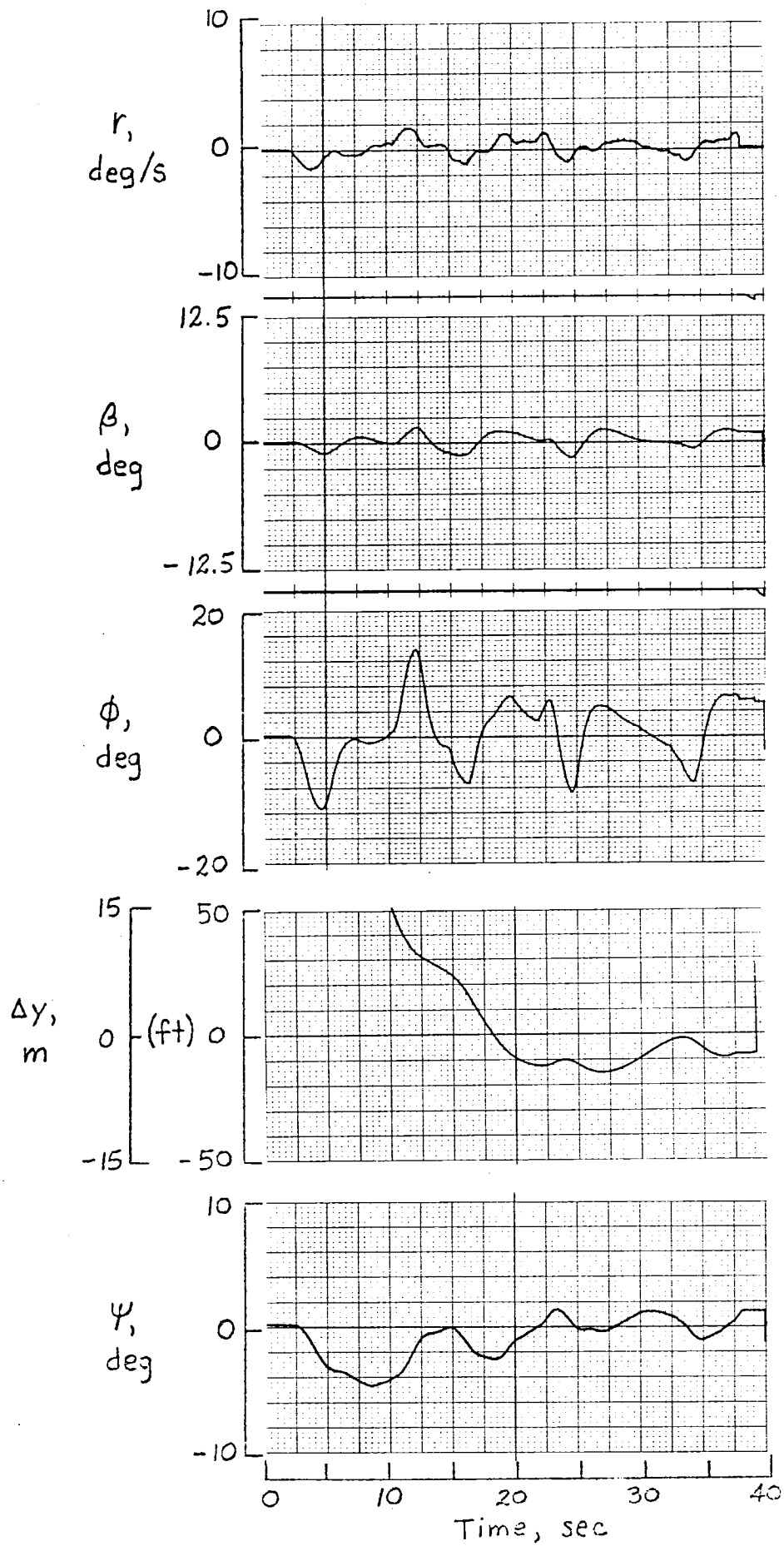

Figure 27.- Concluded.

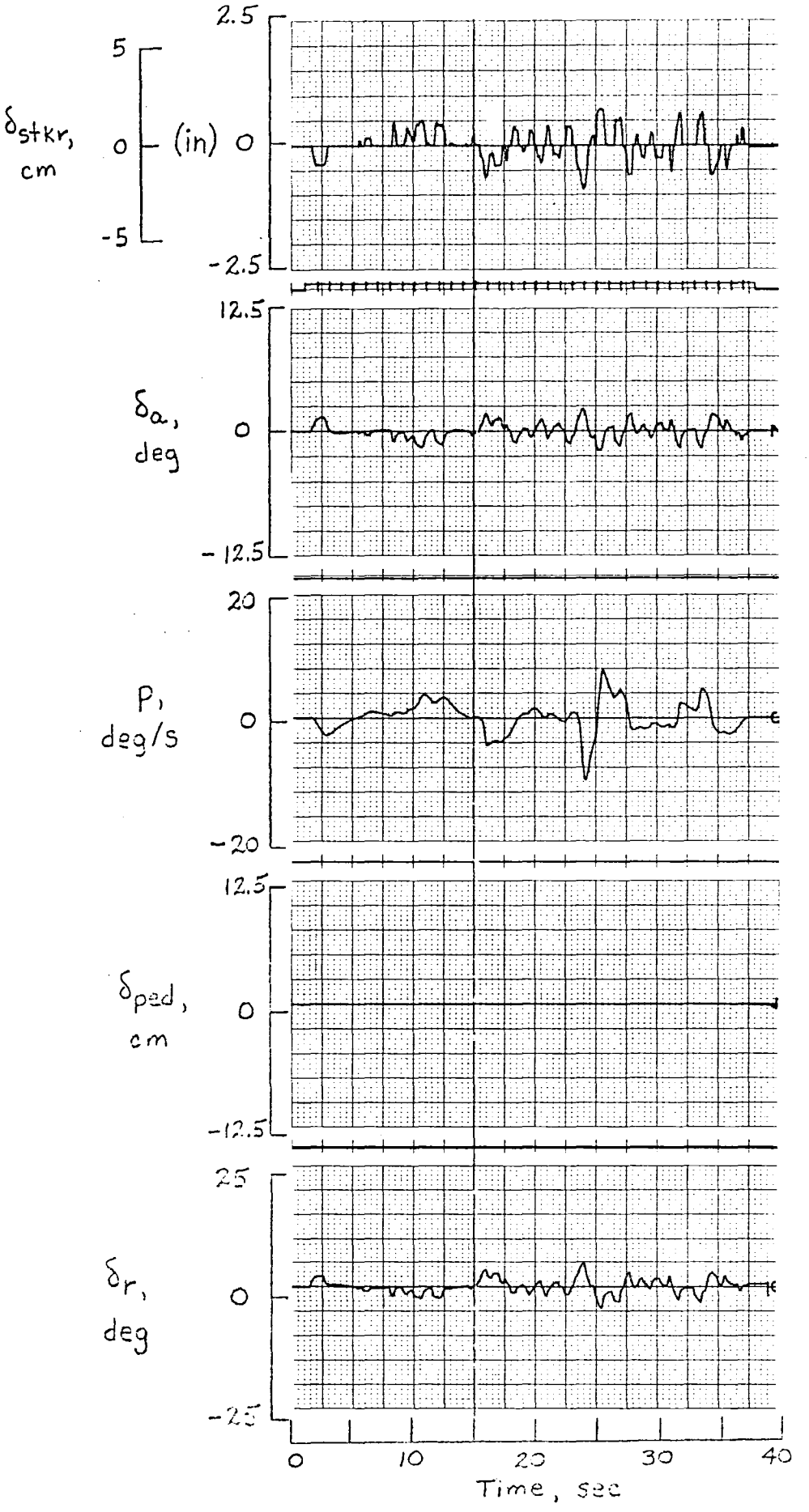

Figure 28.- Carrier approach - Pilot 1, control system C.

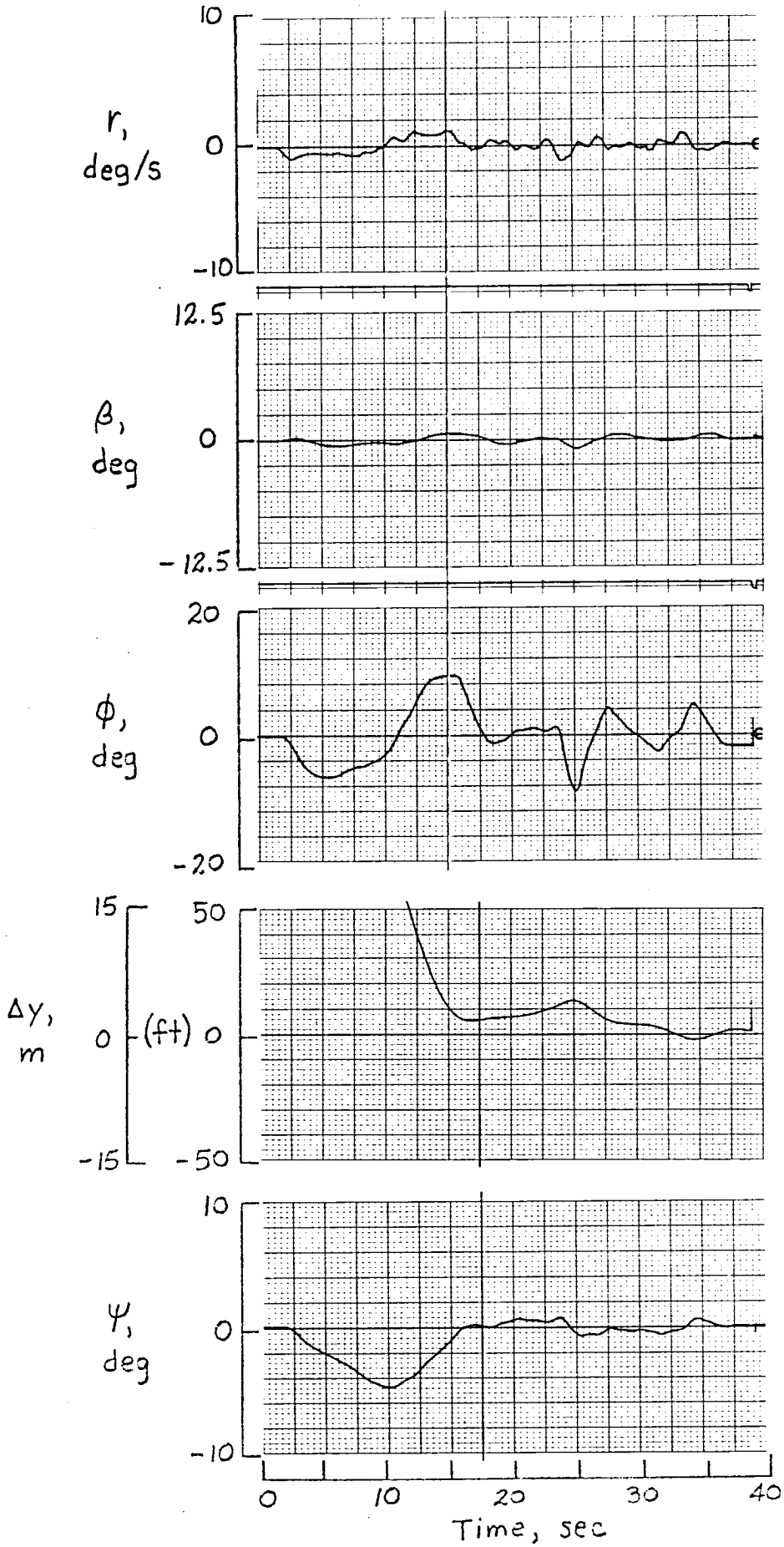

Figure 28.- Concluded.

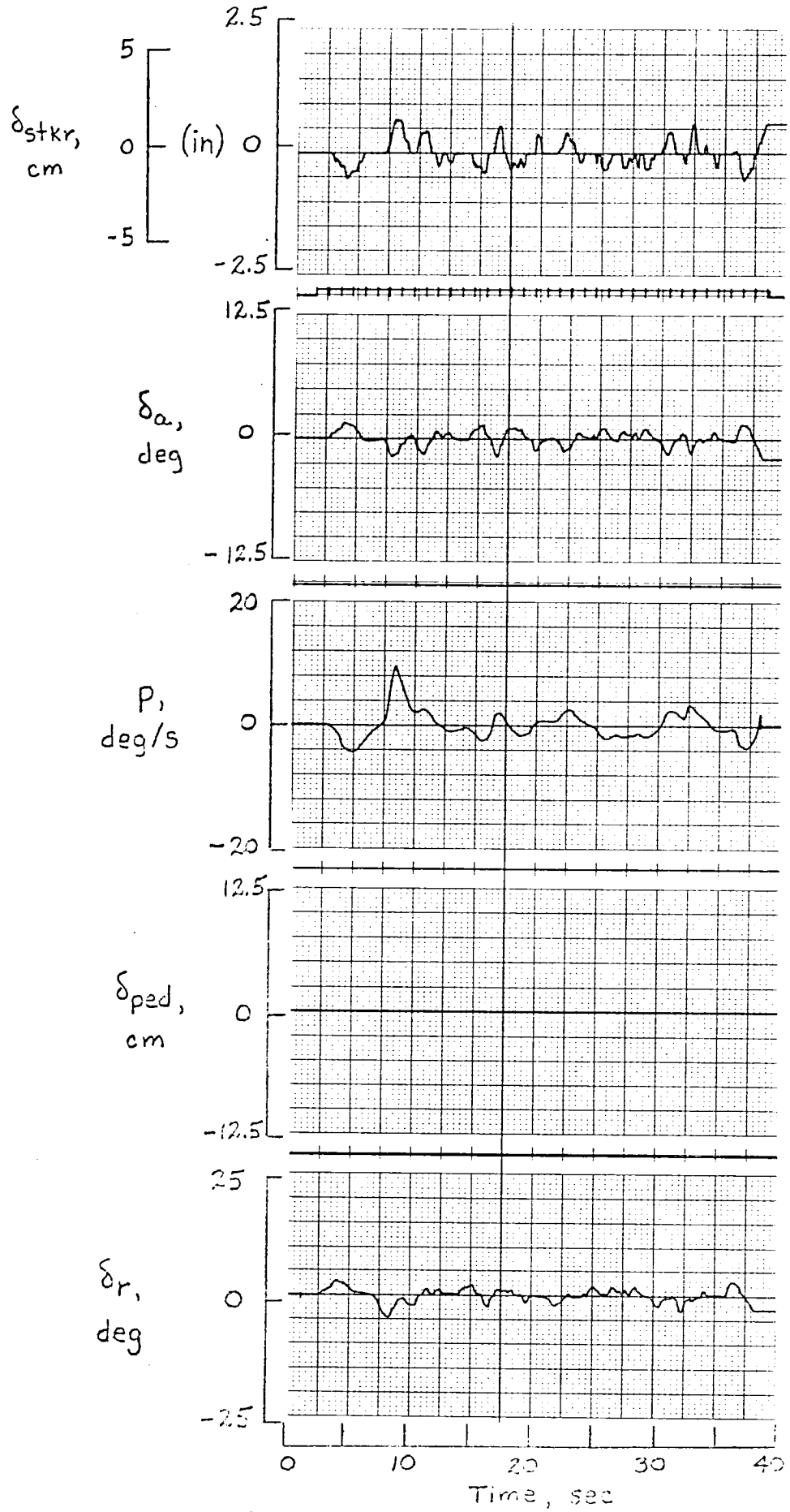

Figure 29.- Carrier approach - Pilot 2, control system C.

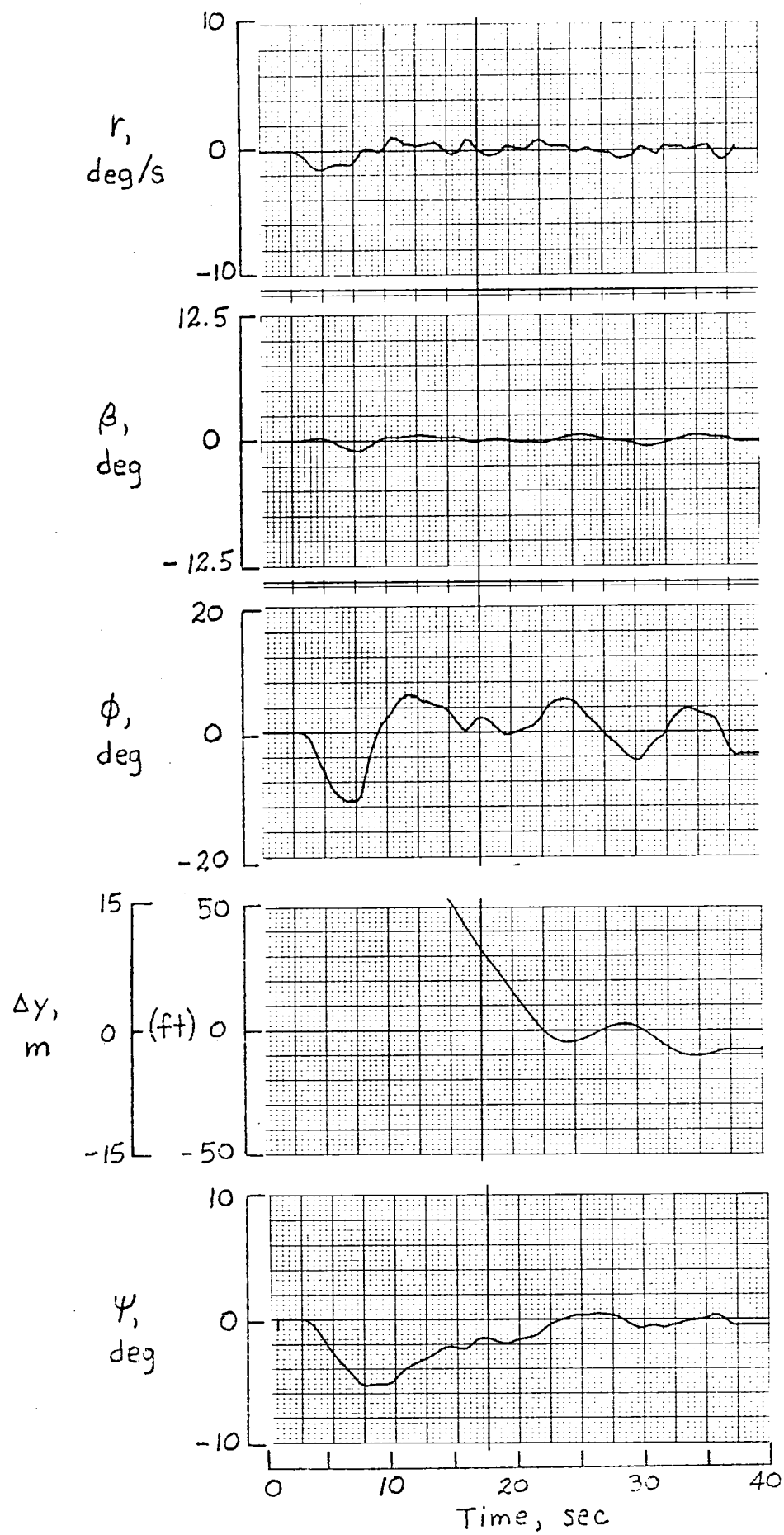

Figure 29.- Concluded.

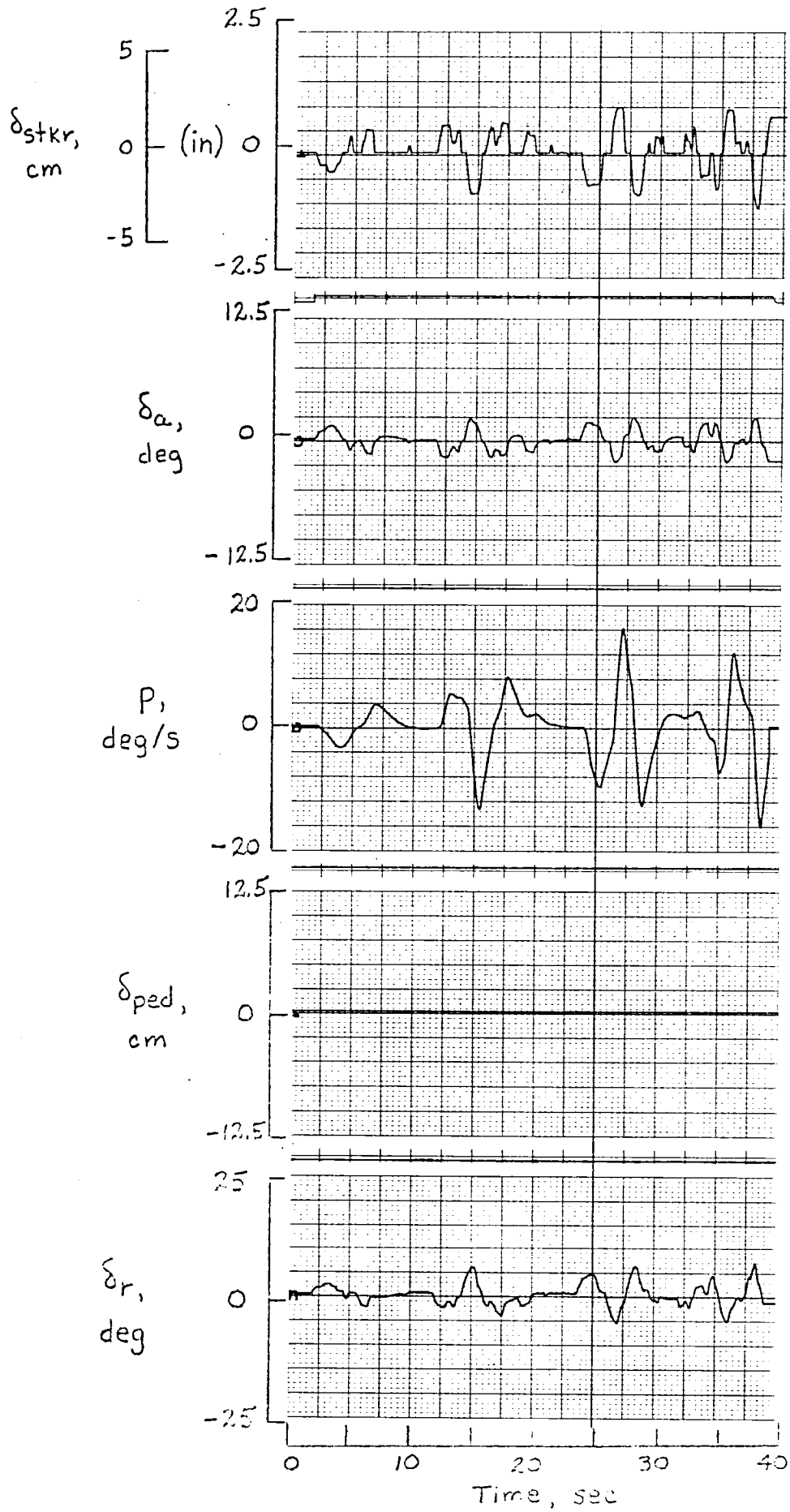

Figure 30.- Carrier approach - Pilot 3, control system C.

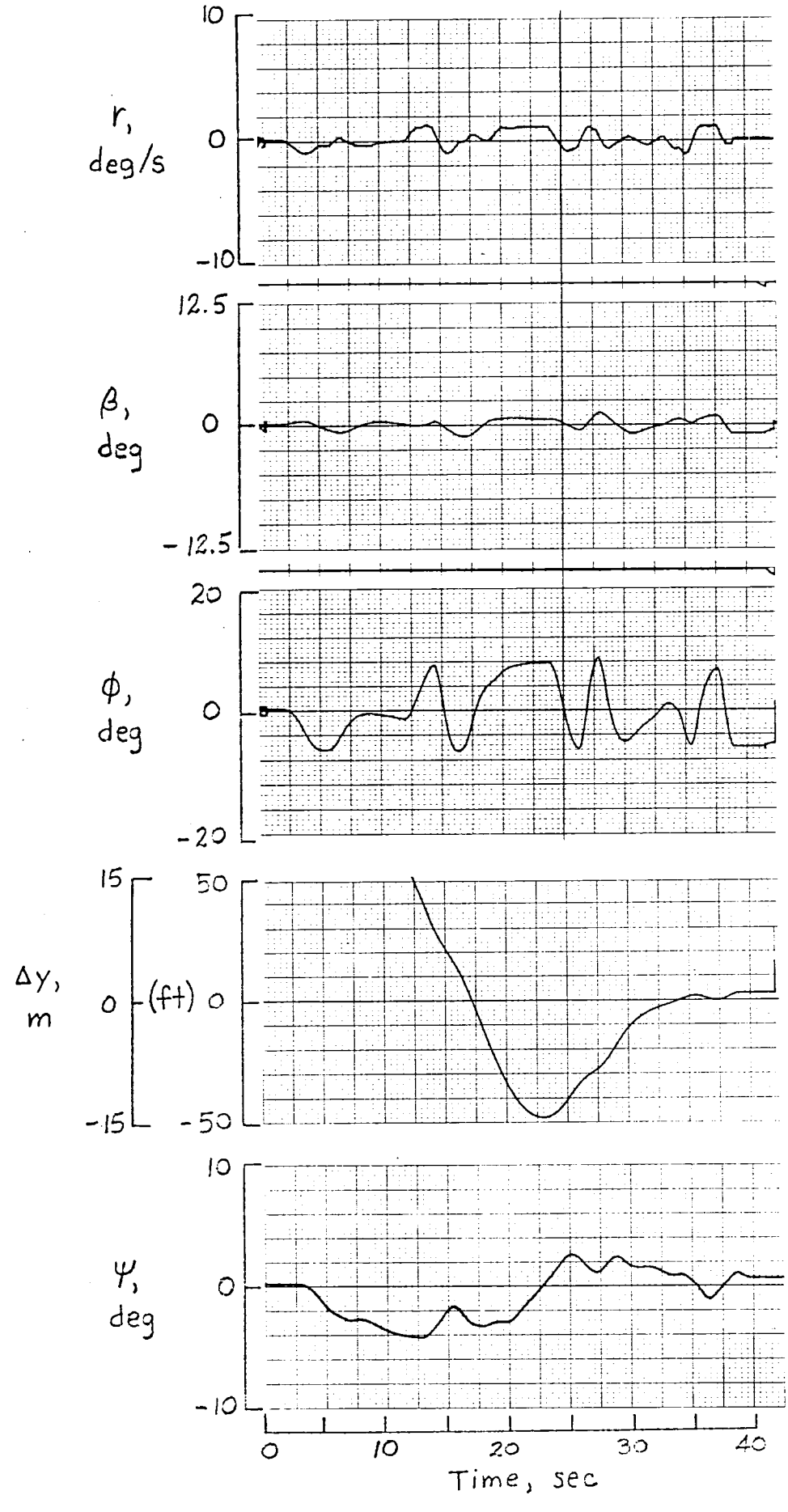

Figure 30.- Concluded.

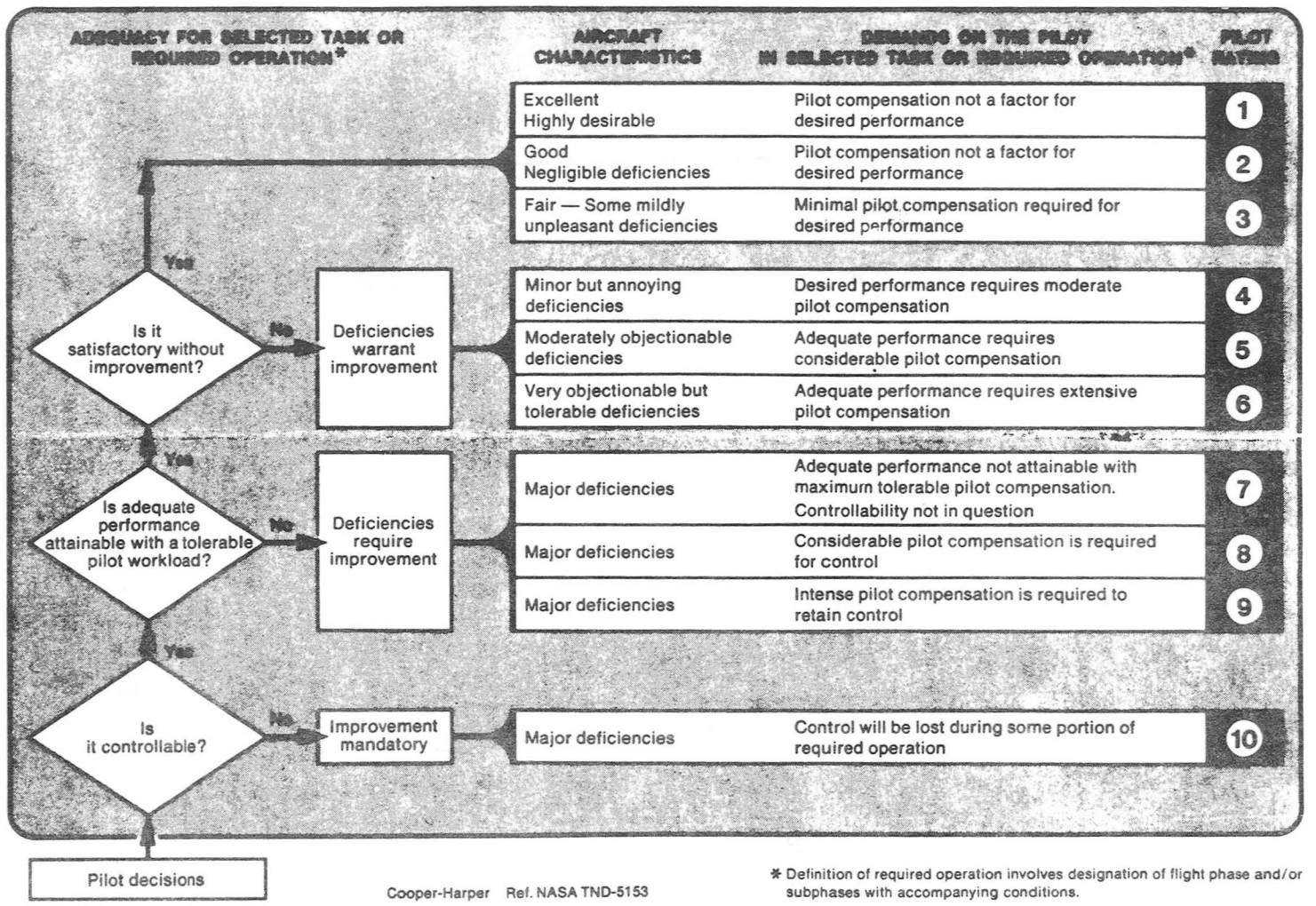

(a) Pilot rating scale.

Figure 31.- Pilot rating scale used and results of pilot ratings.

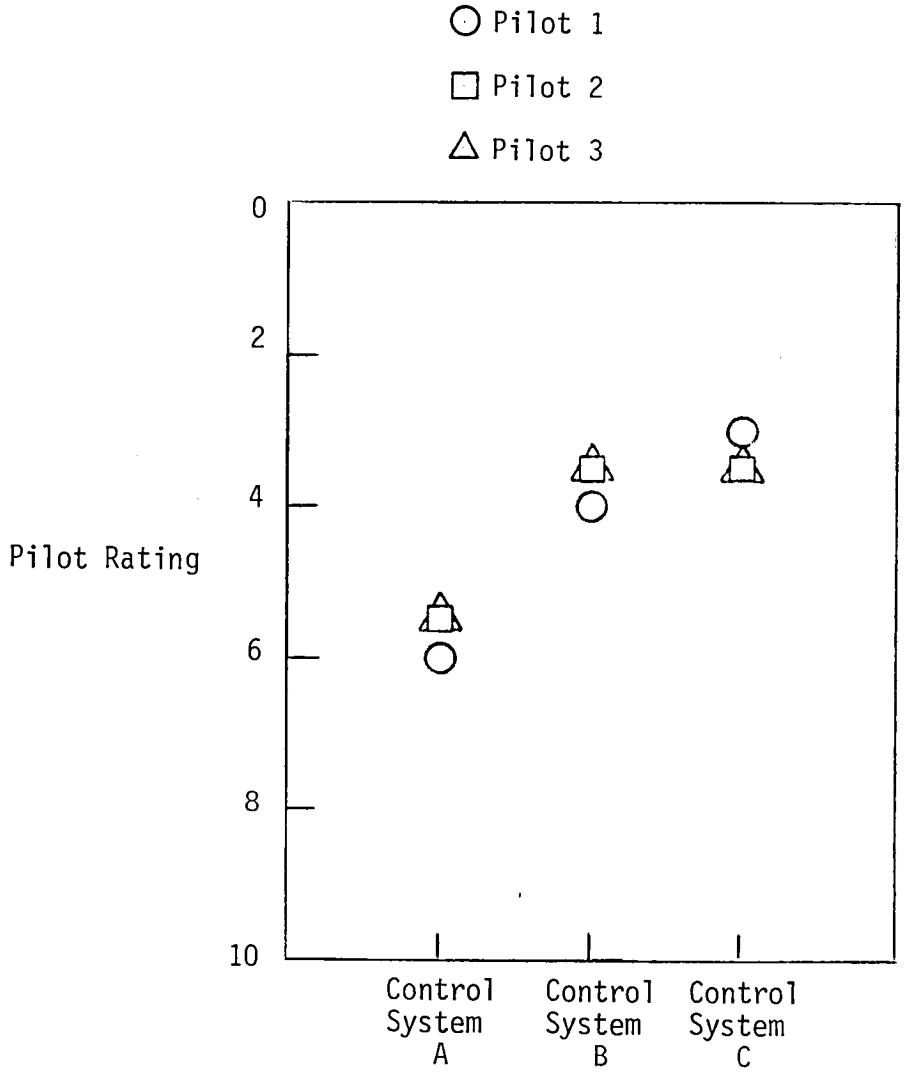

(b) Pilot ratings.

Figure 31.- Concluded.

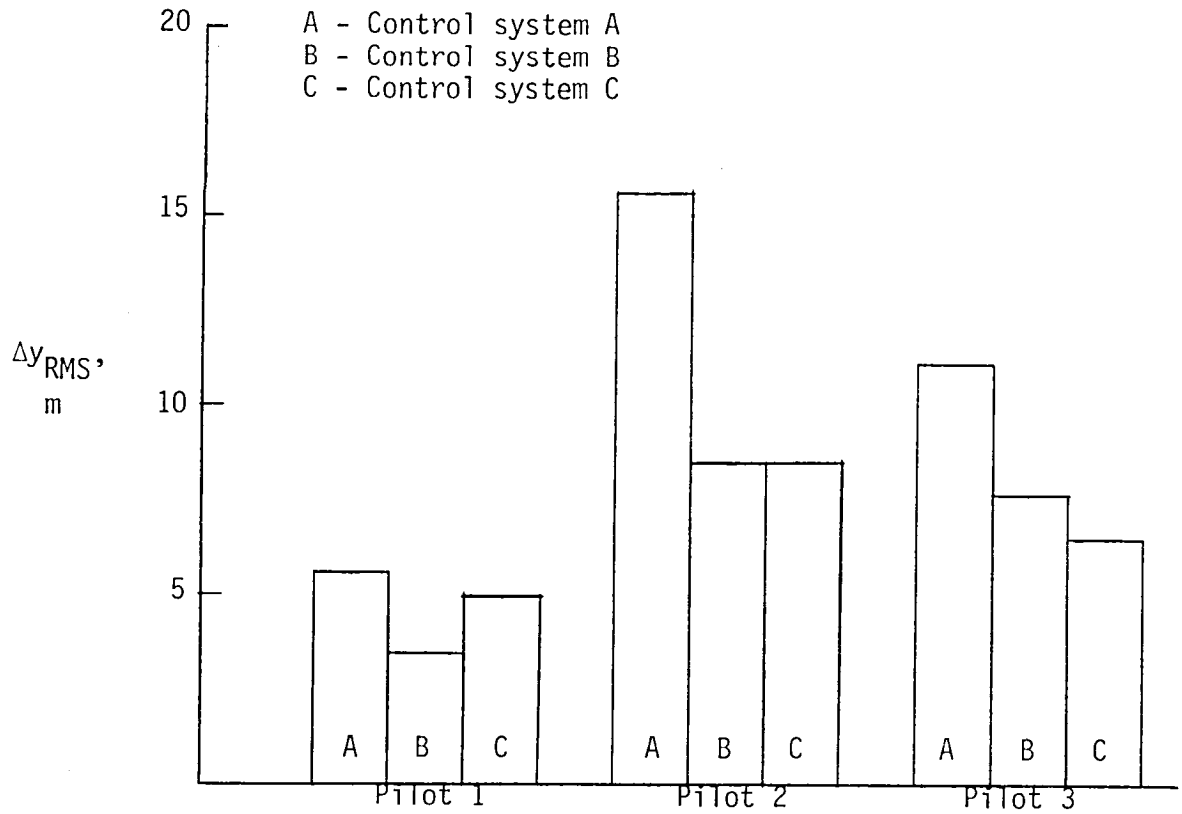

(a) Segment 1.

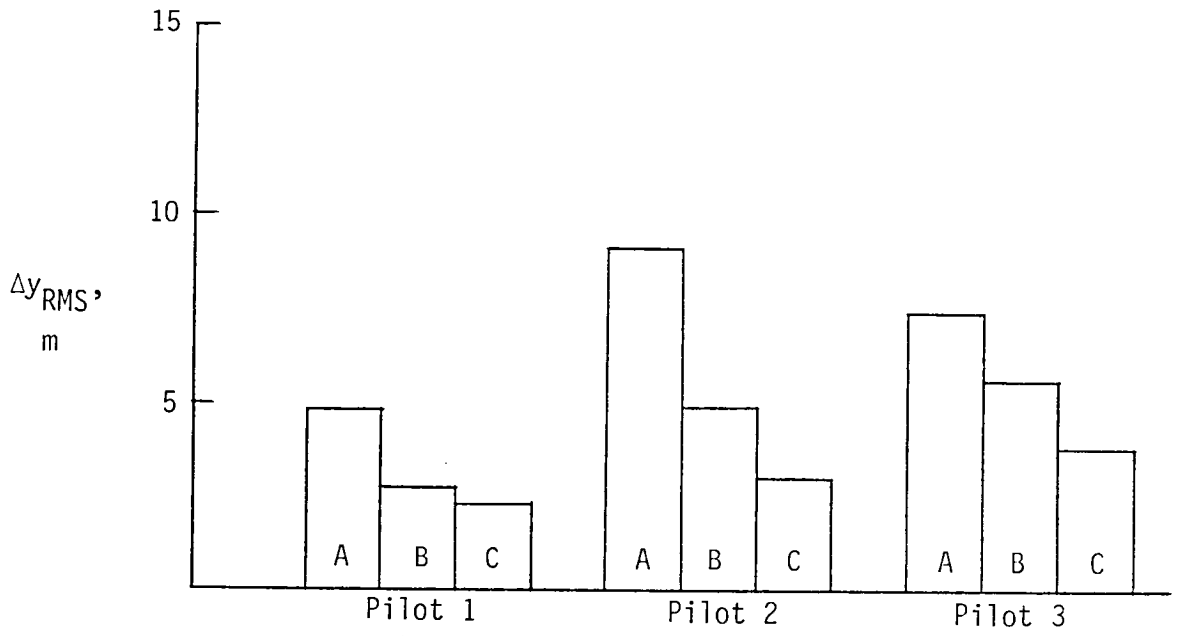

(b) Segment 2.

Figure 32.- Lateral deviation from carrier centerline during approaches.

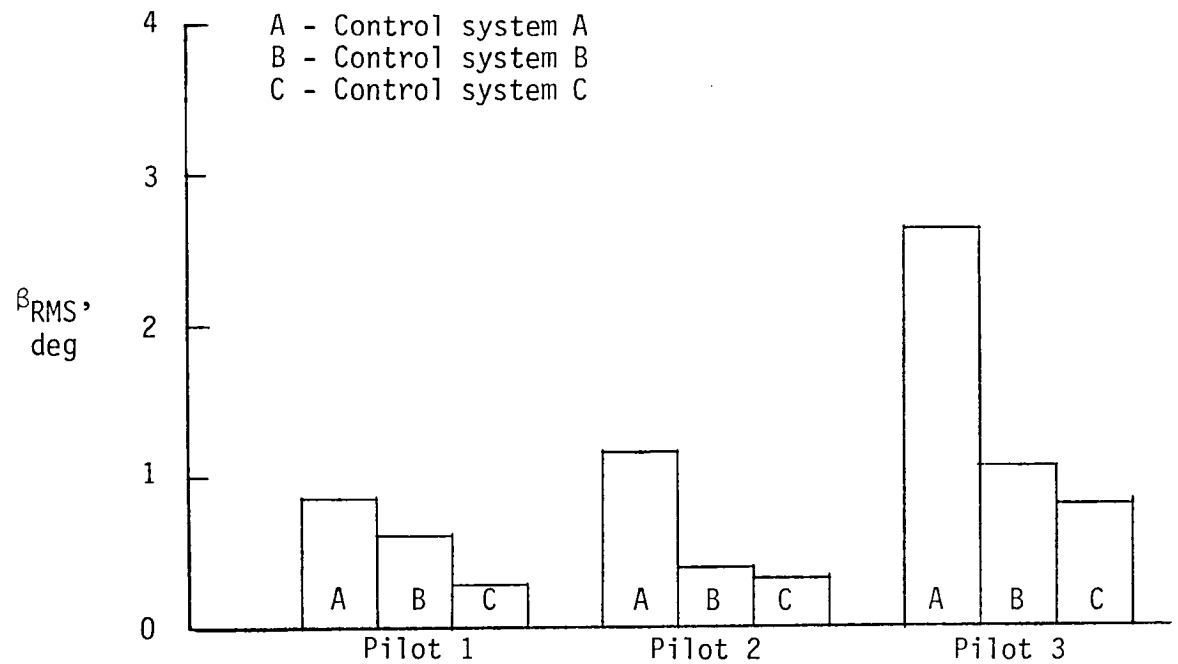

(a) Segment 1.

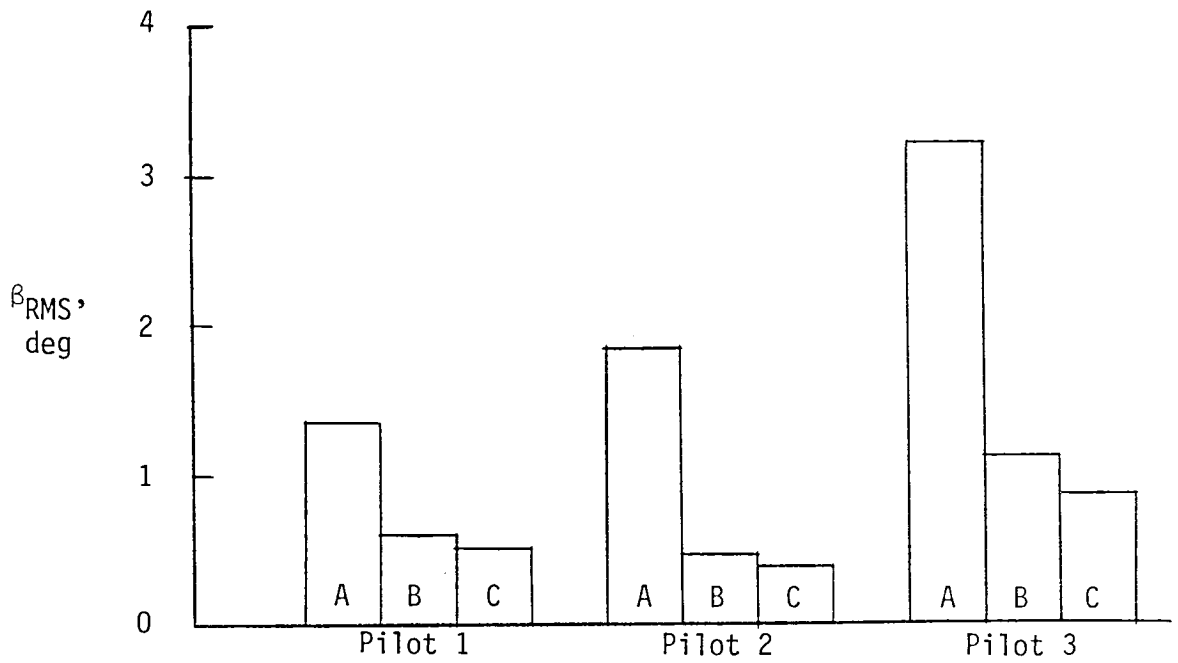

(b) Segment 2.

Figure 33.- Sideslip angles during carrier approaches.

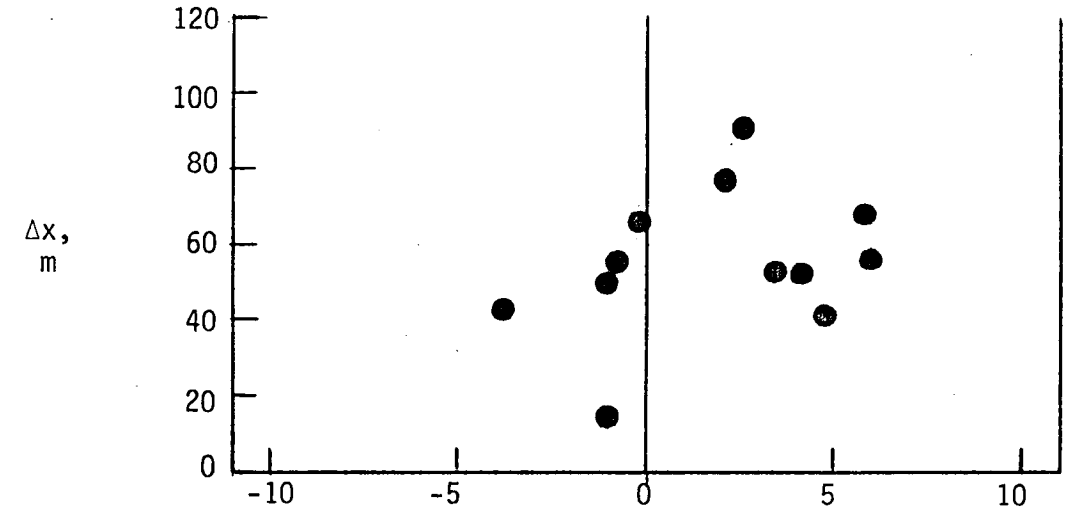

(a) Control system A.

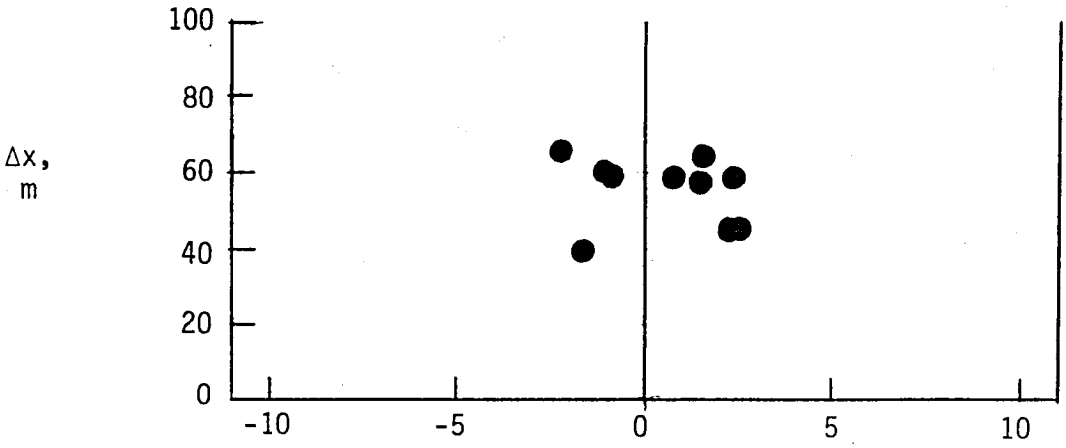

(b) Control system B.

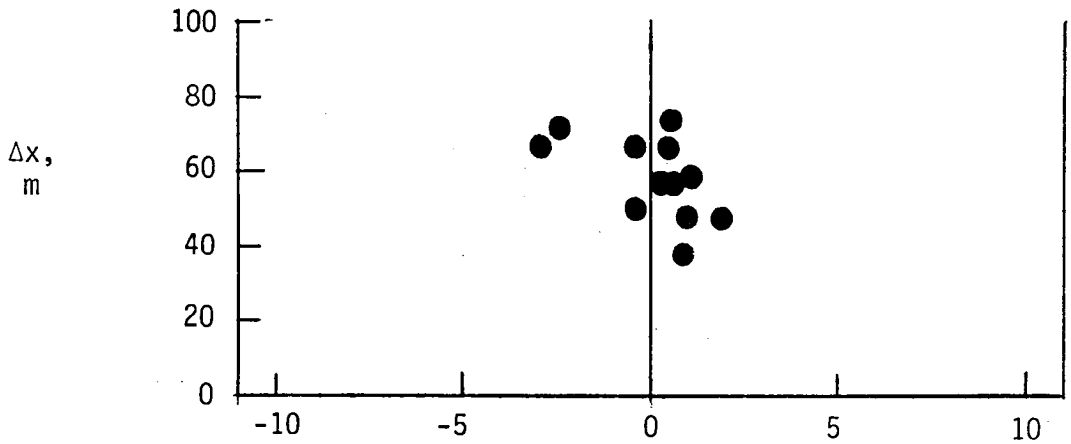

(c) Control system C.

Figure 34.- Touchdown dispersion - Pilot 1.

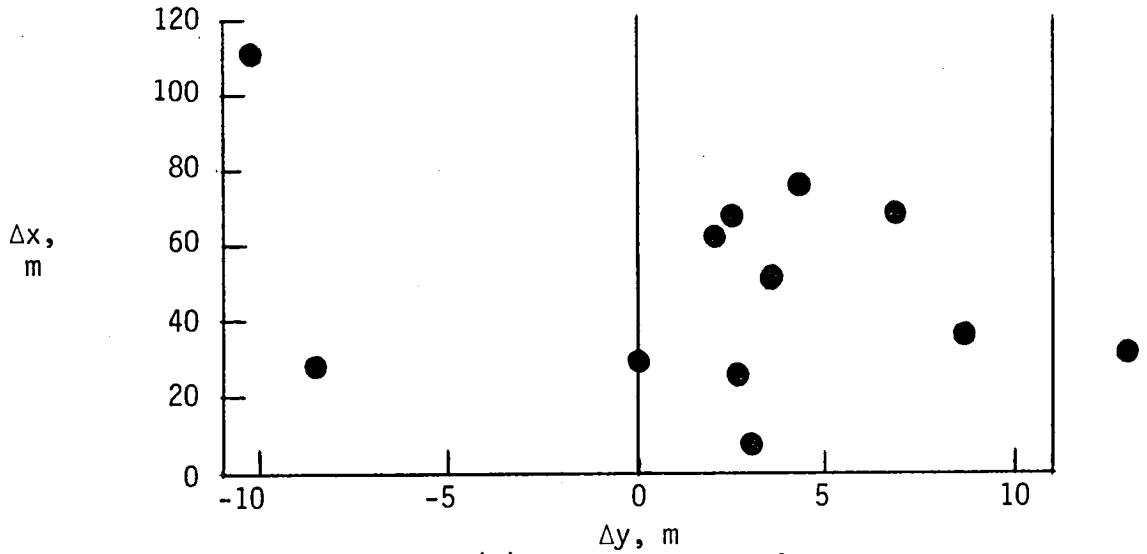

(a) Control system A.

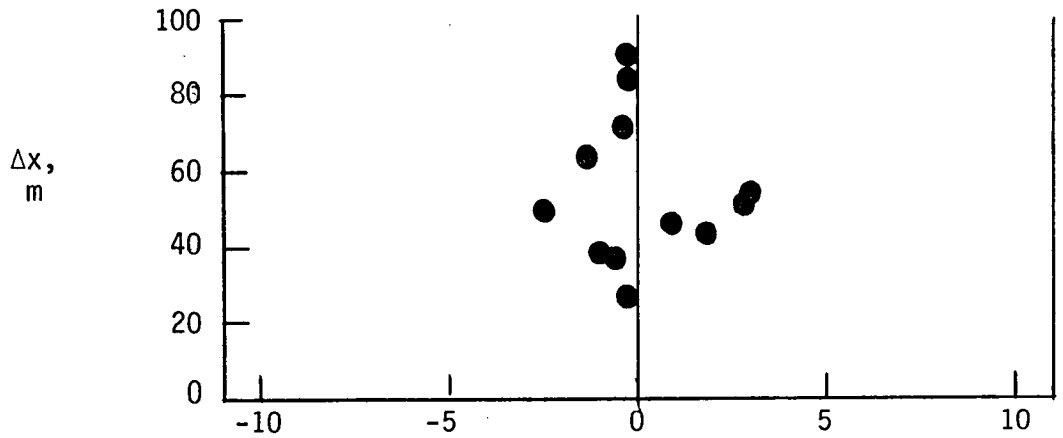

(b) Control system B.

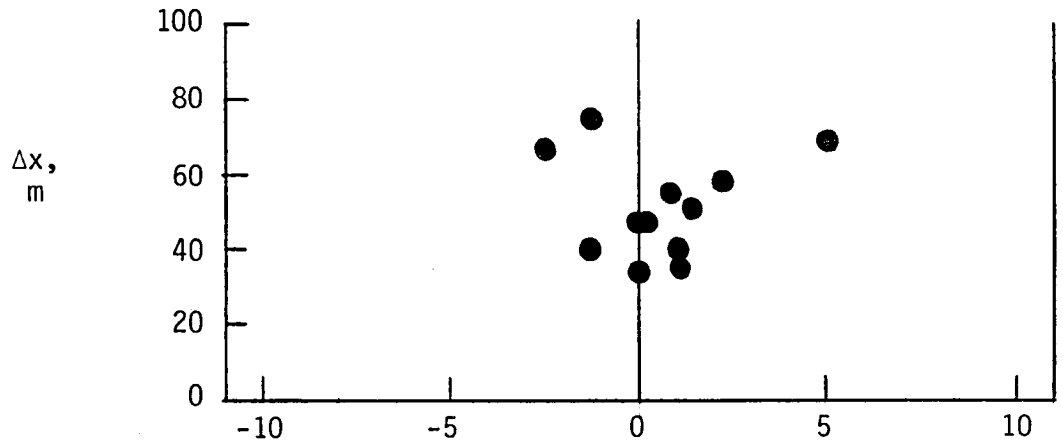

(c) Control system C.

Figure 35.- Touchdown dispersion - Pilot 2.

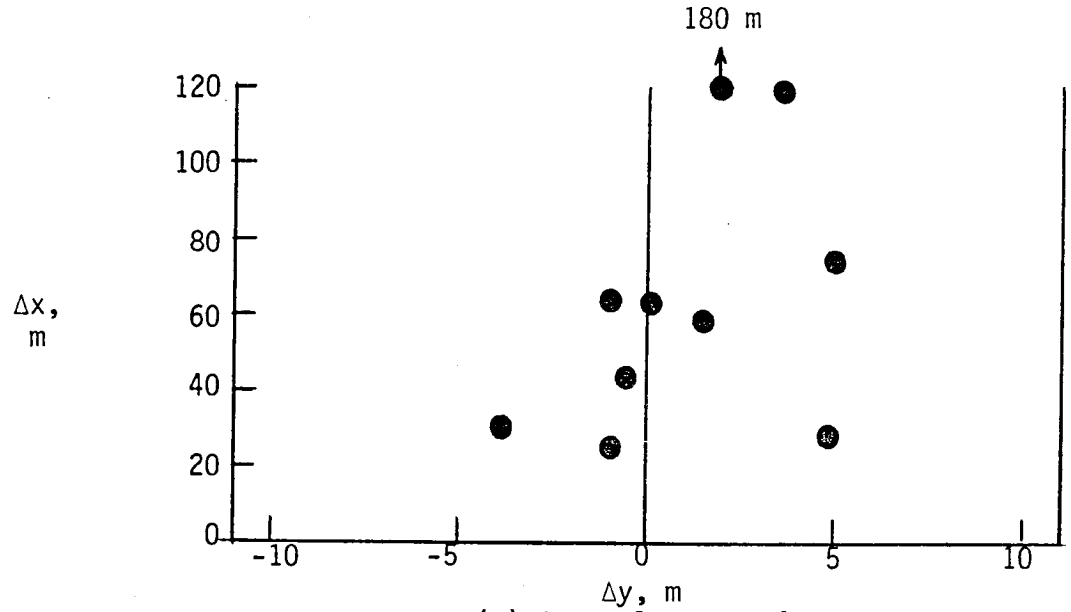

(a) Control system A.

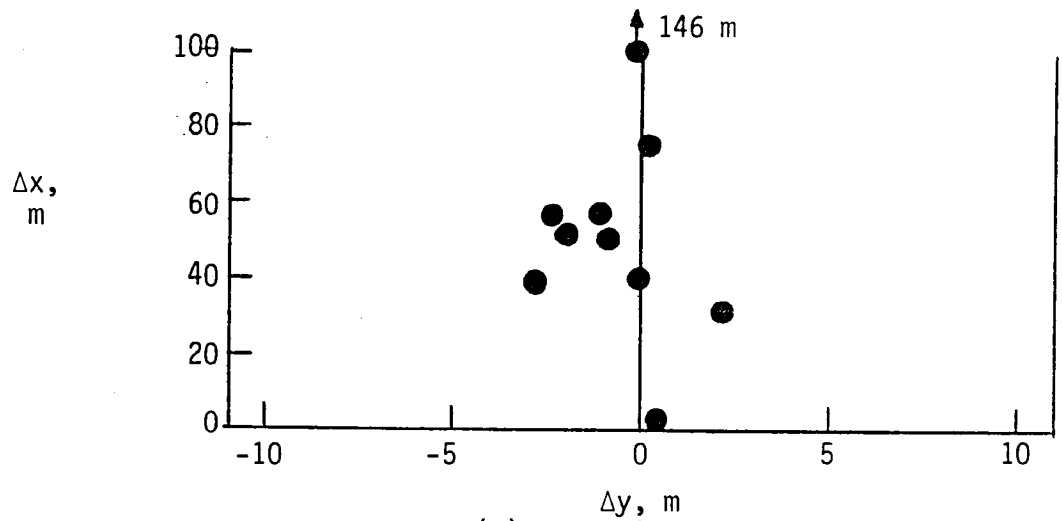

(b) Control system B.

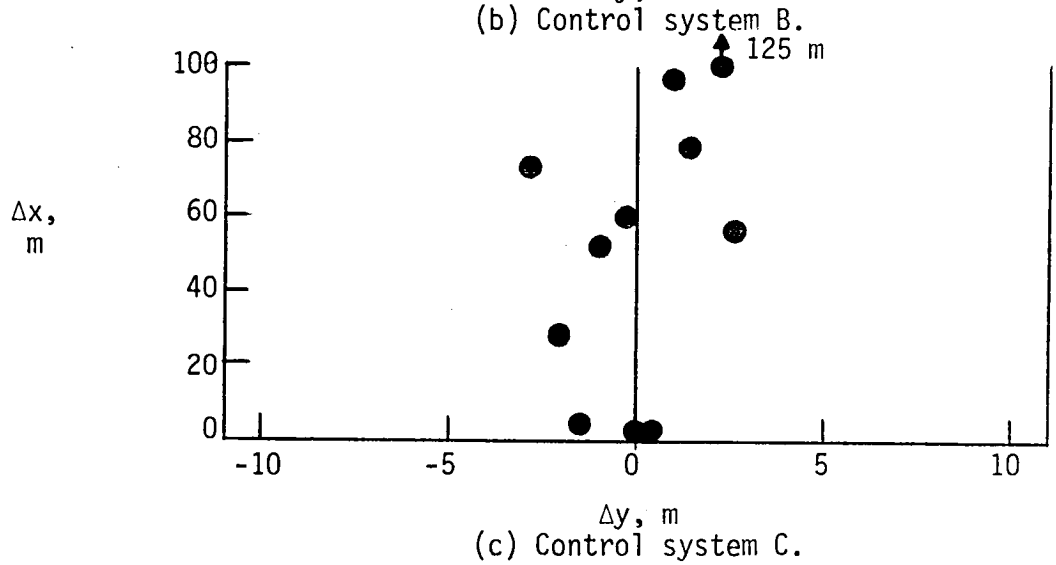

(c) Control system C.

Figure 36.- Touchdown dispersion - Pilot 3.

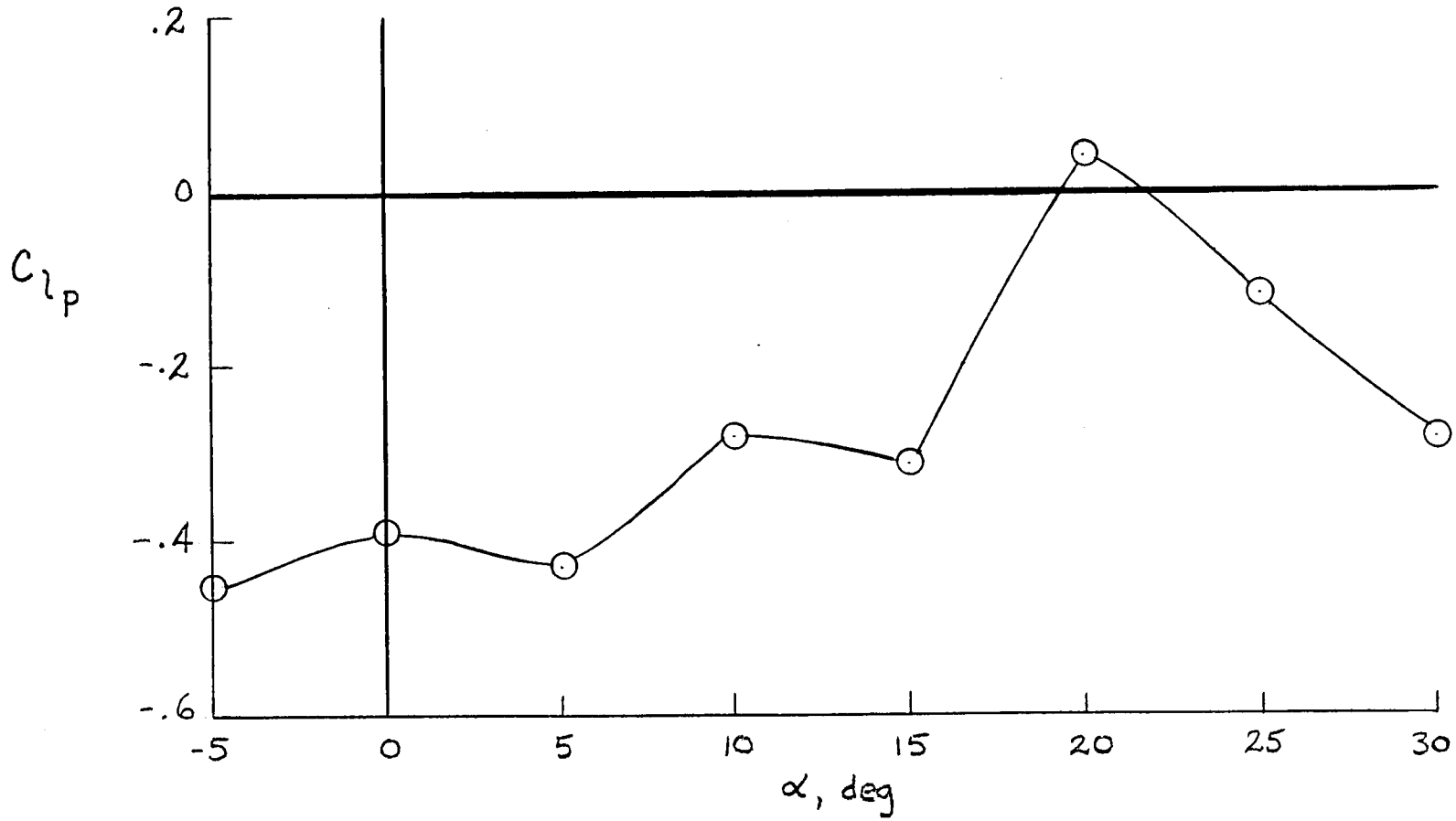

(a) Rolling moment coefficient due to roll rate.

Figure 37.- Aerodynamic data used in simulation.

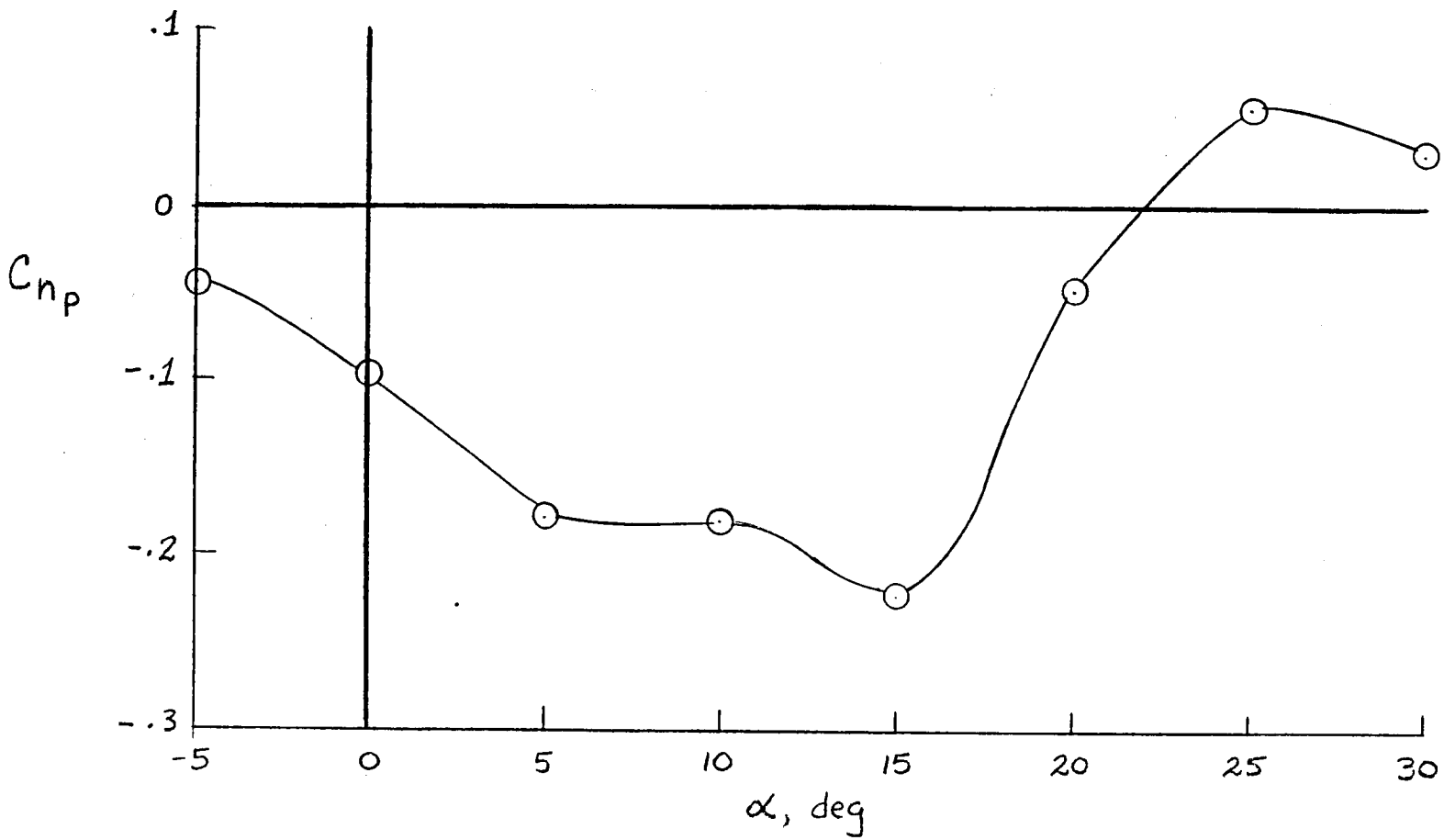

(b) Yawing moment coefficient due to roll rate.

Figure 37.- Continued.

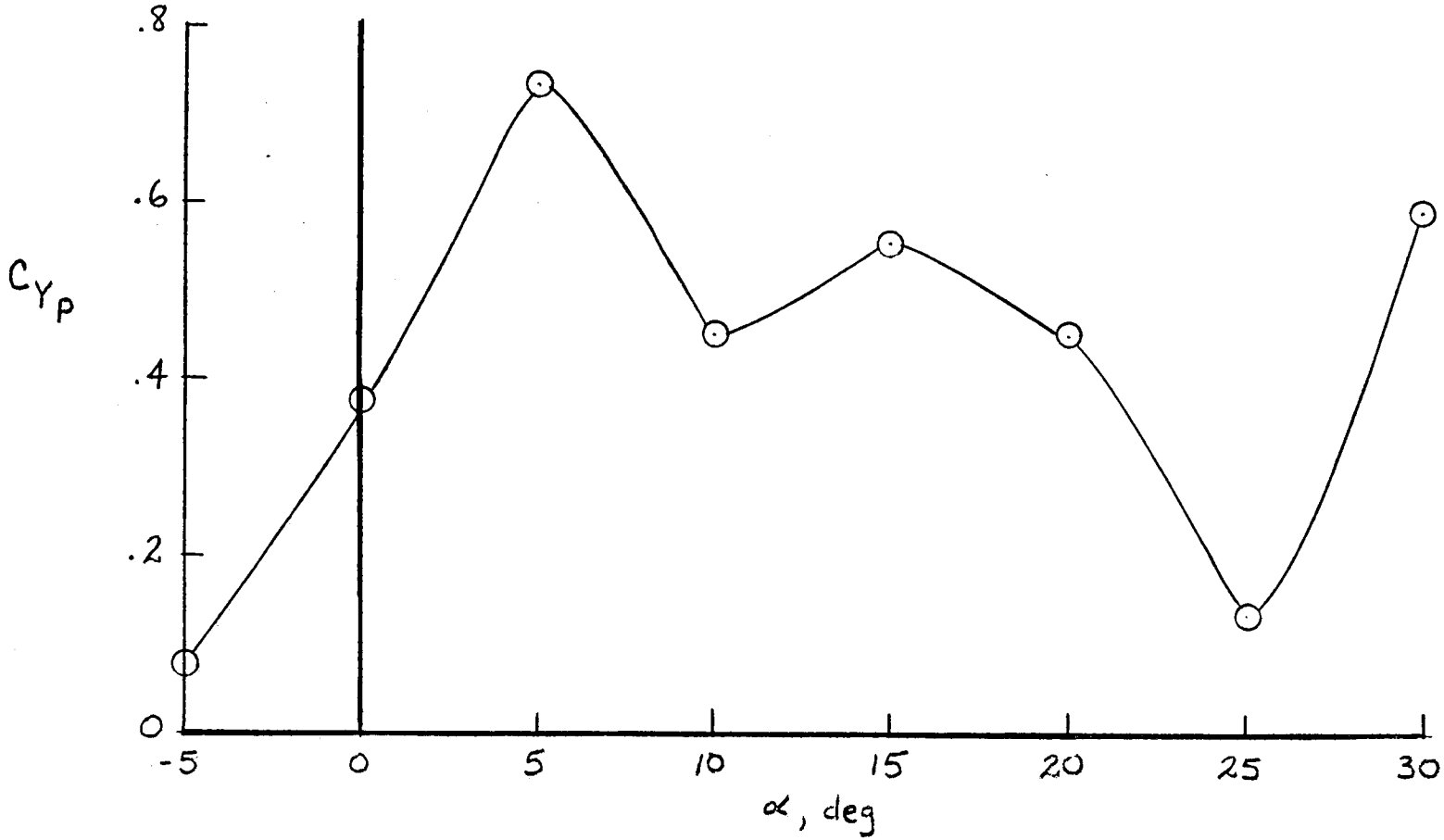

(c) Sideforce coefficient due to roll rate.

Figure 37.- Continued.

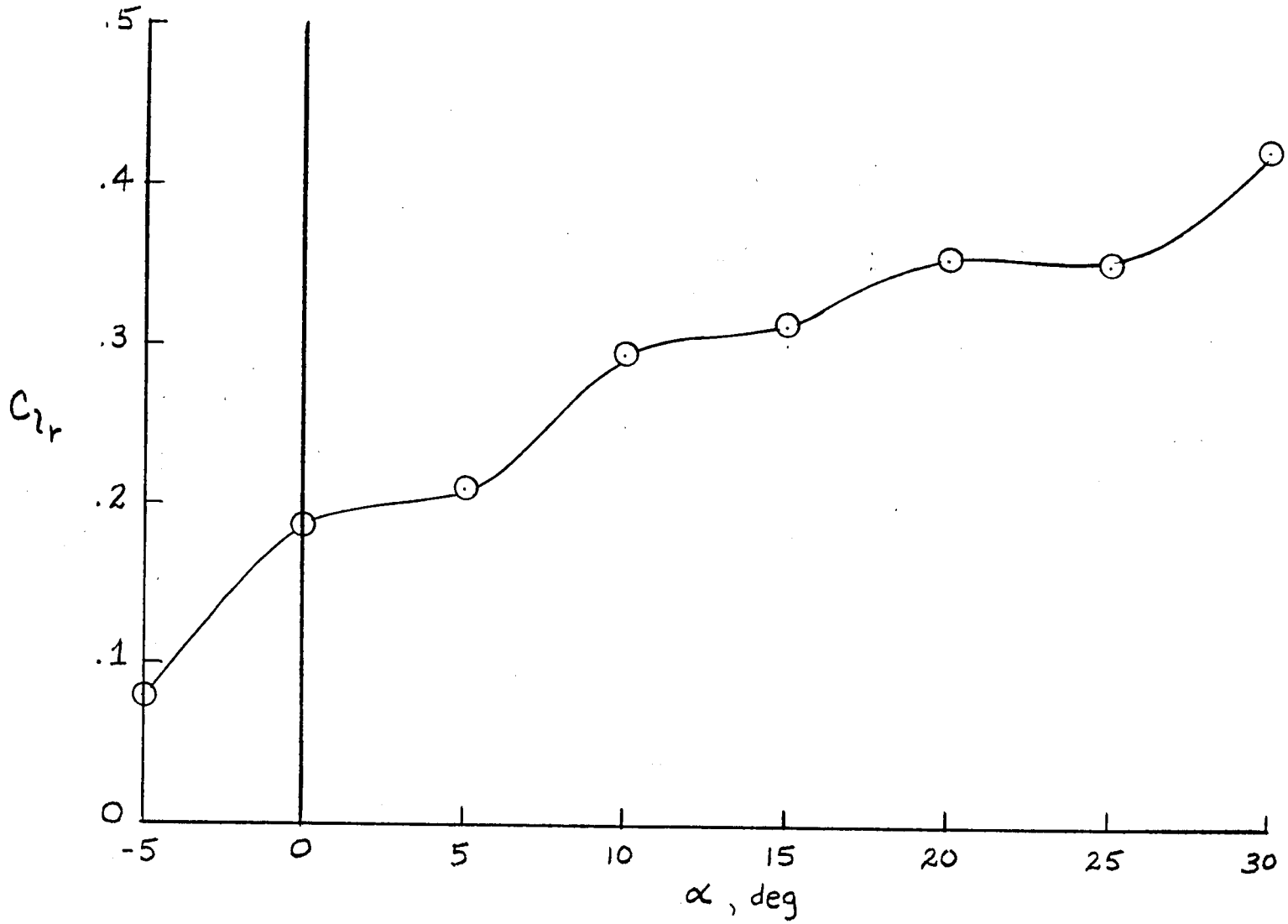

(d) Rolling moment coefficient due to yaw rate.

Figure 37.- Continued.

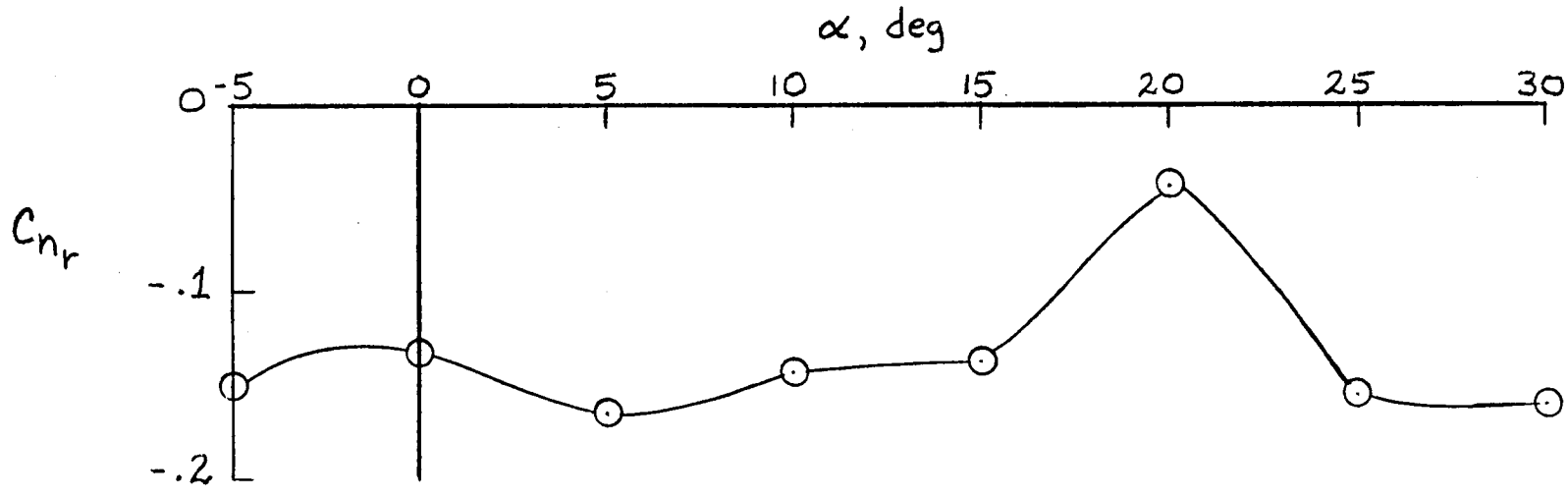

(e) Yawing moment coefficient due to yaw rate.

Figure 37.- Continued.

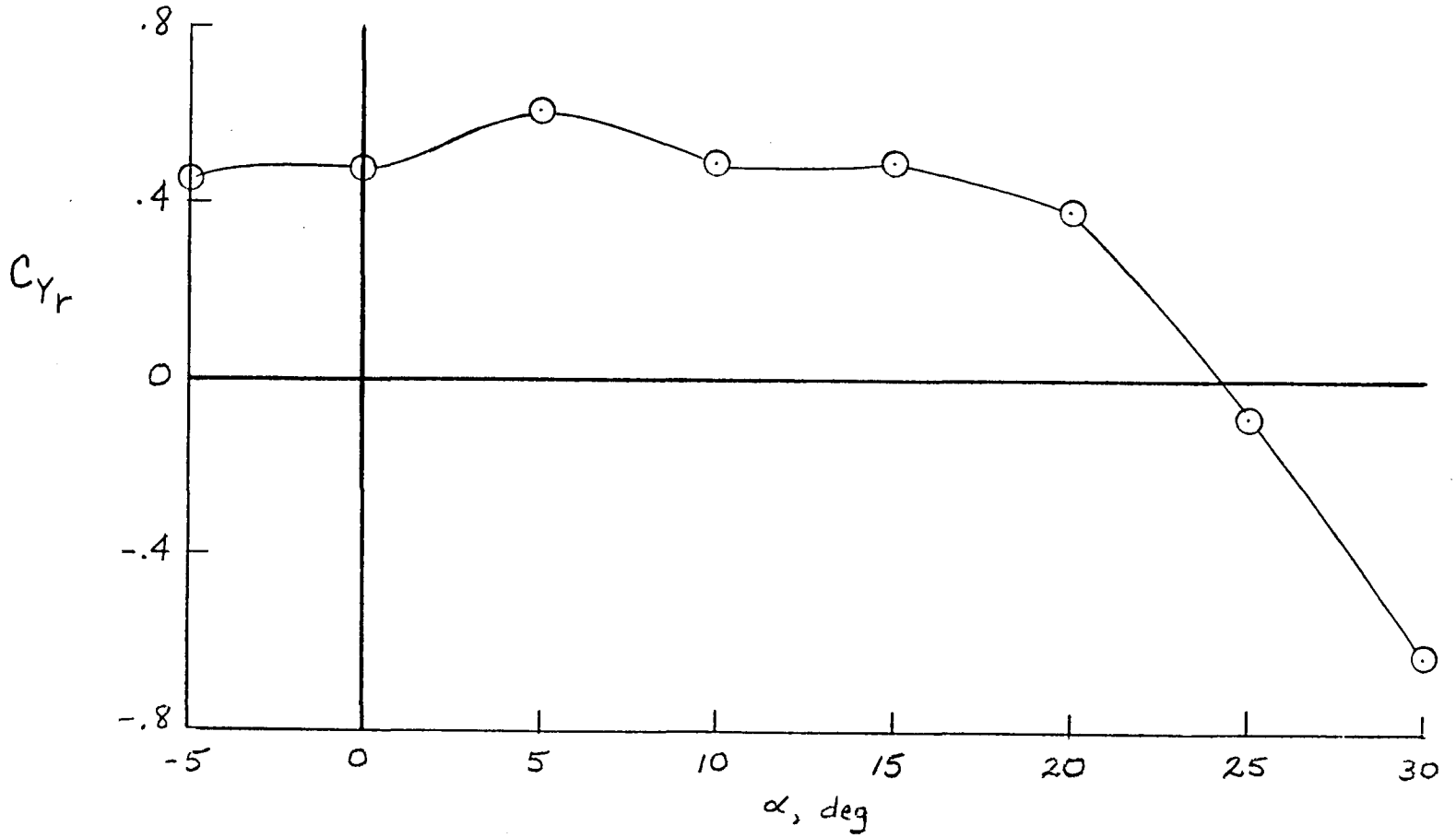

(f) Sideforce coefficient due to yaw rate.

Figure 37.- Concluded.

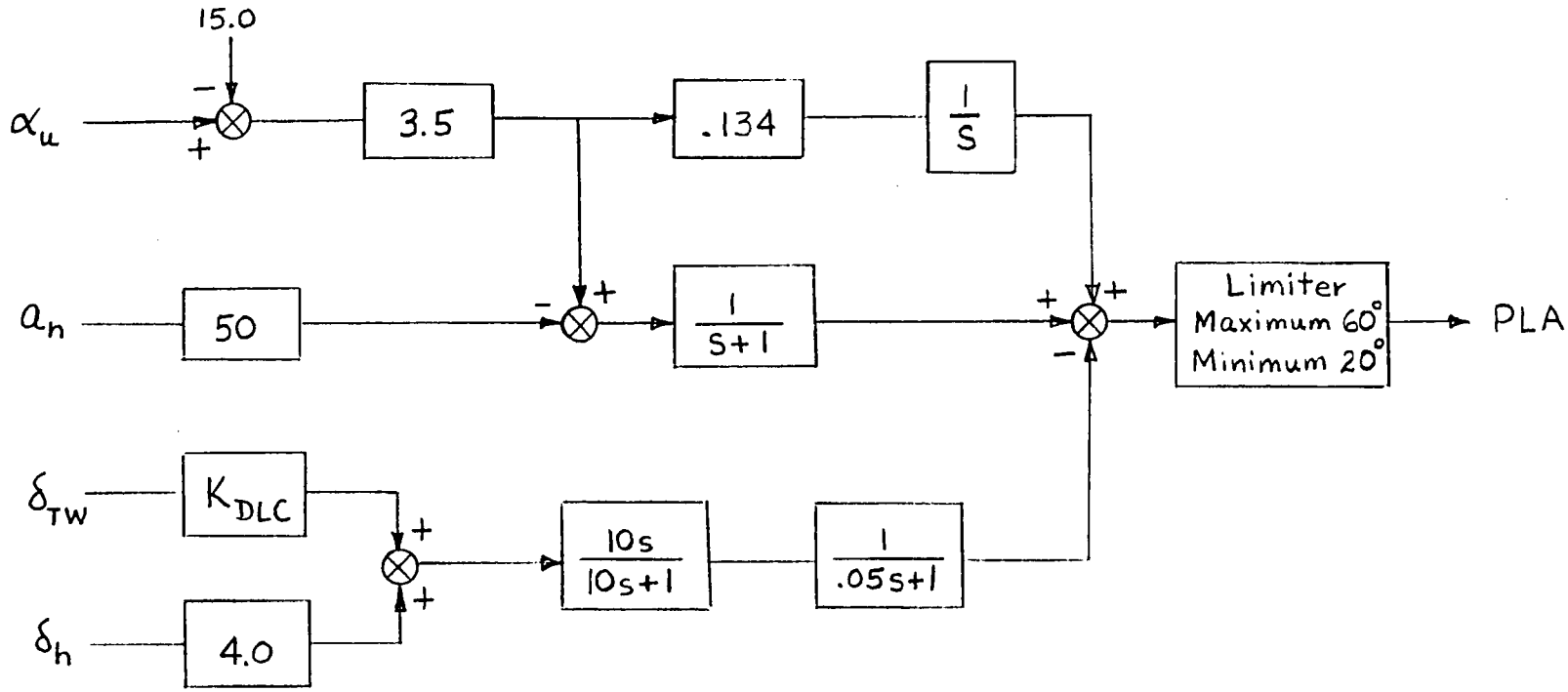

Figure 38.- Schematic of autothrottle control law.

1. Report No.	2. Government Accession No.	3. Recipient's Catalog No.
NASA TM 81833		

4. Title and Subtitle	5. Report Date
Simulator Results of an F-14A Airplane Utilizing an Aileron-rudder Interconnect During Carrier Approaches and Landings	May 1980
	6. Performing Organization Code

7. Author(s)	8. Performing Organization Report No.
Wendell W. Kelley Philip W. Brown	

9. Performing Organization Name and Address	10. Work Unit No.
NASA Langley Research Center Hampton, VA 23665	505-43-1301
	11. Contract or Grant No.

12. Sponsoring Agency Name and Address	13. Type of Report and Period Covered
National Aeronautics and Space Administration Washington, DC 20546	Technical Memorandum Jan. 79 - Feb. 80
	14. Army Project No.

15. Supplementary Notes

16. Abstract

A piloted simulator study was conducted to evaluate an aileron-rudder interconnect (ARI) control system for the F-14A airplane in the landing configuration. Effects on pilot performance and handling characteristics were investigated. Two ARI configurations were tested and compared to the standard F-14 fleet control system. A nonlinear aerodynamic model of the F-14 was used in conjunction with a six degree-of-freedom motion base simulator. The evaluation task, which utilized three subject pilots, consisted of a night carrier approach and landing.

Results of the study showed that both ARI configurations produced improved pilot performance and pilot ratings when compared to the standard control system. Sideslip due to adverse yaw as considerably reduced by the ARI systems and heading control was more stable and precise. Lateral deviation from centerline was reduced during the approach and lateral touchdown dispersion on the carrier deck was reduced with the ARI control systems.

17. Key Words (Suggested by Author(s))	18. Distribution Statement
F-14 ARI flight controls carrier landing piloted simulator aileron-rudder interconnect fighter airplane	Unclassified-unlimited Subject category 08

19. Security Classif. (of this report)	20. Security Classif. (of this page)	21. No. of Pages	22. Price*
Unclassified	Unclassified	90	A05

*For sale by the National Technical Information Service, Springfield, Virginia 22161